



University of
Stavanger

Faculty of Science and Technology

MASTER'S THESIS

Study program/ Specialization:

Spring semester, 2015

Offshore Technology: Marin and Subsea
Technology

Open

Writer:
Sveinung Kleppa

.....
(Writer's signature)

Faculty supervisor: Arnfinn Nergaard

External supervisor: Robert Olsen, GE Oil & Gas

Thesis title:

Dynamic Analysis of Emergency Disconnect during Workover Operations

Credits (ECTS): 30

Key words:

- Dynamic analysis
- Orcaflex
- Intervention
- Workover riser
- Emergency Disconnect Package
- High Angle Release

Pages: 87

+ enclosure: 10

Stavanger, June 15th 2015

Preface and acknowledgments

This thesis has been written as my finalization of my Master's degree program in Offshore Technology with specialization in Marine and Subsea Technology at the University of Stavanger. The work related to this thesis has been carried out from January until June 2015.

This master thesis has been written due to interest from GE Oil & Gas with Robert Olsen as main initiator.

I would like to express my sincere gratitude to Professor Arnfinn Nergaard from the University of Stavanger for his support and enthusiasm throughout this project. Also I would like to thank my external supervisor Robert Olsen from GE Oil & Gas for suggesting this thesis and his expert judgments during this work. I would also like to thank engineering supervisor Olav Ulen for his effort for making this thesis happen in collaboration between GE Oil & Gas and the University of Stavanger. Last but not least I would like thank my fiancée for her invaluable support and patience during my studies.

Sveinung Kleppa
Stavanger, June 14, 2015

Abstract

Emergency disconnect from the stack-up with large rig offset during well intervention is considered as a critical operation. Failure of disconnection from the well can lead to a major accident. Unofficial figures suggest that the connector fails to release 15 – 20 times globally each year. The industry has little detailed knowledge of the kinematics and trajectories of an emergency disconnect. GE Oil & Gas has shown interest of gaining more information regarding this matter. To comply with ISO 13628-7 the industry has developed High Angle Release (HAR) connectors for the Emergency Disconnect Package (EDP). The connector shall be able to safely release with a minimum offset angle of 10° .

The main objective of this thesis is to analyze the motions and the associated forces occurring immediately after disconnecting from the stack-up. To analyze the dynamics of the EDP after emergency disconnect Orcaflex was used. The established model in Orcaflex is verified by manual calculations and reasonable considerations. For better understanding of the dynamics involved, the Emergency Quick Disconnect (EQD) is analyzed with three different water depths and 15 Te overpull at the High Angle Release (HAR) connector.

The rig offset of 10° caused a bending moment of approximately 1000 kNm at the connector with the given riser configuration. The results showed that a large rotational motion dominated immediately after release. The EDP rotated with 12.6° within the first second after initiated EQD. Also an initial horizontal acceleration was found to occur simultaneously. The maximum initial horizontal acceleration was found to be approximately 4.7 m/s^2 . This led to a horizontal displacement of approximately 210 mm and a maximum velocity of 0.25 m/s. Several simulations with different EQD timing in waves were performed. This resulted in a minimum acceleration of approximately 6 m/s^2 and a maximum acceleration of approximately 8 m/s^2 in vertical direction depending on vessels position in the wave.

Table of Contents

| | |
|---|------|
| Preface and acknowledgments | i |
| Abstract | ii |
| Table of Contents | iii |
| List of figures | vi |
| List of tables | viii |
| List of symbols and abbreviations..... | ix |
| 1 Introduction..... | 1 |
| 1.1 Background..... | 1 |
| 1.2 Objectives | 2 |
| 1.3 Structure of thesis | 3 |
| 1.4 Assumptions and limitations | 3 |
| 2 Operations | 5 |
| 2.1 Intervention..... | 5 |
| 2.2 Drilling..... | 5 |
| 2.3 Dynamic positioning systems | 6 |
| 2.3.1 Drift-off | 7 |
| 2.3.2 Drive-off..... | 7 |
| 2.4 Risk involved in well interventions | 7 |
| 2.5 Operational envelope | 9 |
| 3 Standards and regulations | 10 |
| 4 System description | 12 |
| 4.1 C/WO Riser System..... | 13 |
| 4.1.1 Workover risers | 14 |
| 4.1.2 Riser joint | 14 |
| 4.1.3 Stress joint..... | 14 |
| 4.1.4 Tension joint..... | 15 |
| 4.1.5 Safety joint | 15 |
| 4.2 EDP..... | 16 |
| 4.3 LRP | 17 |

| | | |
|-------|---|----|
| 4.4 | HAR Connector | 18 |
| 4.5 | XT | 19 |
| 4.6 | Heave compensating system..... | 20 |
| 5 | Operational conditions | 21 |
| 5.1 | Environmental forces..... | 21 |
| 5.1.1 | Waves | 22 |
| 5.1.2 | Current..... | 22 |
| 5.1.3 | Wind..... | 22 |
| 5.1.4 | Risk related to environmental forces..... | 23 |
| 5.2 | Operational forces..... | 23 |
| 5.2.1 | Risk..... | 23 |
| 6 | Mechanical model..... | 24 |
| 6.1 | Geometry | 24 |
| 6.2 | Axial stiffness | 27 |
| 6.3 | Riser strain..... | 30 |
| 6.4 | Required top tension..... | 31 |
| 6.5 | Bending moment..... | 33 |
| 6.6 | Added mass..... | 34 |
| 6.7 | Acceleration..... | 37 |
| 7 | Modelling system in Orcaflex..... | 39 |
| 7.1 | Modeling of elements | 40 |
| 7.1.1 | Riser | 40 |
| 7.1.2 | Stack-up..... | 41 |
| 7.1.3 | Heave compensating system | 45 |
| 7.2 | Selection of input data | 47 |
| 8 | Verification of model..... | 49 |
| 8.1 | Natural frequency | 50 |
| 8.2 | Tension | 51 |
| 8.3 | Acceleration..... | 52 |
| 8.4 | Selection of time step and key coefficients | 53 |
| 8.4.1 | Time step..... | 53 |

| | | |
|-------|--|----|
| 8.4.2 | Coefficients | 54 |
| 9 | Results from EQD..... | 57 |
| 9.1 | EQD with no environmental forces | 59 |
| 9.2 | EQD with environmental forces | 67 |
| 10 | Comparison of results..... | 77 |
| 10.1 | Different water depths | 77 |
| 10.2 | Environmental conditions..... | 80 |
| 11 | Discussion | 81 |
| 12 | Conclusions | 84 |
| 13 | Uncertainties..... | 85 |
| 14 | Further work..... | 85 |
| 15 | References | 86 |
| | Appendix A | 88 |
| | Appendix B | 93 |

List of figures

| | |
|--|----|
| FIGURE 1: TYPICAL OPERATING ENVELOPE [6]..... | 9 |
| FIGURE 2: STACK-UP FROM GE OIL & GAS [7] | 12 |
| FIGURE 3: TYPICAL C/WO RISER GENERAL ARRANGEMENT IN TREE MODE [6]..... | 13 |
| FIGURE 4: SKETCH OF A RISER JOINT FROM GE OIL & GAS [10] | 14 |
| FIGURE 5: SAFETY JOINT FROM GE OIL & GAS [7] | 15 |
| FIGURE 6: EDP SUBSEA1.COM [11]..... | 16 |
| FIGURE 7: TYPICAL XT FROM [8]..... | 17 |
| FIGURE 8: XTREME RELEASE CONNECTOR™ FROM STL [2] | 18 |
| FIGURE 9: GE OIL & GAS XT [14] | 19 |
| FIGURE 10: ILLUSTRATION OF HEAVE COMPENSATION LIMITS BASED ON [15]..... | 20 |
| FIGURE 11: ENVIRONMENTAL LOADS ON RISERS [15]..... | 21 |
| FIGURE 12: GEOMETRY OF ESTABLISHED MODEL | 24 |
| FIGURE 13: GEOMETRY USED FOR CALCULATIONS..... | 25 |
| FIGURE 14: REMAINING COMPENSATOR STROKE AS A FUNCTION OF OFFSET | 26 |
| FIGURE 15: SKETCH OF THE SIMPLIFIED MODEL | 28 |
| FIGURE 16: TENSION PICTURE | 32 |
| FIGURE 17: CURVATURE DUE TO RIG OFFSET | 34 |
| FIGURE 18: FREE BODY DIAGRAM FOR THE EDP..... | 37 |
| FIGURE 19: ORCAFLEX LINE MODEL | 40 |
| FIGURE 20: APPROXIMATED MODEL OF EDP IN ORCAFLEX..... | 44 |
| FIGURE 21: SIMPLE SPRING AND COMBINED SPRING-DAMPER..... | 45 |
| FIGURE 22: HSC PRIOR STATIC ANALYSIS | 46 |
| FIGURE 23: HSC POST STATIC ANALYSIS | 46 |
| FIGURE 24: SKETCH OF SIMPLIFIED MODEL IN ORCAFLEX..... | 49 |
| FIGURE 25: FORCED OSCILLATIONS OF EDP FROM ORCAFLEX - SIMPLIFIED MODEL | 50 |
| FIGURE 26: TENSION RESULTS FROM ORCAFLEX – SIMPLIFIED MODEL | 51 |
| FIGURE 27: EDP Z-ACCELERATION FROM ORCAFLEX - SIMPLIFIED MODEL 300 METERS..... | 52 |
| FIGURE 28: IMPACT OF TIME STEP IN ORCAFLEX. FIGURE SHOWS EDP ACCELERATION FROM EQD WITH WAVES AND CURRENT AND SERVES ONLY ILLUSTRATIVE SENSITIVITY PURPOSES. | 53 |
| FIGURE 29: EDP TRAJECTORY - SENSITIVITY OF RISER DRAG COEFFICIENT | 54 |
| FIGURE 30: EDP TRAJECTORY - SENSITIVITY OF RISER ADDED MASS COEFFICIENT | 54 |
| FIGURE 31: EDP TRAJECTORY - SENSITIVITY OF EDP ADDED MASS COEFFICIENTS..... | 55 |
| FIGURE 32: EDP TRAJECTORY - SENSITIVITY OF EDP DRAG COEFFICIENT | 55 |

| | |
|---|----|
| FIGURE 33: EDP TRAJECTORY - SENSITIVITY OF EDP MASS COEFFICIENT | 56 |
| FIGURE 34: CONFIGURATION OF EDP AND HAR CONNECTOR WITH COORDINATE SYSTEM | 57 |
| FIGURE 35: GE OIL & GAS HAR CONNECTOR (NOT TO SCALE) [20] | 58 |
| FIGURE 36: BENDING MOMENT AT 300 METERS WD AS A FUNCTION OF OFFSET | 58 |
| FIGURE 37: GLOBAL SET-UP IN ORCAFLEX WITH 300 METERS WD AND 10° OFFSET | 59 |
| FIGURE 38: INITIAL MOTIONS OF THE EDP AFTER EQD | 60 |
| FIGURE 39: EDP ACCELERATION IN Z-DIRECTION IN 300 METERS WD | 61 |
| FIGURE 40: EDP VELOCITY IN X-DIRECTION IN 300 METERS WD | 61 |
| FIGURE 41: EDP ACCELERATION IN X-DIRECTION IN 300 METERS WD | 62 |
| FIGURE 42: EDP VELOCITY IN X-DIRECTION IN 300 METERS WD | 62 |
| FIGURE 43: EDP POSITION IN Z-DIRECTION FOR 300 METERS WD | 63 |
| FIGURE 44: EDP POSITION IN X-DIRECTION FOR 300 METERS WD | 63 |
| FIGURE 45: EDP TRAJECTORY | 64 |
| FIGURE 46: INITIAL EDP TRAJECTORY | 64 |
| FIGURE 47: EDP ANGULAR ACCELERATION | 65 |
| FIGURE 48: EDP ANGULAR VELOCITY | 65 |
| FIGURE 49: CLOSE-UP OF RISER CURVATURE WITH 10° RIG OFFSET | 66 |
| FIGURE 50: Z-VELOCITY OF SEMI-SUBMERSIBLE | 67 |
| FIGURE 51: Z-POSITION | 67 |
| FIGURE 53: SYSTEM SET-UP IN ORCAFLEX | 68 |
| FIGURE 53: DETAIL A | 68 |
| FIGURE 54: CONFIGURATION OF EDP AND HAR CONNECTOR WITH COORDINATE SYSTEM | 69 |
| FIGURE 55: ORCAFLEX SIMULATION - TRAJECTORY OF EDP FOR 300 METERS WD AND 10° OFFSET | 69 |
| FIGURE 56: TENSION VERIFICATION OF GLOBAL MODEL SETTINGS | 70 |
| FIGURE 57: BENDING MOMENT AT HAR CONNECTOR | 71 |
| FIGURE 58: EDP ACCELERATION IN Z-DIRECTION | 72 |
| FIGURE 59: EDP VELOCITY IN Z-DIRECTION | 72 |
| FIGURE 60: EDP ACCELERATION IN X-DIRECTION | 73 |
| FIGURE 61: EDP VELOCITY IN X-DIRECTION | 73 |
| FIGURE 62: EDP MOTION IN Z-DIRECTION | 74 |
| FIGURE 63: EDP MOTION IN X-DIRECTION | 74 |
| FIGURE 64: EDP TRAJECTORY (LOWER EDGE OF EDP) | 75 |
| FIGURE 65: CLOSE-UP OF EDP TRAJECTORY (LOWER EDGE OF EDP) | 75 |
| FIGURE 66: EDP ANGULAR VELOCITY | 76 |
| FIGURE 67: COMPARISON OF Z-ACCELERATIONS | 77 |

| | |
|--|----|
| FIGURE 68: COMPARISON OF EDP ACCELERATION IN X-DIRECTION WITHOUT ENVIRONMENTAL LOADS | 78 |
| FIGURE 69: COMPARISON OF EDP TRAJECTORIES..... | 78 |
| FIGURE 70: CONFIGURATION OF LOWER EDGE COORDINATE SYSTEM | 79 |
| FIGURE 71: LOWER EDGE OF EDP LOCAL TRAJECTORY | 79 |
| FIGURE 72: COMPARISON OF EDP ACCELERATION IN Z-DIRECTION WITH AND WITHOUT ENVIRONMENTAL LOADS..... | 80 |
| FIGURE 73: COMPARISON OF EDP ACCELERATION IN X-DIRECTION WITH AND WITHOUT ENVIRONMENTAL LOADS..... | 80 |

List of tables

| | |
|--|----|
| TABLE 1: TYPICAL PREVENTATIVE MEASURES TO REDUCE PROBABILITY OF DRIFT-OFF/DRIVE-OFF [6] | 10 |
| TABLE 2: TYPICAL PREVENTATIVE MEASURES TO REDUCE THE CONSEQUENCES OF DRIFT-OFF/DRIVE-OFF (ISO, 2005) | 11 |
| TABLE 3: EDP SUBSEA1.COM [11] | 16 |
| TABLE 4: SUBSEA1.COM [11] | 17 |
| TABLE 5: MAXIMUM FEASIBLE RIG OFFSET FOR DIFFERENT WATER DEPTHS..... | 26 |
| TABLE 6: INPUT DATA | 27 |
| TABLE 7: INPUT DATA FOR CALCULATING NATURAL PERIOD | 29 |
| TABLE 8: CALCULATIONS OF AXIAL NATURAL PERIOD OF RISER AND EDP | 29 |
| TABLE 9: AXIAL NATURAL PERIODS FOR DIFFERENT WATER DEPTHS..... | 29 |
| TABLE 10: STATIC ELONGATION OF RISER DUE TO GRAVITY CALCULATED USING HOOKE'S LAW | 31 |
| TABLE 11: RISER DATA | 32 |
| TABLE 12: TENSION VALUES ACCORDING TO FIGURE 16 WITH AND WITHOUT 15 TE OVERPULL | 33 |
| TABLE 13: ADDED MASS COEFFICIENTS (RP-H103, 2011) | 35 |
| TABLE 14: ADDED MASS CALCULATIONS [17] | 35 |
| TABLE 15: RELEVANT ADDED MASS DATA FOR EDP AND RISER..... | 36 |
| TABLE 16: NATURAL PERIODS OF DEFINED SYSTEM WITH AND WITHOUT ADDED MASS | 36 |
| TABLE 17: EDP ACCELERATION IN Z-DIRECTION | 38 |
| TABLE 18: ORCAFLEX EDP COEFFICIENTS AND MOMENT OF INERTIA | 47 |
| TABLE 19: ORCAFLEX RISER COEFFICIENTS..... | 47 |
| TABLE 20: KEY OUTPUT OBTAINED FROM ORCAFLEX | 66 |
| TABLE 21: COMPARISON OF AXIAL PERIODS..... | 77 |

List of symbols and abbreviations

Symbols:

| | |
|-------------|--|
| a_z | Acceleration in Z-direction |
| a_x | Acceleration in X-direction |
| b_{riser} | Buoyancy of riser [kg/m] |
| C_d | Drag coefficient |
| C_m | Mass coefficient |
| d | Water depth |
| d_i | Internal diameter |
| d_o | Outer diameter |
| F_T | Tension force |
| g | Acceleration of gravity |
| M_{bR} | Bending moment riser |
| M_{bWH} | Bending moment Well Head |
| m_{riser} | Mass of riser [kg/m] |
| T_n | Natural period |
| v_z | Velocity in Z-direction |
| v_x | Velocity in X-direction |
| x | Position of wave |
| ΔX | Rig offset |
| Δx | Distance from riser to drill floor |
| α | Angular acceleration [rad/s ²] |
| θ | Offset angle |
| ρ | Density [kg/m ³] |
| ρ_w | Density of seawater |
| ω_n | Natural frequency |

Abbreviations:

| | |
|----------|---|
| C/WO | Completion/Workover |
| DP | Dynamic Positioning |
| EDP | Emergency Disconnect Package |
| EDS | Emergency Disconnect Sequence |
| EQD | Emergency Quick Disconnect |
| HAR | High Angle Release |
| HCS | Heave Compensation System |
| ISO | International Standard Organization |
| Lock-up | Dysfunctional heave compensation system |
| LRP | Lower Riser Package |
| NCS | Norwegian Continental Shelf |
| RAO | Response Amplitude Operator |
| RL | Rapid Lock |
| SG | Specific Gravity |
| Stack-up | Includes XT and LRP |
| STL | Subsea Technologies Ltd |
| Te | Metric ton |
| WD | Water depth |
| WOR | Workover Riser |
| WORS | Workover Riser System |
| XT | Christmas Tree |
| XR | Xtreme Release |

1 Introduction

As there consists over 6000 subsea wells worldwide [1], well intervention is a large business. In order to obtain maximum and continuous production of hydro carbons wells need modifications while producing. The frequency of well intervention depends on several parameters; single- or multiphase flow, flow rate, external environment, content of fluid, water and reservoir depth and reliability of equipment. Accessing a subsea well is a complex task with a high degree of safety precautions implemented. The industry has gained lots of experience of entering subsea wells using a variety of methods. Typical intervention operations are performed using a Workover Riser (WOR) combined with an Emergency Disconnect Package (EDP) and a Lower Riser Package (LRP). The EDP allows the vessel to safely disconnect from the well in required situations. Not only will the vessel be free to move, but the well is also secured by active barriers in the LRP. Disconnection from a well is considered as a last option to maintain the integrity and safety of the vessel and the well. The primary reasons of initiating an Emergency Quick Disconnect (EQD) is either rough weather or problems with staying positioned. EQD is defined as the sequence from initiation of emergency disconnect procedure to the EDP has released from the stack-up. The procedure can take up to 1 minute from the operator initiates the Emergency Disconnect Sequence (EDS) until the EDP is released. The weather can be predicted to a certain degree, but the integrity of the vessel can be lost with little or no warning. This thesis will focus on the initial forces and trajectories of the EDP after initiated EQD. The trajectory describes the motion of the EDP with respect to X and Z-coordinates.

1.1 Background

The oil and gas industry have shown interest in the dynamic forces in the riser and EDP and the trajectory of these. In the wake of the Macondo incident, the industry has focused on development of methods to recover from similar incidents. There is no official record of the numbers of times the emergency release connectors fail to release due to rig offset, but unofficial figures suggests that such events occurs 15 to 20 times globally each year [2]. In order to verify the design of a High Angle Release (HAR) connector, a thorough analysis of

the emergency disconnect scenario is needed. The analysis is required to ensure that the EDP will not suffer any damage and not cause any damage to surrounding equipment on the seabed during EQD. National regulations also set requirements to zero discharge after initiated EQD, which means in practice that the EDP has to seal off the riser content prior EQD. This master thesis was requested by GE Oil & Gas to investigate the forces and trajectories associated with EQD. GE Oil & Gas has have developed a high angle release connector based on a design from Subsea Technologies Ltd (STL).

1.2 Objectives

The objective of this thesis is to analyze and understand the dynamics associated with an emergency disconnect. Accelerations, velocities and trajectory are the primary values of interest. For better understanding of the dynamics of the EQD water depths (WD) of 300, 500 and 1000 meters are to be investigated. The first few seconds after release are considered most critical. This thesis will only consider the time interval from release until the EPD is safely removed from the stack-up. The main objectives are presented below:

- Description of the system components and expressions
- Establish a mechanical model including required calculations
- Dynamic analysis of EQD using Orcaflex
 - Analyze the EDP motions for 300, 500, and 1000 meters WD
 - Analyze the EDP motions for 300, 500, and 1000 meters WD including waves and current
- Discussion and comparison of results
- Suggestion for HAR connector design improvements

1.3 Structure of thesis

This thesis is divided into four main parts. The first chapter gives an introduction to the scope of this thesis and why it is relevant for the industry. For clarification reasons description of limitations and assumptions are also included.

The following four chapters present the theoretical background, description of the system and addressing the forces involved. From chapter six to eight the mechanical system is explained, Orcaflex is presented and used to perform a dynamic analysis of the emergency disconnect. Finally the results are presented with a comparison, discussion and conclusion.

1.4 Assumptions and limitations

This thesis will be focused on intervention operations with a certain system set-up. Water depths of 300, 500 and 1000 meters will be considered. As the objective for this thesis is to gain information of the dynamics of the EDP after EQD, advanced wave spectra is not used. Ordinary Stokes 5th order waves are used to clarify the effect of wave loads subjected to the vessel. This thesis is limited by following assumptions:

- The stack-up and wellhead is considered to be infinitely stiff.
- The annulus line will not contribute to added mass, drag forces, axial or bending stiffness.
- The riser is considered a homogenous pipe with constant material properties, except the stress joint.
- Complexity of the EDP is not considered. Added mass and drag forces could be incorrect due to assumptions made in Orcaflex.
- The riser is always operating in the elastic region because of the safety joint.
- No marine growth on riser due to temporary operational time period.
- Zero gauge pressure inside riser – only hydrostatic.
- Response amplitude operator (RAO) for semi-submersible is not assessed or questioned.
- Thermal elongation of riser is not considered.

- Total heave compensator stroke length is assumed to be 10 meters.
- Material properties and geometric dimensions are treated equally for all types of riser joints, except the stress joint which is tapered.
- In general when this thesis refers to 300 meters WD, this implies usage of a riser length of 308 meters. The same goes for 500 and 1000 meters with 508 and 1008 meters respectively. Further explanation is presented later.
- Moon pool collision is not addressed in this thesis

2 Operations

To fully understand the scope of this thesis a description the different operations and systems involved are presented.

2.1 Intervention

Any inspection and modification performed in a well are called well intervention. Causes that can reduce or block the production rate of a well are mechanical failure, plugging of flowlines or changes in production characteristics [3]. To maintain the integrity of the wells they need service and maintenance. The main types of well configuration are differentiated by either surface X-mas Tree (XT) or subsea XT. Surface wells are easier to maintain and intervene, as the XT are located at surface onboard a vessel/rig. A major advantage with surface XT's are that they are accessible at all time. Subsea wells on the other hand are more limited. For accessing a subsea well a suitable vessel must be available to rent and the weather conditions must be appropriate. This explains why many subsea wells have a planned maintenance schedule instead of a reactive maintenance plan. This means that the maintenance is primarily performed during summer season. If similar activities is to be performed during winter season, a suitable vessel would be significant larger in size and hence have a higher cost. The risk involved in performing an intervention during the winter season is also considerable higher than during summer season.

During intervention the vessel have physical connection to the subsea well using a WORS. Operations such as coiled tubing, wire line and fluid displacement are typical intervention operations.

2.2 Drilling

Drilling is a discipline of its own. The mechanical configuration of the system is much similar to the workover operation, but usually with greater dimensions. The physical connection between a drilling vessel and the BOP/LMRP is a marine riser. The marine riser is connected to the LMRP which enables the quick disconnect feature corresponding to the EDP during

interventions. As the marine riser is larger in diameter than the WOR, this implies significant larger forces on the stack-up during rig drift off. This thesis is limited to workover operations and will not explain further on drilling operations.

2.3 Dynamic positioning systems

Floating vessels typically use two main types of station keeping; Dynamic positioning (DP) and mooring lines. The idea is to keep the vessel at the same geographical location during the entire operation. The two systems are sometimes used together to obtain higher reliability [4]. A suitable solution will vary for each specific operation and depend on environmental conditions along with which operation to be performed. Mooring systems require costly installation and handling of the anchors and will delay the operation with the installation time. DP vessels can start operating almost immediately after entering the location, but will consume more fuel to stay positioned. A big drawback for using DP is the risk of loss of power. The thrusters require a large amount of power and cannot rely on uninterrupted power supply system (UPS). This is one of the failures that caused the Deepwater Horizon incident. The blowout caused the diesel engines supplying the vessel with electricity to break down. As a result of loss of power, the DP system was no longer operational and the rig started to drift of its location. Drilling vessels prefer DP systems due to enormous rig rates and the fact that the rigs will not be stationed for long. DP systems are divided into three different classes. Class one is the most critical system and relies on only one system without any redundancy. Class 2 has two fully functional separate DP systems. DP 3 systems also consist of two systems, but the second system is physical isolated from each other. In case of failure of one system, the other is capable of holding position. Mooring systems are mainly used in shallow water because the weight will be very high in deep waters. This means that the tension applied to the vessel will increase significantly. Many vessels are designed to operate at deep water and are capable of coping with these tension forces. However, using fiber or Kevlar mooring lines in deeper water can be a cost efficient solution due to their low weight and high strength. The disadvantage with Kevlar mooring lines are mainly high cost.

Loss of position can be caused by either drift off or drive off.

2.3.1 Drift-off

If a vessel loses position due to external loads such as winds, waves and currents it is addressed as a drift-off. Initiating events can be malfunction of DP system, breakage of mooring lines, loss of power, engine breakdown, software or human failure. During intervention operations a drift-off can have significant consequences to the vessel and subsea structures. Schematic diagram of a drift-off situation are presented in section 6 in this thesis. As the vessel moves horizontally, the riser will be affected to high tension forces and bending moments. The figure shows that the initial riser length will be too short compared to the new geometry. Active heave compensators will comprehend some of the change in required riser length, but as the stroke length is limited, the heave compensator will stop to move. At that point the vessel can no longer account for heave movement and the riser will be exposed to enormous forces. To avoid this situation GE Oil & Gas have developed a Safety Joint to protect against excessive top tension.

2.3.2 Drive-off

Drive off is a special case of drift-off, involving only malfunction of the DP system. The thrusters will force the vessel to change position and may be considered to be far more dangerous than drift-off due to less time to react. Typical average velocity of a semi-submersible with full thrust is 1 m/s. In shallow waters this implies that the operator have less than one minute to react prior to gaining a critical offset. Drive-off can occur due to software failure including but not limited to loss of GPS signal or receiving a false GPS signal and poor communication between thrusters and computer system.

2.4 Risk involved in well interventions

DNV has published a paper called "Workover/Well Intervention and Regulatory Challenges" [5]. It describes the concerns regarding lack of international regulations. As rigless well intervention business is a rather new business with many new companies involved, dangerous

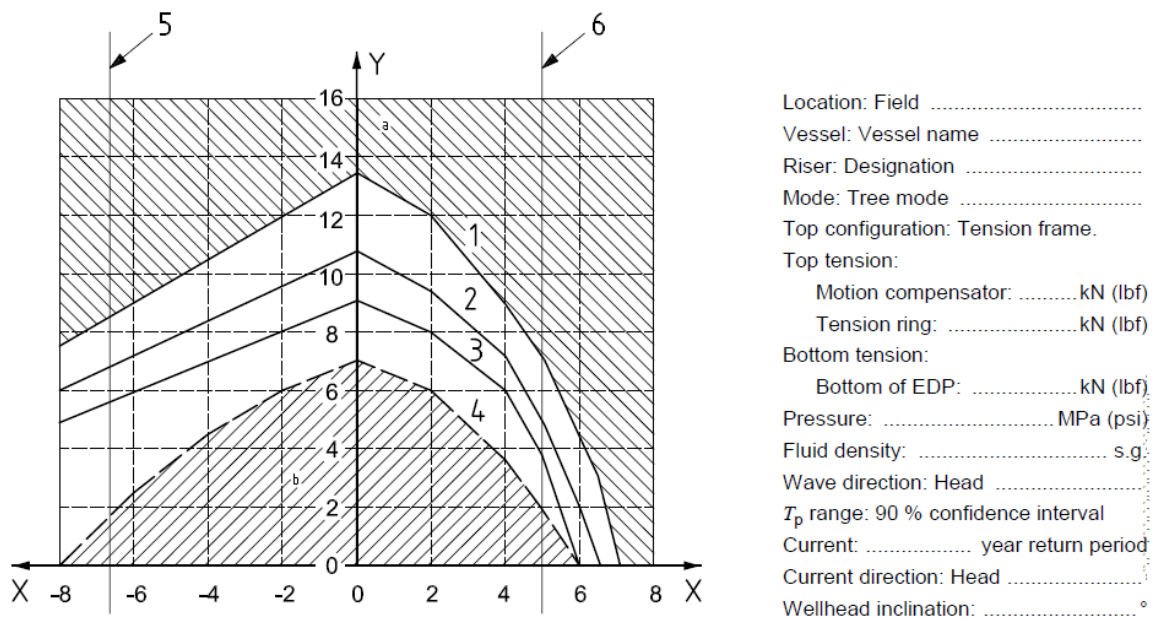
situations can arise. Many operators are focusing on drilling and exploration and not intervention operations. This is mainly because drilling operations obviously has greater risk than interventions. However, serious accidents have occurred during well interventions even though it is less frequent and often involves both human error and barrier failure. Intervention vessels used are often not designed to perform these operations, but are customized and equipped with required components. As long as the vessel have a heave compensated crane and a system for station keeping, there are no clear guidelines for requirements of an intervention vessel. In many parts of the world the requirements for well intervention units are mostly regulated by the industry itself [5].

During normal operations the EDS system will never have to be utilized. However, it is even more important that the system is operative at all times in case of emergency. As described above, this thesis will focus on rig drift-off and drive-off. The critical phase is the short interval from disconnecting the well until the EDP is removed from the stack-up. Unless the forces, accelerations and trajectories are established, expensive equipment can be damaged and the probability for an unwanted event is unknown.

Another situation that may occur is an uncontrolled blowout. The EDS system is designed to be fail-safe, which implies that if communication with the subsea equipment is lost, the system automatically initiates the EDS.

2.5 Operational envelope

In order to minimize the risk involved with marine operations, operational envelopes for the vessel have to be established. The main objective of the operating envelopes is to produce a set of operating limitations that can be used as a guideline to ensure that all equipment relating to the riser system is being used within its design limits. By relating information regarding static vessel offset, current and significant wave height to allowable bending moment data, a series of operating envelopes are developed.



Key

- X vessel static offset, L_{so} , from wellhead extension, measured as percentage of water depth, positive in direction of current
- Y significant wave height, H_s
- 1 strength limit: accidental
- 2 strength limit: extreme
- 3 strength limit: normal
- 4 stroke limit: motion compensator
- 5 EDP angle limit: upstream
- 6 EDP angle limit: downstream
- a Unsafe operating area.
- b Safe operating area.

Figure 1: Typical operating envelope [6]

3 Standards and regulations

According to ISO 13628-7 the minimum allowable emergency disconnect angle for the connector between the EDP and LRP should be 10°. The disconnect angle shall also be qualified by testing.

The designer of C/WO equipment should account for both planned disconnection and emergency disconnection. All parameters regarding vessel characteristics, operational conditions and environmental conditions must be evaluated. Preventative measures related to rig drift-off/drive-off can be divided into two categories [6]:

- a) Measures directed toward reducing the probability of experiencing a drift-of/drive-off situation.
- b) Measures directed towards reducing the consequences following a drift-off/drive-off situation.

The consequences are again split into different categories involving possibility for blow-out, consequences for the subsea equipment and risers. Table 1 shows typical preventative measures for reducing the probability of drift-off/drive-off.

| System | Preventative measures | Comments |
|----------------------------|---|--|
| Dynamic positioning system | Specification of dynamic positioning consequence class | Typically IMO consequence class 3. Not less than IMO, class 2 |
| Reference system | Specification of minimum number of independent position reference systems, positioning accuracy and repeatability | A minimum of three independent systems is recommended, irrespective of dynamic positioning class |
| | For shallow water (< 350 m), special consideration shall be given to positioning accuracy and repeatability | Typical reference systems: GPS Hydro-acoustic Taut wire Riser angle |
| Power system | Maximum utilization of the dynamic positioning system during operation | Weather criteria for the 80 % limit should be established and documented |
| | Should not exceed 80 % of total capacity | - |

Table 1: Typical preventative measures to reduce probability of drift-off/drive-off [6]

If a drift-off/drive-off situation occurs there are several preventative actions to reduce the consequences. Table 2 shows some typical preventative measures:

| System | Preventative measures | Comments |
|---|--|--|
| Reservoir | Operations performed with well in overbalance | - |
| Drilling riser and C/WO riser | Weak link philosophy | Risers unable to transmit forces of such magnitude as to threaten the barriers |
| BOP, LMRP, lower workover riser package, subsea test tree | Rapid emergency shutdown and emergency disconnect response | Fully automated and tested emergency disconnect systems |
| Vessel | Active positioning of vessel | Suitable for drift-off only. Increase time to reach critical limits |
| BOP, LMRP, subsea test tree | Procedures | Combined operating procedures for drilling riser and C/WO riser systems |

Table 2: Typical preventative measures to reduce the consequences of drift-off/drive-off (ISO, 2005)

4 System description

This thesis is limited to intervention equipment and hence WOR is used as interface between floating vessel and the subsea well. There are a large variety of configurations of C/WO risers depending on environmental conditions and reservoir properties. A typical WORS configuration and specifications will be considered.

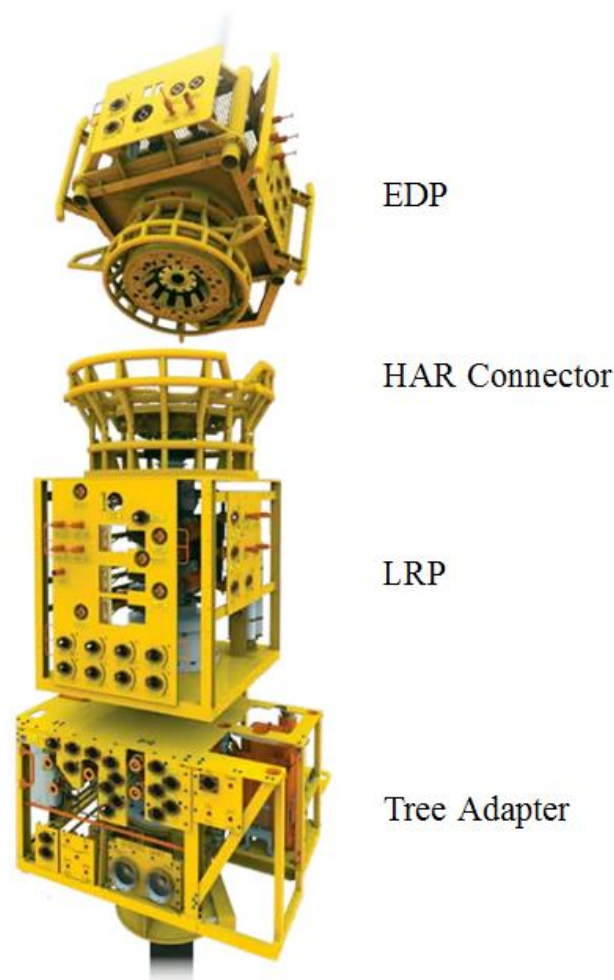


Figure 2: Stack-up from GE Oil & Gas [7]

Figure 2 shows a stack-up from GE Oil & Gas including EDP, LRP and tree adapter. The XT is a part of the stack-up, but not shown in this figure. The tree adapter is optional and enables an interface with non-GE tree mandrels. Tree adapter is only of illustrative purposes and is not of further use in this thesis.

4.1 C/WO Riser System

Figure 1 shows a typical configuration of a C/WO riser from a floating vessel.

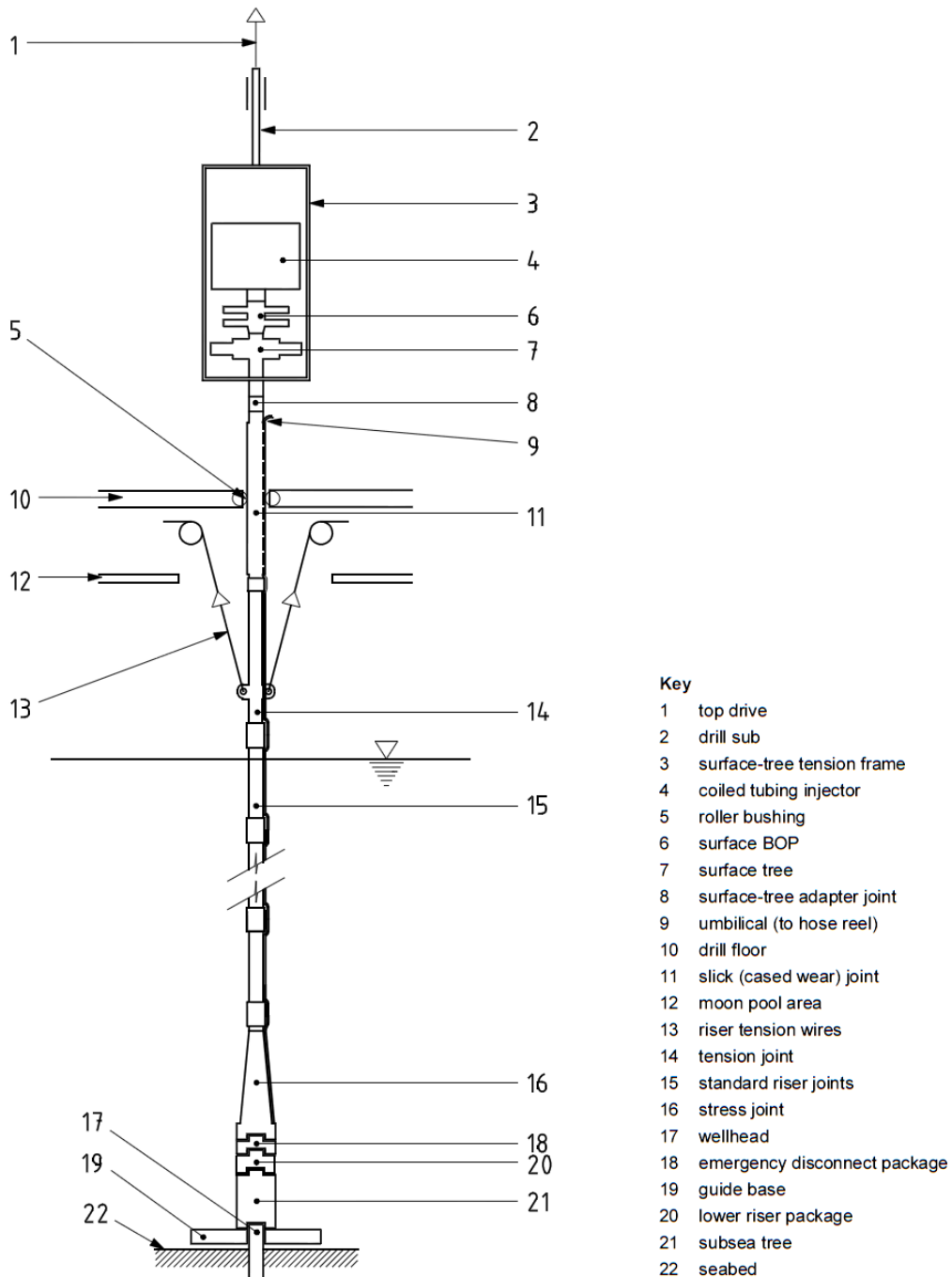


Figure 3: Typical C/WO riser general arrangement in tree mode [6]

4.1.1 Workover risers

The WOR is the main mechanical interface between subsea tools and topside equipment on the vessel. The WOR enables passage for running tools downhole and allows for circulation of fluids and well stream [8]. With constantly installing subsea wells at larger water depths, the top tension requirements increases significantly. The industry has been performing research in composite risers to reduce the top tension.

4.1.2 Riser joint

The main part of the WOR system consists of riser joints. These are normally provided in 30 – 50 ft lengths depending on the water depth in each field. The annulus line is usually clamped onto the riser during operation and provides the opportunity of circulating fluids during operations. Shorter riser joints may be addressed as pup joints and may provide the needed distance while running subsea trees, tubing hangers or during workover operations [9].



Figure 4: Sketch of a riser joint from GE Oil & Gas [10]

Figure 4 shows a typical riser joint from GE Oil & Gas with the annulus line clamped onto the riser.

4.1.3 Stress joint

The stress joint is located right above the EDP in the WOR system. This is a riser joint with a tapered cross section to withstand local curvature and reduce local bending stresses. Its objective is also to increase the systems fatigue life and improve the operational envelope of the system. The upper design criterion for the outer diameter is to fit down the rotary table on the operating vessel.

4.1.4 Tension joint

The tension joint is a special riser joint with interface to the tensioning system on the vessel. The joint is subjected to largest tension forces and is located near the vessels deck. This thesis treats the tension joint as any other riser joint. This assumption will slightly reduce the weight of the riser system.

4.1.5 Safety joint

To prevent unnecessary damage to the WORS safety joints are introduced. The safety joint handles two types of failure mechanisms. If the heave compensation system fails and cause a lock-up, excessive tension would quickly arise in the riser system due to heave motion of the vessel. Lock-up occurs during failure of the HCS, hence the system becomes fixed in Z-direction. The safety joint ensures a controlled and safe fracture close to the seabed. The second failure mechanism is too large vessel offset. Too large offset in deep waters will cause the heave compensation system to stroke out and give the same effects as the lock-up situation. New technology allows the safety joint to seal the riser from the environment and prevent content in the riser to discharge.



Figure 5: Safety joint from GE Oil & Gas [7]

Figure 5 shows the safety joint provided from GE Oil & Gas. The protection load can be adjusted according to fulfill requirements of field specific global riser analysis.

4.2 EDP

The EDP and LRP are situated on top of the XT that is connected to the well. In required situations the EDP shall ensure safe and quick disconnect from the riser so that the rig is free to move. The main function of an EDP is to act as a barrier against the well together with the LRP during workover and intervention operations. The EDP also provides an interface between the LRP, Workover Riser and workover control system [11]. Figure 6 shows a typical EDP:



Figure 6: EDP Subsea1.com [11]

The EDP consists of the following main components:

| Pos. no. | Description | Purpose |
|----------|------------------------------------|--|
| 1 | Valve Block/Wing Blocks | Pressure containing with different valves installed. |
| 2 | Protection Frame | Protect the item during operations in addition to provide a structure for installation of different auxiliary items. |
| 3 | Protection Roof / Working Platform | Protect the item during operation, in addition to provide a working platform for operators topside. |
| 4 | Hydraulic Actuators | Hydraulic opening and closing of valves |
| 5 | Accumulators | Reservoir for pressurized hydraulic fluid required for hydraulic operation of connector and valves. |
| 6 | Flowloop | For routing of well/service/annulus flow |
| 7 | Connector with Stabplate | To connect the Emergency Disconnect Package to the Lower Riser Package |

Table 3: EDP Subsea1.com [11]

4.3 LRP

The main purpose of the LRP is to provide well control during workover and intervention operations. For safe operations the LRP consists typically of minimum two barriers located in the main bore; the isolation valve and the shear seal ram. Both these valves are capable of sealing the well from the environment and able to cut wireline and coiled tubing. The LRP have interfaces with the EDP and XT.

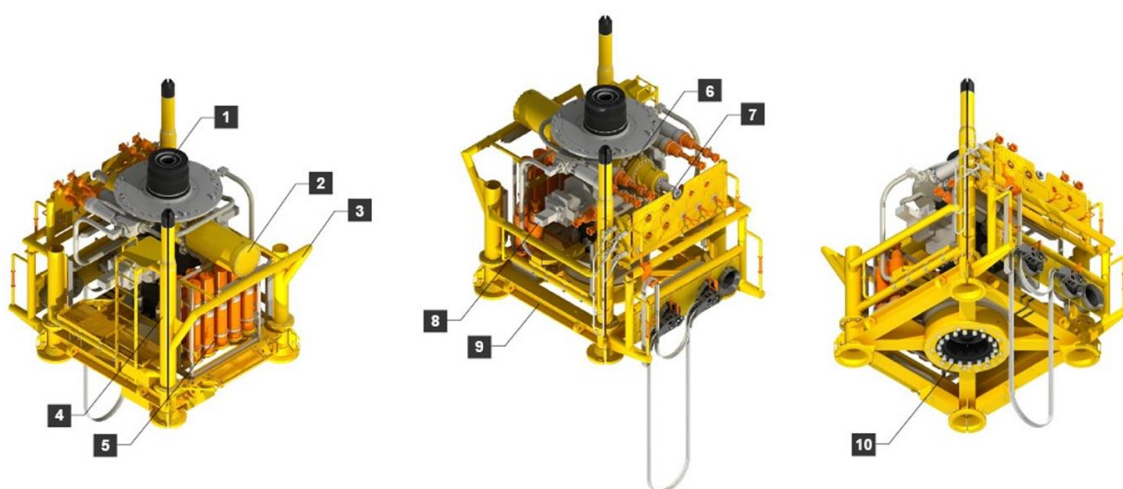


Figure 7: Typical XT from [8]

Main components of the LRP:

| Pos. no. | Description | Purpose |
|----------|--|--|
| 1 | Hub | Hub for Emergency Disconnect Package connector. |
| 2 | Isolation Valve | One of the main barriers against wellflow. |
| 3 | Bumper bar | Protect the Lower Riser Package during operations. |
| 4 | Valve block with wing blocks | Pressure containing with different valves/rams installed. |
| 5 | Accumulators | Reservoir for pressurized hydraulic fluid required for hydraulic operation of connector and valves/rams. |
| 6 | Wing valves actuator with ROV override interface | Hydraulically operated valves with ROV override. |
| 7 | Isolation valve actuator with ROV override interface | Hydraulically operated valve with ROV override. |
| 8 | Shear Seal Ram | Primary barrier against wellflow. |
| 9 | Protection Frame | Protect the item during operations in addition to provide a structure for installation of the different items. |
| 10 | Connector | To connect Lower Riser Package to Xmas Tree. |

Table 4: Subsea1.com [11]

4.4 HAR Connector

The interface connector between the EDP and LRP has several names. Emergency release connector, high angle release connector and Xtreme Release (XR) connector are some of these. Even though the design may differ, they all serve the same purpose. The main purpose of these connectors is to ensure quick and reliable disconnection of the WORS. Conventional technology consisting of male-into-female engagement are known to be unable to separate with high bending loads applied [12]. The Xtreme Release Connector™ from STL releases at 100% bending moment without requirements to axial tension in order of separation. Maximum bending moment prior to leakage is 2020 kNm [13].

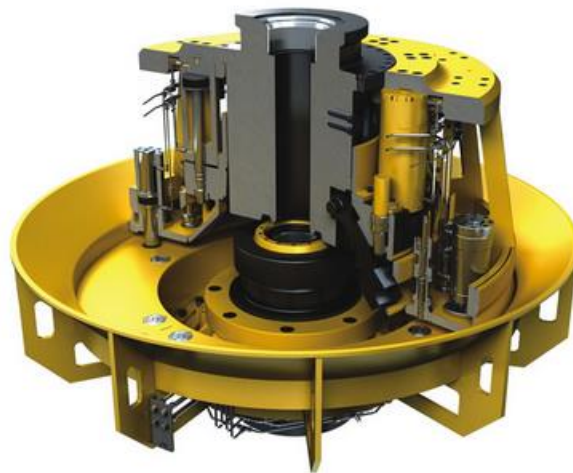


Figure 8: Xtreme Release Connector™ from STL [2]

Figure 8 shows the connector from STL. The connector is based on a face-to-face technology, making it possible to disconnect repeatedly with no angle restrictions. The XR connector is used as basis for the analysis performed in this thesis and is referred to as the HAR connector.

4.5 XT

The main purpose of XT is to isolate the well against the environment and well control during production. It is also providing flow control from and into the well. The XT accommodates injection systems, flow control elements, monitoring systems, downhole control systems and ROV interface panels. The XT is designed to withstand installation, operational and removal loads. This thesis will not consider any forces from the operational loads during intervention. The XT is not considered as a part of the workover system as it is placed stationary on the seabed during production.



Figure 9: GE Oil & Gas XT [14]

Figure 9 shows a production XT from GE Oil & Gas. During production a tree cap is installed on top of the XT as a barrier element against the bore in the tree. During installation and workover, the barrier functions are transferred to the LRP.

4.6 Heave compensating system

The main objective for the heave compensating system (HCS) is to always maintain tension in the riser. Due to the relative small diameter compared to the height, even small a compression of the riser may cause buckling. In an EQD scenario the recoil from the riser can be substantial. It is preferred to limit the overpull prior to disconnecting the well, but in reality there may not be much time to prepare for an emergency disconnect. A 10% safety margin of the physical stroke amplitude is assumed to be sufficient. Additionally a large part of the stroke is designated or lost to tide, setdown and make-up of tolerances. The remaining part of the stroke is left to counterbalance the vessel heave motions.

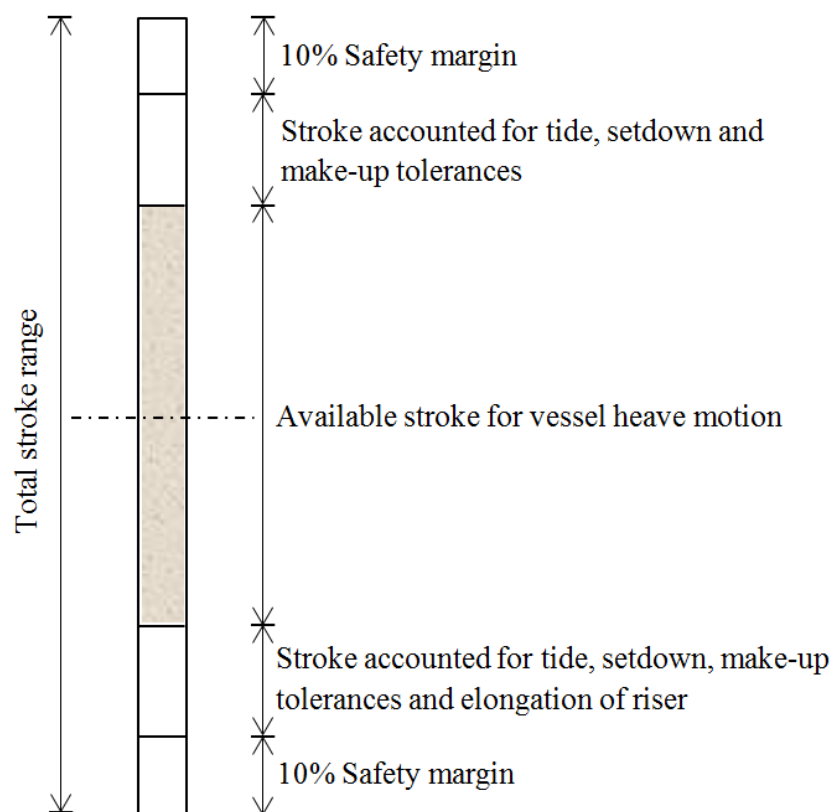


Figure 10: Illustration of heave compensation limits based on API 17G [15]

Figure 10 shows dedicated stroke lengths of a HCS. During this thesis the total stroke range is assumed to be 10 meters. This means that the HCS can travel 5 meters up and down from the center line. If the stroke exceeds 5 meters, a lock-up scenario will occur.

5 Operational conditions

A WORS is subjected to both environmental and operational forces. Execution of an emergency disconnect sequence must be available regardless of environment and operational scenario. Forecasting may allow for preparation prior to effects from environmental loads

5.1 Environmental forces

Intervention performed from a floating vessel is always depending on environmental loads such as wind, wave and current loads. Wind loads acts as an indirect source of load on the riser due to its affection on the waves and vessel. Reliable weather forecasts are critical to ensure a safe operation and reduce the non-productive time. Each vessel has a safe operating criterion depending on these parameters, primarily dependent of wave height.

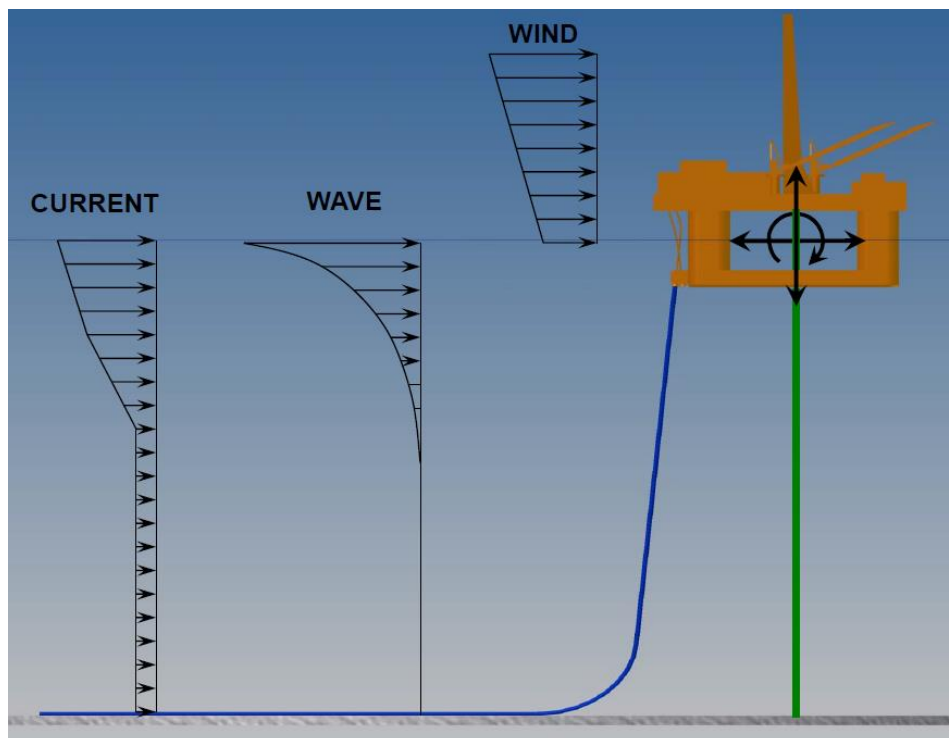


Figure 11: Environmental loads on risers [15]

Figure 11 shows the location of operational loads. Further descriptions are presented in next section.

5.1.1 Waves

Waves can approach the vessel from one or several different directions simultaneously. The waves may also be a combination of wind and swell waves from different directions. Waves have the largest impact on a floating vessel due to the change of buoyancy center and water particle velocity causing drag force. Waves may cause large heave motion to the vessel especially if the wave frequency coincides with the vessels natural frequency. Waves will also contribute to fatigue to the WORS together with the current. Wave forces influences the riser over the whole length.

5.1.2 Current

The current velocity profile is varying from maximum velocity at sea surface to zero at the seabed as shown in Figure 11. The figure shows a conservative current profile which may be used for calculations. The profile between can change depending on the weather and sea state. Currents are typically in the range of 0 to 1.5 m/s and may affect the riser of its entire length. The current profile varies from region to region and may consist of surface currents, deep water currents or a combination of both. Deep water risers are especially subjected to vortex induced vibrations and can hence be subjected to fatigue unless actions are taken. Due to the increased length of the riser, the axial natural frequency is reduced. Also deep water vessels do not have the opportunity to clamp the riser onto a fixed structure from the seabed to surface. The current cause the risers curvature to deflect since an unevenly load is distributed over the risers length.

Vortex induced vibration is a local mode effect that depends on the magnitude of the current. Generally VIV have a great impact on fatigue life on a riser, but due to the limited and periodic usage of WORS this is not considered as a big issue.

5.1.3 Wind

The North Sea experiences extreme wind conditions. In combination with wave loads these will cause significant forces on floating structures setting high requirements to the mooring lines or DP system. Both semi-submersibles and ship-shaped intervention vessels have a large freeboard to be affected by the wind. Wind forces will not be considered in this analysis.

5.1.4 Risk related to environmental forces

A worst case scenario is an unpredicted storm surprising the crew in the middle of an operation. Some operations have extensive rig-down time, causing a demand for reliable and precise weather forecasts. Storms might cause anchor lines to break or overloading of DP system. Weather forecasts are normally reliable and the operation may be stopped while the bad weather passes. The WORS is then released from the stack-up performing a planned EQD.

5.2 Operational forces

To reduce the risk of riser buckling, the vessel exerts a constant tension force to the WORS. The vessel is allowed to heave up and down, even with nearly constant tension. There will be some variation in tension when the vessel is heading upwards and downwards. This occurs due to the damping effect in the HCS. Typical allowable stroke for the heave compensating systems are up to 10 m. Some operators use buoyance elements in deep waters to reduce the required pre tension of the WORS.

5.2.1 Risk

Operating with a constant tension there is always a risk of system failure. One failure mode is heave compensator lock-up. This may subject the riser to enormous tension and/or compression forces. In rough weather a lock-up can cause the riser to snap with little or no warning. To address this risk the industry has introduced a product called a safety joint. This is installed as a part of the riser stack and is manufactured with a weak link to control the point of fracture. Another failure mode is loss of tension. This is less critical than the heave compensator lock-up and will only cause large compression forces to the WORS. A combination of large compression forces and environmental loading can cause the riser to buckle. This is considered as very critical as fatigue is accumulated in a short time period and the riser will fracture at some point in time. This is why there is a safety margin on the tension applied to the WORS, to allow for loss of a tension wire.

6 Mechanical model

To show the basic geometry of the model a sketch is established. It is important to understand the model and define all variables and parameters. Geometric calculations are performed to extract realistic parameters. The calculations are presented in section 8.

6.1 Geometry

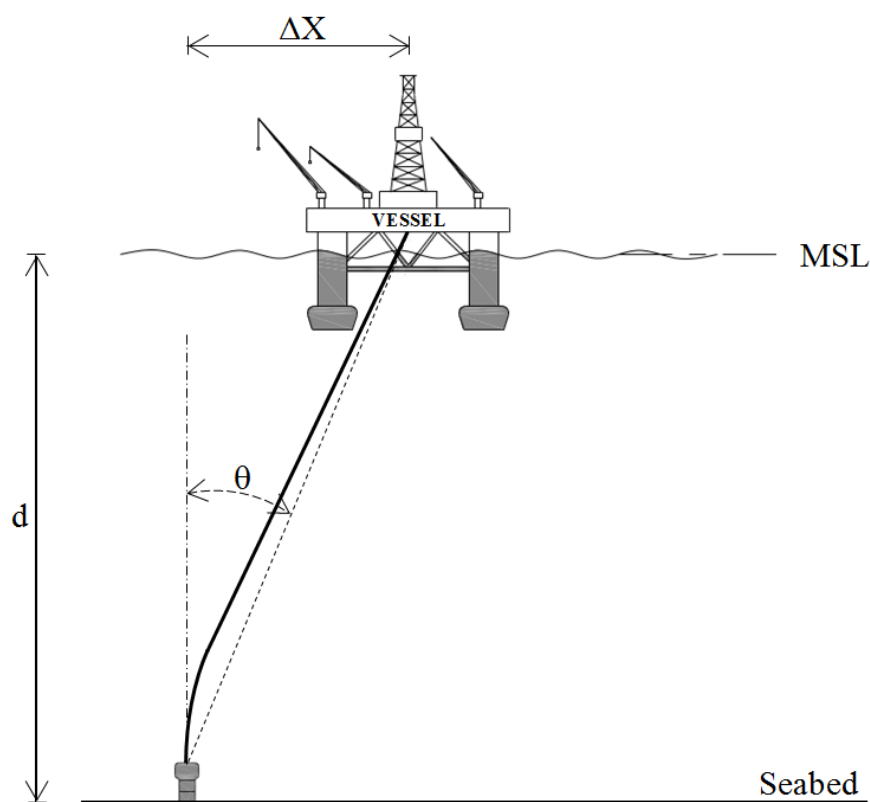


Figure 12: Geometry of established model

Figure 12 shows a simple system containing the stack-up at the seabed, the WOR and the vessel that has deployed the equipment. Initial position is when the center of the vessel is positioned vertically above the stack-up. The water depth, d , is varying from case to case. The angle, θ , describes the rig offset in degrees from initial position. The distance from the original position to the point of disconnect is denoted with ΔX . There are two ways to consider this model, either assume that the tensioners are fixed in X-direction, i.e. infinite rotational stiffness that causes a bending moment or assume that they are free to move. This

thesis will consider the latter. To analyze the EQD, a homogenous 7 inch riser is used in all calculations. The heave compensator system is assumed to have a total stroke length of 10 meters. General data such as sizes and weights of the equipment used are generalized values from GE Oil & Gas.

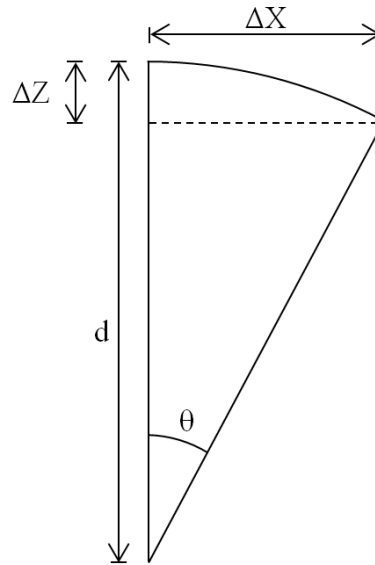


Figure 13: Geometry used for calculations

Figure 13 shows the basic foundation of calculating the limits for vessel offset. The HCS limits the ΔZ in terms of maximum physical available stroke length.

Vessel offset ΔX :

$$\Delta X = d \cdot \sin(\theta) \quad (1)$$

Required stroke length ΔZ :

$$\Delta Z = d - d \cdot \cos(\theta) \quad (2)$$

With the heave compensator stroke limit set to 10 meters, the amplitude is 5 meters from centered position; hence remaining ΔZ is 5 meters.

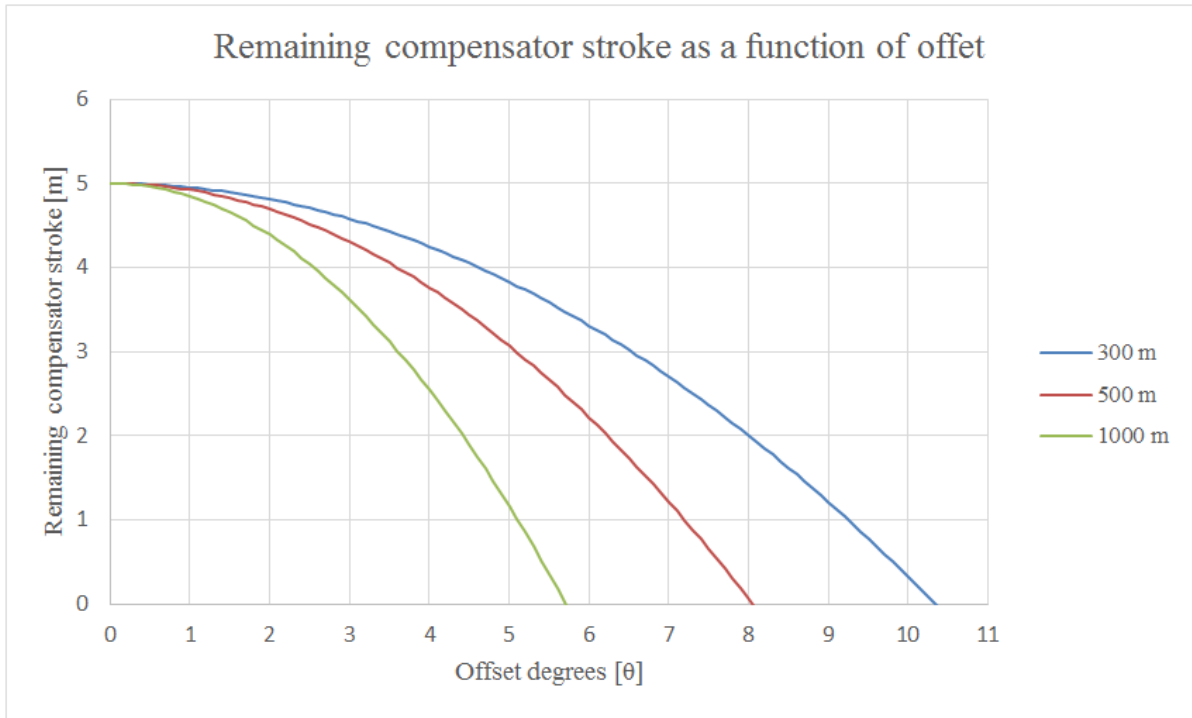


Figure 14: Remaining compensator stroke as a function of offset

Figure 14 shows geometric offset limits given maximum amplitude of 5 meters, thus the vessel cannot gain more offset than the figure shows. However, if the offset exceeds the associated physical stroke amplitude, the HC will stroke out and the tension force will increase rapidly.

| Description | Value | Annotation |
|-----------------------|-------|------------|
| Offset 300 meters WD | 53 | m |
| Offset 500 meters WD | 70 | m |
| Offset 1000 meters WD | 100 | m |

Table 5: Maximum feasible rig offset for different water depths

Table 5 present the geometric offset limits calculated from equation 1 with input from Figure 14.

The stack-up at the seabed will reduce the required length of the riser. The distance from mean sea level to the drill floor at the semi-submersible will add additional length to the riser. Typical distance from mean sea level to the drill floor on a semi-submersible is in the range of

15 – 30 meters. It is assumed that the length from mean sea level to the drill floor is 17 meters. It is also assumed that the initial position of the top end of the riser is placed at this point. The stack-up height is assumed to be 9 meter, i.e. the bottom end of the riser is positioned 9 meters above the seabed. With these assumptions in mind the resulting length of the riser in 300 meters WD is 308 meters.

| Description | Value | Annotation |
|------------------------------|-------|------------|
| Overpull at HAR connector | 15 | Te |
| HC stroke | 10 | m |
| Safety Joint strength | 400 | Te |
| Module of elasticity (Riser) | 210 | Gpa |
| Base material in riser (80K) | 552 | Mpa |
| Sea water density | 1025 | kg/m3 |
| Riser ID | 0,18 | m |
| Riser OD | 0,23 | m |
| Steel density | 7850 | kg/m3 |
| LRP mass | 35 | Te |
| EDP mass | 15 | Te |
| XT mass | 30 | Te |

Table 6: Input data

6.2 Axial stiffness

The systems natural frequency is determined by a static analysis under pure axial displacements. Depending on the length of the riser, cross section and the material properties, the natural frequency will change. The riser can be compared with a spring with a specific stiffness. Interaction between the EDP and water can be compared with the associated damping of the system. The formula presented below assumes a negligible mass of the spring. Since the riser represents a larger part of the total weight of the system than the attached EDP, this equation cannot be used to obtain an accurate result. However, the result will give a rough approximation of the natural frequency.

Natural period:

$$T_n = \frac{2\pi}{\omega_n} \quad (3)$$

Natural frequency:

$$\omega_n = \sqrt{\frac{k}{m}} \quad (4)$$

Spring constant:

$$k = \frac{EA_0}{L_0} \quad (5)$$

Where:

k : Stiffness

A_0 : Initial area

L_0 : Initial length

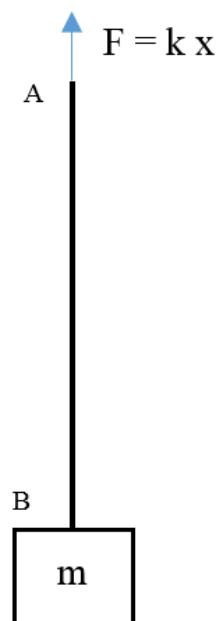


Figure 15: Sketch of the simplified model

As shown in Figure 15 end A represents the top of the riser and end B represents the bottom of the riser. F corresponds to the force that the riser is subjected from the HCS. M correspond to the mass of the EPD.

| Description | Value | Annotation |
|------------------------------|---------|-------------------|
| Module of elasticity (Riser) | 210 000 | Mpa |
| Riser length | 308 | m |
| Riser ID | 0,18 | m |
| Riser OD | 0,23 | m |
| Steel density | 7850 | kg/m ³ |
| M_{EDP} (submerged) | 13 050 | Kg |
| M_{RISER} | 35 941 | Kg |

Table 7: Input data for calculating natural period

Table 7 presents required inputs for calculating the natural period. The natural period can be calculated from equation 3.

| Description | Value | Annotation |
|--------------------------------|--------|----------------|
| A: Cross sectional area riser | 0.0161 | m ² |
| k: Spring constant | 10 977 | kN/m |
| m: $M_{EDP} + M_{RISER}$ | 48 991 | Kg |
| ω_n : Natural frequency | 14.8 | rad/s |
| T_n : Natural period | 0.42 | s |

Table 8: Calculations of axial natural period of riser and EDP

Table 8 shows the natural period for a simplified WORS in 300 meters WD. The axial natural period is calculated to be 0.42 second. Added mass is excluded from this calculation.

| Description | Value | Annotation |
|------------------------|-------|------------|
| T_n : 300 meters WD | 0.42 | s |
| T_n : 500 meters WD | 0.65 | s |
| T_n : 1000 meters WD | 1.23 | s |

Table 9: Axial natural periods for different water depths

Table 9 shows the natural period for the three considered cases. The natural frequency including added mass will be presented in section 6.6.

6.3 Riser strain

To simplify this calculation it is assumed that the internal pressure is zero and the riser is homogenous during the entire length. The submerged mass of a 7 inch WOR is approximately 114 kg/m. This results in a linear varying stress condition, reducing the stress and strain along the riser. Calculations shown in Table 10 are based on equation 6. The riser is divided into sections to include the changing stress. The riser will only operate in elastic area due to the safety joint will release with too high tension force. Main contributor the riser elongation is the weight of the riser. Presented elongation includes the submerged weight of the EDP and 15 Te overpull. Hooke's law is used to calculate the total riser strain [16]:

Hooke's law:

$$\varepsilon = k \cdot \sigma = \frac{1}{E} \cdot \sigma = \frac{\sigma}{E} \quad (6)$$

Strain:
$$\varepsilon = \frac{\Delta L}{L} \quad (7)$$

Force:
$$F = k \Delta L \quad (8)$$

Where:

ε : Relative strain

k: Material constant

E: Module of elasticity

ΔL : Elongation

L: Unit length

Depending on material and geometric properties the riser will have a certain elongation in static equilibrium state. With the data presented in this thesis the structural weight of the riser and EDP is calculated to an elongation of 27 mm. The required force of causing an elongation is found by equation 8.

| Static elongation of riser when connected to EDP excluding overpull | | Static elongation of riser when connected to EDP including 15 Te overpull | |
|---|-----------------|---|-----------------|
| Water depth [m] | Elongation [mm] | Water depth [m] | Elongation [mm] |
| 300 | 27 | 300 | 41 |
| 500 | 62 | 500 | 84 |
| 1000 | 207 | 1000 | 251 |

Table 10: Static elongation of riser due to gravity calculated using Hooke's law

Table 10 presents riser elongation of 300, 500 and 1000 meters WD.

6.4 Required top tension

Required tension consists of submerged weight of the equipment together with an overpull to ensure no form of buckling. Typical steel used in risers are 80KSI low alloy steel. The riser dimensions are approximately corresponding to a 7" workover riser joint from GE Oil & Gas. A steel density of 7850 kg/m^3 is assumed for all steel types addressed in this thesis. To calculate the required tension from the vessel, weight are calculated and combined with Archimedes' law. An immersed body experiences an upthrust equal to the weight of the fluid displaced.

The mass per unit length of the riser is calculated by using equation 9:

$$m_{riser} = \rho \pi \left(\frac{d_o^2 - d_i^2}{4} \right) \quad (9)$$

Buoyancy per unit length is calculated by using equation 10:

$$b_{riser} = \rho_w \pi d_o^2 \quad (10)$$

| Description | Value | Annotation |
|-------------------------------------|---------------|------------|
| m_{riser} : Riser mass | 126.39 | [kg/m] |
| m_{mud}^* : Mud mass | 30.54 | [kg/m] |
| b_{riser} : Riser buoyancy | 42.59 | [kg/m] |
| Submerged weight | 114.34 | [kg/m] |
| *Mud density of SG: 1,2 | | |

Table 11: Riser mass data

With data from Table 7 and Table 11 the total required topside tension on a vessel at 300 meters WD is 64 metric tonnes (Te). Submerged weight of steel structures is approximated to multiply the weight in air with a factor of 0.87. The factor implies that seawater density is 1025kg/m^3 and steel density is 7850kg/m^3 , hence the buoyancy of the equipment is included in this factor. Confined space inside the equipment is neglected in this approximation. The submerged weight of EDP is hereby approximated by this method.

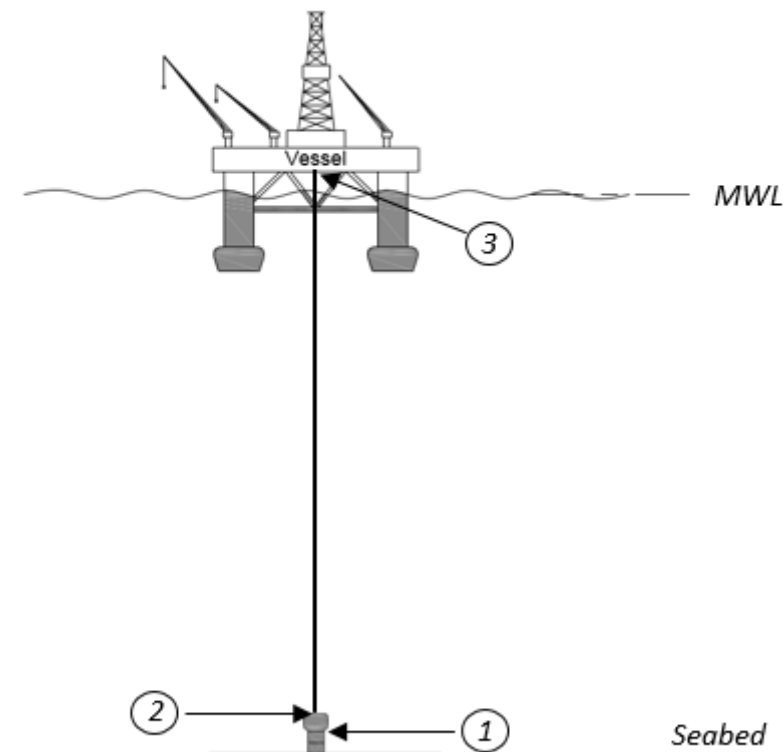


Figure 16: Tension picture

Figure 16 shows the points of interest regarding tension. Point number one represents the tension at the HAR connector between the EDP and LRP. Point number two represents the tension in the bottom part of the riser and number three represents the tension in the upper part of the riser.

| Tension values along the riser | | | | |
|--------------------------------|--------------------------------|---------------|------------------|------------|
| No. | Description | With overpull | Without overpull | Annotation |
| 1 | Tension at HAR connector | 147 | 0 | kN |
| 2 | Tension at lower riser end | 275 | 128 | kN |
| 3 | Top tension at upper riser end | 629 | 481 | kN |

Table 12: Tension values according to Figure 16 with and without 15 Te overpull

Table 12 shows the tension values of the riser system at 300 meters WD. There is a difference of 147.15 kN (15 Te) between the case with and without overpull.

6.5 Bending moment

The connection between the riser and the semi-submersible is assumed to behave as a free hinge. This means that zero bending moment is assumed at the top drive. However, a bending moment will occur if the riser engages contact with the drill floor due to the gained offset. The bending moment located at the lower end of the riser near the stress joint will depend on the bending curvature of the riser and the properties of the material used.

The curvature of the riser will continuously change along with the water depth. The weight of the riser will impose a catenary shape from the top until the fixed connection (HAR connector) will counteract the shape.

$$\left(\frac{1}{R}\right) = \frac{d^2y}{dx^2} = \frac{M_b}{E \cdot I} \quad (11)$$

Equation 11 may be used to determine the curvature of the riser. However this equation is limited to beam with a uniform load and of constant properties. As a stress joint is used at the

lower end of the WOR, the properties are not constant. The curvature will vary along the riser depending on the bending moment at each section.

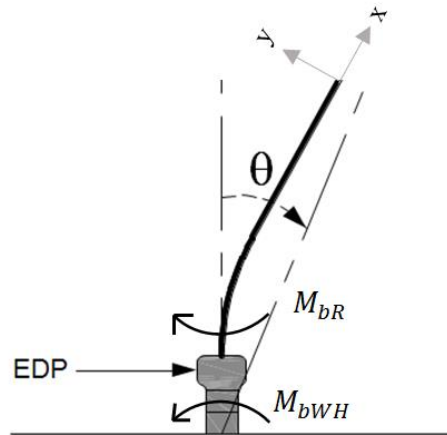


Figure 17: Curvature due to rig offset

Figure 17 shows a principal sketch of the curvature occurring in the lower part of the riser with rig offset. Equation 11 can be used to calculate the curvature in each section of the riser if the bending moment is known.

6.6 Added mass

Only the riser and the EDP will be affected of added mass during disconnect. When current and waves are included, the rest of the stack-up will also have a small contribution. DNV RP-H103 Appendix A states that long circular cylinders in infinite fluid will have added mass per unit length based on the following formula:

$$A_{ij} = \rho_w C_A A_R \quad (12)$$

$$A_{33} = A_{ij} L \quad (13)$$

Where:

A_{ij} : Added mass per unit length

ρ_w : Seawater density

C_A : Added mass coefficient

A_R : Reference area

A_{33} : Added mass

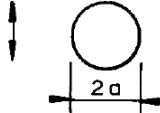
| Section through body | Direction of motion | C_A | A_R | Added mass moment of inertia [(kg/m)*m ²] |
|---|---------------------|-------|-----------|---|
|  | | 1.0 | πa^2 | 0 |

Table 13: Added mass coefficients (RP-H103, 2011)

Using formula 12 and Table 13, the added mass of the riser is calculated to be 42.6 kg/m.

The EDP is approximated to be a perforated square prism shape with 3000 x 3000 x 3000 mm with a hollow cylinder inside, representing well bore access. Added mass in heave for a solid square prism must be found using Table 15.

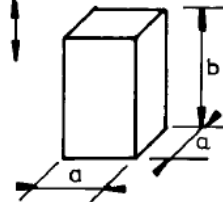
| Square prisms |  | Vertical | b/a | C_A | $a^2 b$ |
|---------------|--|----------|-------|-------|---------|
| | | | 1.0 | 0.68 | |
| 2.0 | 0.36 | | | | |
| 3.0 | 0.24 | | | | |
| 4.0 | 0.19 | | | | |
| 5.0 | 0.15 | | | | |
| 6.0 | 0.13 | | | | |
| 7.0 | 0.11 | | | | |
| 10.0 | 0.08 | | | | |

Table 14: Added mass calculations [17]

The added mass in heave direction for a solid square prism is calculated to 18800 kg. Since the structure is perforated, the actual added mass will be reduced.

DNV RP-H103 is used to estimate the added mass and the effect of perforation. The following equations are obtained directly from the standard.

For perforation rate below 5%:

$$A_{33} = A_{33s} \quad (14)$$

For perforation rate between 5% and 34%:

$$A_{33} = A_{33s} \cdot \left(0.7 + 0.3 \cdot \cos \left[\frac{\pi \cdot (p - 5)}{34} \right] \right) \quad (15)$$

For perforation rate between 34% and 50%:

$$A_{33} = A_{33s} \cdot e^{\frac{10-p}{28}} \quad (16)$$

Where:

A_{33} : Added mass

A_{33s} : Solid added mass

p : Perforation rate (percentage)

Assuming the EDP has a perforating rate of 35% formula 16 is used to estimate the reduction in added mass due to transparency of structure. The resulting added mass in heave direction is 7700 kg.

| Description | Value | Annotation |
|--------------------|--------|------------|
| A_{33} Riser X-Y | 42.6 | Kg/m |
| A_{33s} EDP Z | 18 800 | Kg |
| A_{33} EDP Z | 7 700 | Kg |
| Perforation rate P | 35 | % |

Table 15: Relevant added mass data for EDP and riser

The natural frequency will slightly increase when added mass is affecting the system. The calculations remain the same, except for the change in mass.

$$m_{tot} = m_{EDP} + m_{riser} + m_{added\ mass} \quad (17)$$

Both calculated natural periods including and excluding added mass are presented in Table 16.

| Description | T_n | T_{n_added} | Annotation |
|----------------------|-------|----------------|------------|
| T_n 300 meters WD | 0.42 | 0.45 | s |
| T_n 500 meters WD | 0.65 | 0.69 | s |
| T_n 1000 meters WD | 1.23 | 1.27 | s |

Table 16: Natural periods of defined system with and without added mass

The calculated added mass is considered to be conservative due to the structural shape of the EDP.

6.7 Acceleration

As the top tension is larger than the weight if the WORS, an upwards acceleration will occur with disconnecting the HAR connector. The instantaneous acceleration depends on the magnitude of operational overpull. To prevent stress both to the riser and the HCS, a recoil system is enabled after initial release. However, if the vessels off-set is larger than the physical stroke length, the HCS will stroke out and cause excessive tension. In shallow waters the safety joint can have a typical maximum allowable tension of 4000 kN, which corresponds to 408 Te. This will lead to an elongation of the riser of 574 mm. The large magnitude of tension forces will only appear with high drift-off angles or heave compensator lock-up. With high drift-off angles, the heave compensator stroke will be too short and the situation can be compared to the HCS lock-up scenario. As the stroke of the HCS is no longer available, the increased tension is coming from the increased distance needed from the riser. This creates additional buoyancy of the vessel and results in an upwards tension. Instant acceleration of the EDP after release is calculated from Newton's 2nd law and Figure 18.

$$F = m \cdot a \quad (18)$$

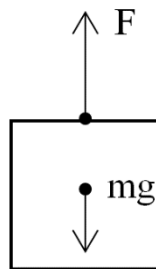


Figure 18: Free body diagram for the EDP

Figure 18 shows the forces the EDP is subjected to. In addition added mass will affect the motion of the EDP the moment the body starts accelerating. The positive force F is equal to the overpull of 15 Te (147.15 kN).

$$a = \frac{F}{m_{EDP} + m_{added}} \quad (19)$$

| EDP acceleration in Z-direction for 300 meters WD | | |
|---|--------|----------------|
| Description | Value | Annotation |
| m: EDP submerged mass + added mass | 20 750 | Kg |
| F_{overpull} : Tension at HAR connector | 147.15 | kN |
| $F_{\text{lock-up}}$: Assumed tension at HAR connector in lock-up | 4 000 | kN |
| $a_{\text{overpull_zero_added_mass}}$: EDP acceleration with 15 Te overpull | 11.28 | m/s^2 |
| $a_{\text{overpull_with_added_mass}}$: EDP acceleration with 15 Te overpull | 7.09 | m/s^2 |
| $a_{\text{lock-up}}$: EDP acceleration in lock-up scenario with m_a | 193 | m/s^2 |

Table 17: EDP acceleration in Z-direction

Table 17 show the accelerations of the EDP with and without added mass. It is considered an overpull of 15 Te at the HAR connector. Lock-up scenario is only included for comparison reasons. Depending on accuracy of added mass values, the EDP will have a theoretical local acceleration between 7.09 and 11.28 m/s^2 .

7 Modelling system in Orcaflex

In order to analyze the model established in chapter 6, Orcaflex is used. Orcaflex is a marine dynamics program developed by Orcina. The program is used for static and dynamic analysis of various offshore systems, such as riser systems, mooring systems, lifting operations and installation and towed systems. The user can analyze custom made systems with different environment settings. When a suitable model is established, the user can extract motions, forces, stresses and moments.

As the objective of this thesis is to analyze the disconnect scenario, a basic semi-submersible model was used from Orcina's webpages with its default size and RAO settings [18]. The response of the semi-submersible is considered as low impact of this thesis, hence the RAO values are not questioned. The riser, EDP, LRP and XT is modelled with data from the industry. However, the used data are not field specific. With a proper base model, Orcaflex is able to simulate the EQD and show the trajectory of the riser and EDP.

A comparison of dynamics of the EDP and riser are made with different water depths. The main case presented involves the WORS in 300 meters WD. For better visualization the cases for 500 and 1000 meters WD are only highlighted with the main differences. Full results for these can be found in the appendices.

Prior to any simulation a static analysis has to be performed. Orcaflex calculates the static equilibrium of the system in a series of iterative stages. The initial positions of the buoys and vessels are defined by the given data. Static equilibrium for each line is then calculated with the ends fixed. Out of balance load acting on each free body is calculated and the new position for the body is estimated. At this point the static elongation of the riser will be included. If there are any constraints that are not defined, the static analysis will not be succeeded.

7.1 Modeling of elements

7.1.1 Riser

Orcaflex does not differentiate between massive steel pipes or chain in respect of initial modelling. Any circular shaped component can be modelled as a line. The user defines material properties, geometric dimensions and connection stiffness prior to running the analysis. Orcaflex uses a finite element model for a line as shown in Figure 19.

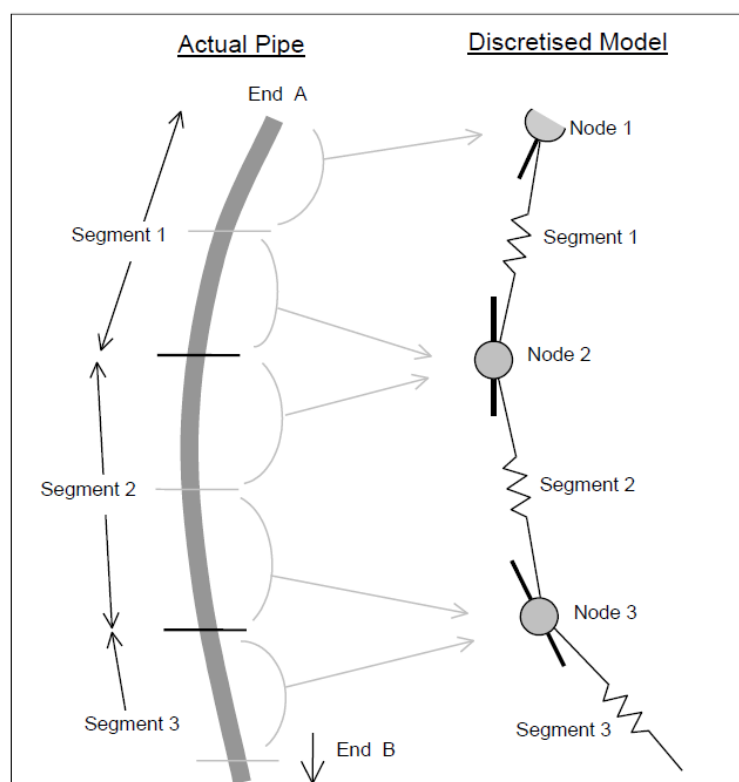


Figure 19: Orcaflex line model

Orcaflex defines the line with a series of segments. Nodes are modelled at the end of each segment. Calculations are only performed at each node and the part in between the nodes is considered massless and straight. This means that a limited number of nodes will give a false curvature. Orcaflex version 9.7a has a limit of 2000 nodes per line. Orcaflex then calculates axial stiffness and bending stiffness which can be manually verified. Internal fluid in the riser is also specified by fluid density.

The riser is divided into 3 main sections with different segment length due to limited node capacity of the program. The ideal riser calculation consists of infinite amount of nodes, but since the available version limits the amount to 2000, the nodes are concentrated at the critical sections. Sections of interest are the upper and lower part of the riser. The node spacing is set to 0.1 meter at the upper and lower part of the riser. The middle part of the riser is set to 1 meter between each node. The stress joint will be modeled with a tapered cross section with uniform internal diameter. This will give a reasonable result of the curvature and bending moments.

When geometries and material properties are defined, Orcaflex runs a static analysis to check the suitability. It is important to consider the elongation in order to get proper results. To be able to trust Orcaflex, hand calculation is performed for comparison. The simplest method of verifying the results is to compare the tension forces. When modelling the riser as a line, Orcaflex has a default setting of defining this as catenary method followed by a full static calculation. Orcina states that this is often a good choice to give good initial estimate of the equilibrium position.

The riser is modelled as a homogenous pipe with constant diameter. The annulus bore is neglected as it does not contribute much to the bending stiffness or drag force and does not affect the tensile stresses in the riser. The stress joint is modelled with constant internal diameter corresponding to the riser joints. Outer diameter of the stress joint equals the riser joint at the top end, and expands to 0.5 meter at the bottom end. To make a proper connection between the EDP and LRP a massive steel joint was used to simulate the HAR connector. This means that the connector adds 0.155 Te to the submerged system.

7.1.2 Stack-up

The EDP is modelled and approximated by a 6D buoy. As the name suggests the 6D buoy is treated as a rigid body with 6 degrees of freedom, 3 translational and 3 rotational. The 6D buoy behaves like a cylinder shaped model of a length equivalent to the specified buoy height. A limitation of the 6D lumped buoy is that it is not suitable to represent a surface-piercing model. This is not a problem as the buoy is fully submerged in this project. The equation of

motion for the 6D buoy consists of weight, buoyancy, hydrodynamic loads, hydrodynamic damping and hydrodynamic moments. The weight is calculated as $m \cdot g$ and is applied at the center of the mass. The buoyancy is calculated $\rho \cdot g \cdot V_{\text{wet}}$ and works vertically upwards from the center of the wetted volume. The volume is specified in Orcaflex and is calculated by hand using the submerged coefficient of 0.87 as explained earlier.

Hydrodynamic loads are calculated by Orcaflex using the fluid kinematics at the center of the wetted volume (V_{wet}). All the following equations are extracted from Orcina's webpage [19]. The buoy translational inertia for each local axis direction is calculated by:

$$\text{Added mass} = P_w \cdot C_a \cdot \text{HydroMass} \quad (20)$$

Where:

P_w : Proportion wet = H_{wet}/H

C_a : Added mass coefficient for translations in that direction.

HydroMass: Reference hydrodynamic mass

The buoy rotational inertia for each local axis direction is calculated by:

$$\text{Added mass} = P_w \cdot C_a \cdot \text{HydroInertia} \quad (21)$$

Where:

C_a : Added mass coefficient for rotations about that direction.

HydroInertia: Reference hydrodynamic inertia

The fluid inertia force applied in each local axis direction is calculated by:

$$\text{Force} = P_w \cdot C_m \cdot \text{HydroMass} \cdot A \quad (22)$$

Where:

HydroMass: Reference hydrodynamic mass

C_m : Mass coefficient in that direction

A : Local water particle acceleration relative to earth in that direction

Damping force applied in each local direction is given by:

$$F_x = -P_w \cdot UDF_x \cdot V_x \quad (23)$$

$$F_y = -P_w \cdot UDF_y \cdot V_y \quad (24)$$

$$F_z = -P_w \cdot UDF_z \cdot V_z \quad (25)$$

Where:

UDF : Unit Damping Force in given direction specified in buoy data

V : Buoy velocity relative to water velocity

Damping moment applied about each local axis direction is given by:

$$M_x = -P_w \cdot UDM_x \cdot \omega_x \quad (26)$$

$$M_y = -P_w \cdot UDM_y \cdot \omega_y \quad (27)$$

$$M_z = -P_w \cdot UDM_z \cdot \omega_z \quad (28)$$

Where:

UDM : Unit Damping Moment in given direction specified in buoy data

ω : Angular velocity of the buoy

The drag force applied in each direction is given by:

$$F_x = -P_w \cdot \frac{1}{2} \cdot \rho_w \cdot C_{dx} \cdot A_x \cdot V_x \cdot |V| \quad (29)$$

$$F_y = -P_w \cdot \frac{1}{2} \cdot \rho_w \cdot C_{dy} \cdot A_y \cdot V_y \cdot |V| \quad (30)$$

$$F_z = -P_w \cdot \frac{1}{2} \cdot \rho_w \cdot C_{dz} \cdot A_z \cdot V_z \cdot |V| \quad (31)$$

Where:

A : Drag area specified in buoy data

The drag moment applied about each local axis direction is given by:

$$M_x = -P_w \cdot \frac{1}{2} \cdot \rho_w \cdot C_{d_x} \cdot AM_x \cdot \omega_x \cdot |\omega| \quad (32)$$

$$M_y = -P_w \cdot \frac{1}{2} \cdot \rho_w \cdot C_{d_y} \cdot AM_y \cdot \omega_y \cdot |\omega| \quad (33)$$

$$M_z = -P_w \cdot \frac{1}{2} \cdot \rho_w \cdot C_{d_z} \cdot AM_z \cdot \omega_z \cdot |\omega| \quad (34)$$

Where:

AM: Moment of area specified in buoy data

Only heights of the LRP and XT are considered in this analysis. The horizontal deflection of the stack-up is assumed to be zero. This will be a conservative consideration as the relative angle of attack decreases when the stack-up is deflecting. Hence the bending moment will also be reduced at the HAR connector.

To achieve the proper model set-up in Orcaflex, the HAR connector between the EDP and LRP has to be a stiff line with only 2 nodes to handle the bending moment. A solid steel pipe with outer diameter of 0.5 meter and length of 0.1 meter is used.

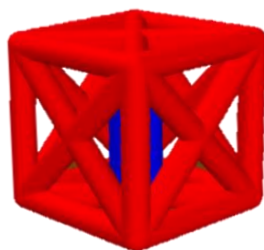


Figure 20: Approximated model of EDP in Orcaflex

Figure 20 shows the modelled EDP in Orcaflex. The trapped cylinder inside and the diagonal frame structure serves only visual effects. Added mass and drag forces are defined by the input coefficients in Orcaflex. The actual coefficients used are presented in Table 18 and Table 19.

7.1.3 Heave compensating system

The model in Orcaflex is based on a simple heave compensated work-over riser system. The heave compensating system is simplified using links in Orcaflex. The user can choose between simple spring or combined spring and damper connection linking two points or objects in the model. The spring-damper shown in Figure 21 is used to simulate the heave compensating system. In this thesis the links are used to connect the semi-submersible to the WORS. The links have no mass and are defined by tension force per unit length. The damping is defined by force per unit velocity. As the main objective for the spring is to represent the top tension and not a correct recoil motion, the link is considered as acceptable.

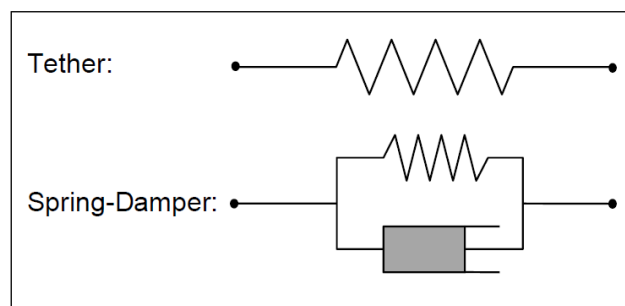


Figure 21: Simple spring and combined spring-damper

Four tensioners are used to connect the riser to the semi-submersible. A tensioner ring is used as an interface between the riser and tensioner link. The tensioner ring is configured as a negligible 6D buoy, i.e. it has no mass and volume. The tensioner links are connected to the semi-submersible at the upper end. There is no connection stiffness affecting the links, causing freedom in all direction for the upper end of the riser. The tension values of the links are set equal to the mass of the attached equipment times gravity plus overpull. To achieve the correct tension values, the angle between the riser and tension links has to be included by simple geometry calculations.

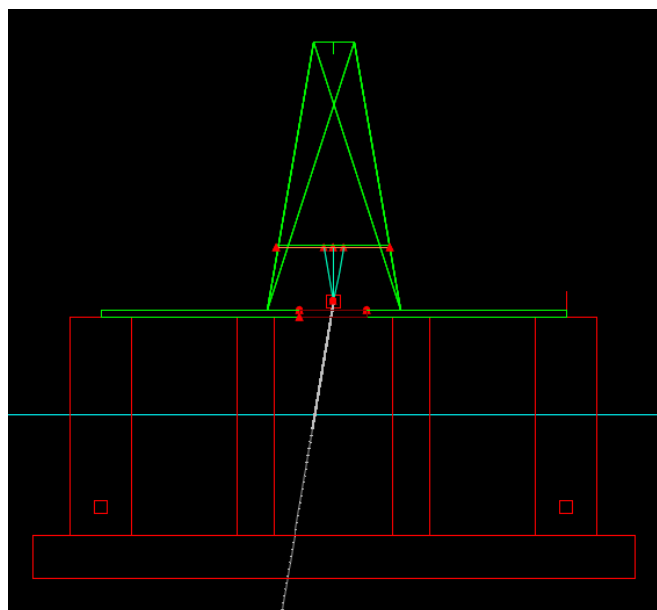


Figure 22: HSC prior static analysis

Figure 22 shows the tensioner lines connected to the semi-submersible. Each line is 8 meters prior to the static analysis.

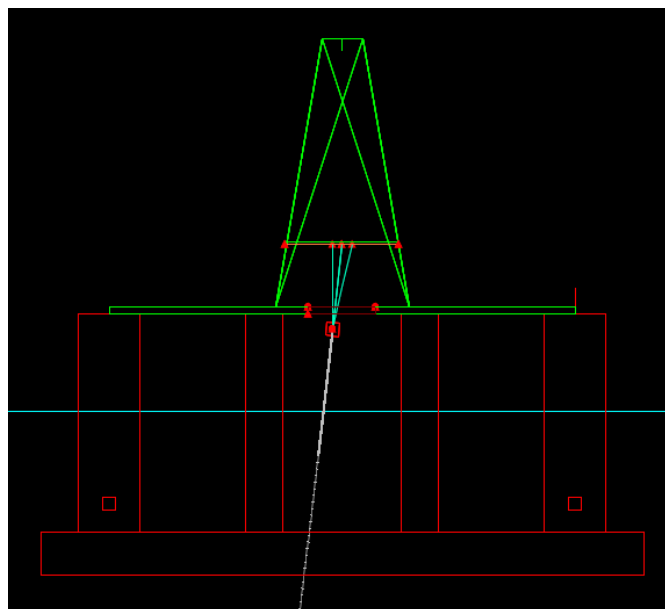


Figure 23: HSC post static analysis

Figure 23 shows the tensioners connected to the semi-submersible post static analysis. Each line is approximately 13 meters post static analysis. The 5 meters difference prior and post the static analysis, corresponds to the remaining compensator stroke length discussed earlier.

7.2 Selection of input data

Unless the boundary conditions and input parameters are correct, Orcaflex cannot give reasonable results. The coefficients for both EDP and riser were generalized from previous performed riser analysis in GE Oil and Gas.

| Input data EDP | | |
|--------------------------------|--------|----------------------------|
| Description | Values | Annotation |
| Drag coefficient C_d | 2.0 | - |
| Inertia coefficient C_m | 2.5 | - |
| Added mass coefficient C_a | 1.5 | - |
| Moment of inertia I_{xx} EDP | 20.7 | $\text{Te}\cdot\text{m}^2$ |
| Moment of inertia I_{yy} EDP | 20.7 | $\text{Te}\cdot\text{m}^2$ |
| Moment of inertia I_{zz} EDP | 12.7 | $\text{Te}\cdot\text{m}^2$ |

Table 18: Orcaflex EDP coefficients and moment of inertia

The moments of inertia were obtained from GeniE. The EDP was modelled as a cubed shell with a trapped hollow cylinder. The cubed shell was assumed to represent 30% of the mass and the cylinder to represent the remaining 70%. The shell was calculated to a wall thickness of 13.7 mm. The cylinder was assumed to have an external diameter of 1 meter and an internal diameter of 0.43. The cylinder represents a gathered mass of all the components inside the EDP.

| Input data riser | | |
|------------------------------|--------|------------|
| Description | Values | Annotation |
| Drag coefficient C_d | 0.7 | - |
| Inertia coefficient C_m | 2.0 | - |
| Added mass coefficient C_a | 1.0 | - |

Table 19: Orcaflex riser coefficients

Table 19 presents the chosen riser coefficients. Depending on surface roughness of the riser, the drag coefficient of a slender circular cylinder is between 0.65 and 1.05 for high Reynolds number [17]. The coefficients could have been manually calculated or established in a CFD

analysis. There would still be many uncertainties involved, hence using industrial common practice is considered acceptable for this thesis. As the velocities of the EDP and riser are considered small and occurring over a small time interval, the coefficients are not considered critical to this thesis. A sensitivity analysis is performed in section 8.4 to verify this statement. Moments of inertia are not applicable in this thesis due to zero rotational motion of the riser.

8 Verification of model

To be able to compare the manually calculated results in section 6 with Orcaflex, a simplified model was established. The simplified model only consists of the riser and EDP. This analysis was performed to confirm that the input parameters to Orcaflex were correct to gain confidence in the program. The riser was configured with given geometric dimensions and material properties and checked against the theoretical elongation due to mass of riser and EDP. The simplified analysis was performed with water depths of 300 and 1000 meters.

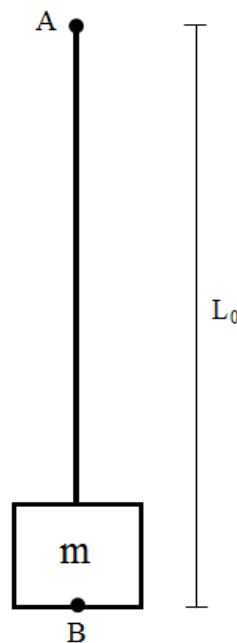


Figure 24: Sketch of simplified model in Orcaflex

Figure 24 illustrates the simplified model in Orcaflex. End A is fixed in all degrees of freedom. End B is initially fixed in all degrees of freedom. L_0 represents the static determined length of the riser and EDP, including the elongation of 27 mm. When these conditions are set in Orcaflex, the riser is configured to a smaller length than L_0 causing tension. After setting a length corresponding to the weight of the structures and overpull, point B is released. This will cause an oscillation at end B.

A 308 meters long riser was modelled and subjected to an axial force corresponding an overpull of 15 Te. This was achieved by stretching the riser as explained above. With the

given riser properties an elongation of 14 mm equals a pretension of 15 Te. This means that the total riser elongation is 41 mm including overpull and associated mass.

8.1 Natural frequency

The oscillations showing in Figure 25 are caused by 15 Te overpull and sudden release.

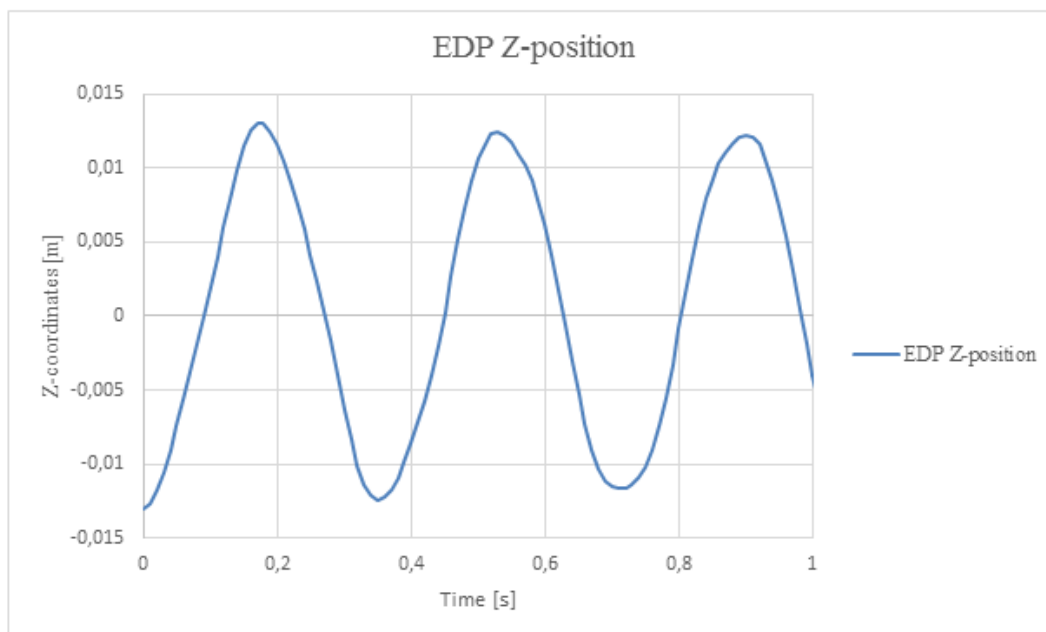


Figure 25: Forced oscillations of EDP from Orcaflex - Simplified model

The figure shows that the natural period for the simplified system is approximately 0.35 seconds. The manually calculated natural period of 0.42 second is considered as acceptable compared to the result from Orcaflex of 0.35 second. The same simplified setup in 1000 meters WD resulted in a natural period of approximately 0.97 seconds. More details regarding simplified analysis in 1000 meters WD can be found in Appendix A.

The damping observed in Orcaflex is caused by the water particles moving around the structure. Orcaflex does not account for different structural shapes, but combines the affected area and corresponding coefficients. As the motion amplitude in Z-direction is small, the associated damping is also small. The damping is considered negligible after a couple of minutes after releasing the lower end of the riser.

8.2 Tension

The tension values obtained in Orcaflex are checked towards the manually calculated values presented in Table 12 presented at page 33.

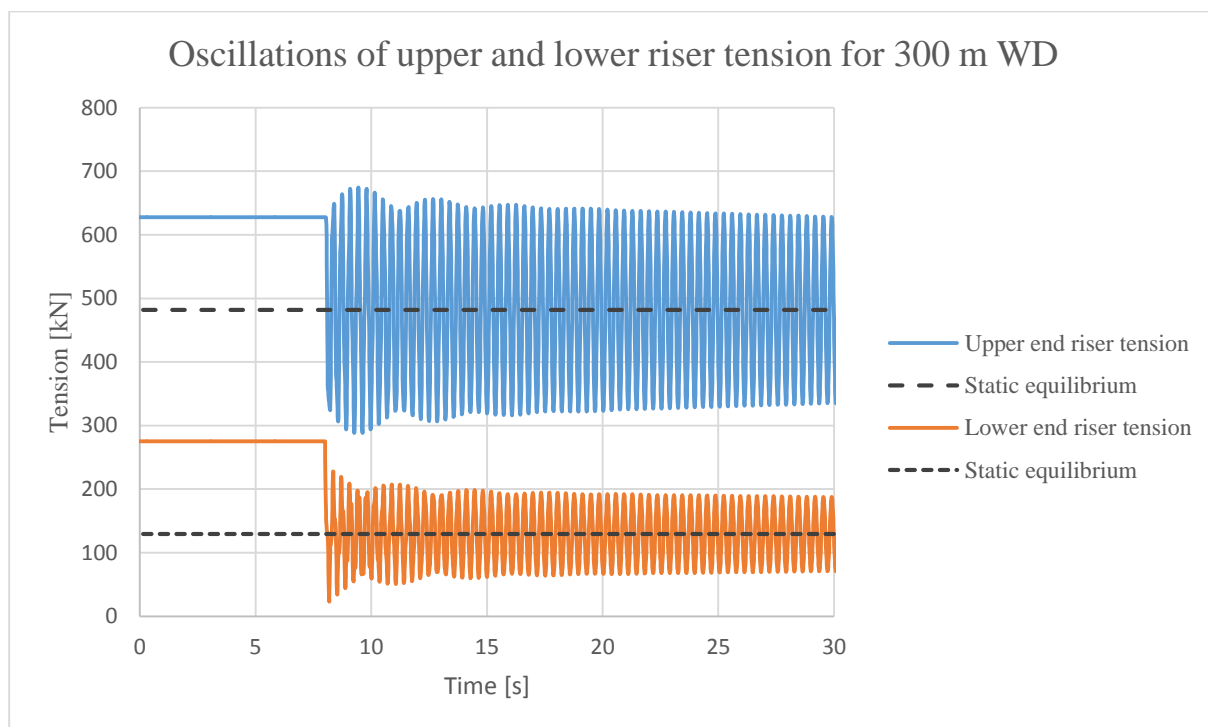


Figure 26: Tension results from Orcaflex – Simplified model

Figure 26 shows the tension in the riser prior and after releasing the EDP connector. The dotted lines show the manually calculated tension for the upper and lower ends of the riser. The EDP was released at $t = 8$ seconds.

The figure shows several modes of response. The observed response modes are caused by a complex dynamic response of the riser. As the riser represents a large part of the total weight, interaction between the mass elements in the riser causes a complex response picture. The tension oscillates with a period equal to the natural period of the riser and EDP in Z-direction. This means that the physical motion of the connected EDP oscillates with ± 13 mm (refer +

8.3 Acceleration

Theoretical accelerations of the EDP are presented in Table 17 at page 38. Verification of the model is partially performed by comparing these values.

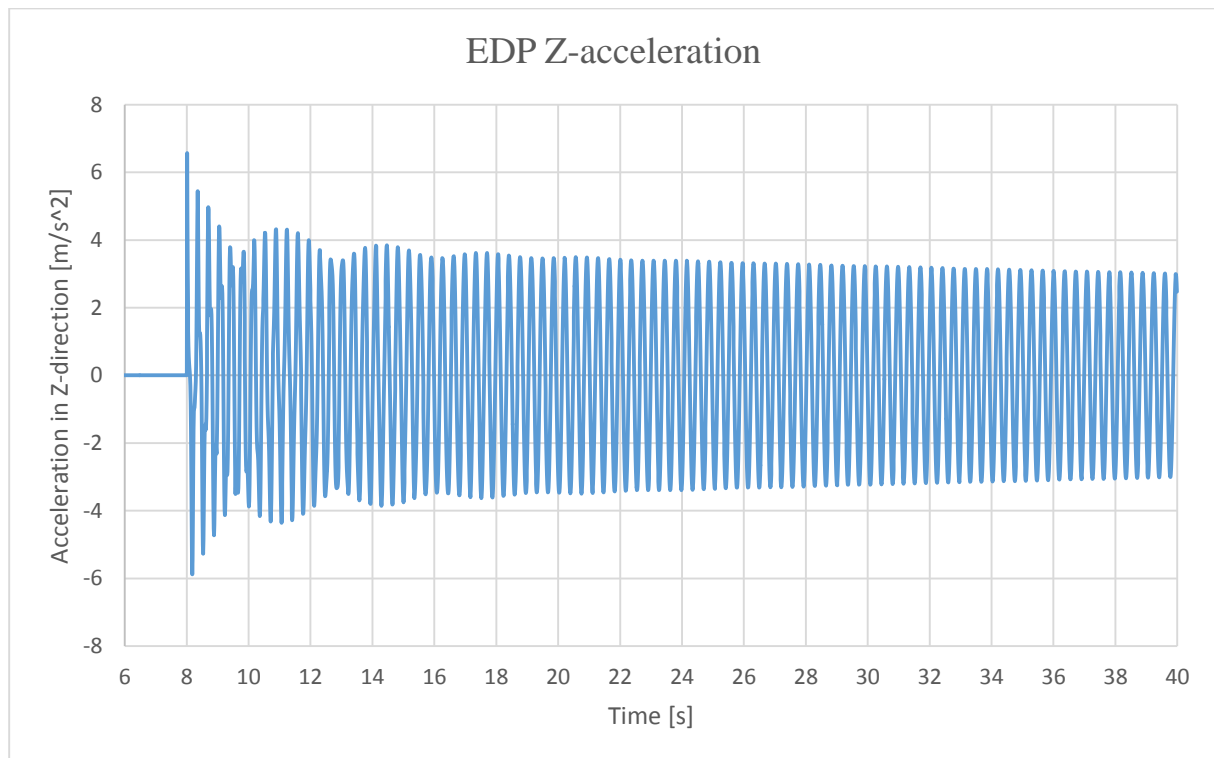


Figure 27: EDP Z-acceleration from Orcaflex - Simplified model 300 meters

As seen in Figure 27 the HAR connector releases at $t = 8$ seconds in the analysis. A complex acceleration picture is presented from Orcaflex. The acceleration oscillates with the same period earlier presented. The previous presented manual calculations of accelerations fit the initial acceleration well. Depending on added mass, calculations resulted in accelerations between 7.1 and 11.3 m/s^2 . The initial acceleration from Orcaflex is approximately 6.5 m/s^2 . The acceleration from Orcaflex is smaller than the theoretical acceleration. This indicates that the manually calculated added mass is too small compared to the calculation in Orcaflex. .

8.4 Selection of time step and key coefficients

8.4.1 Time step

Depending on required accuracy, different time steps can be determined in Orcaflex. An optimum time step gives short analysis time and accurate results. Several experiments have to be performed to identify the optimum time step. EDP acceleration in Z-direction was affected significantly by the time step due to the low natural period in the system.

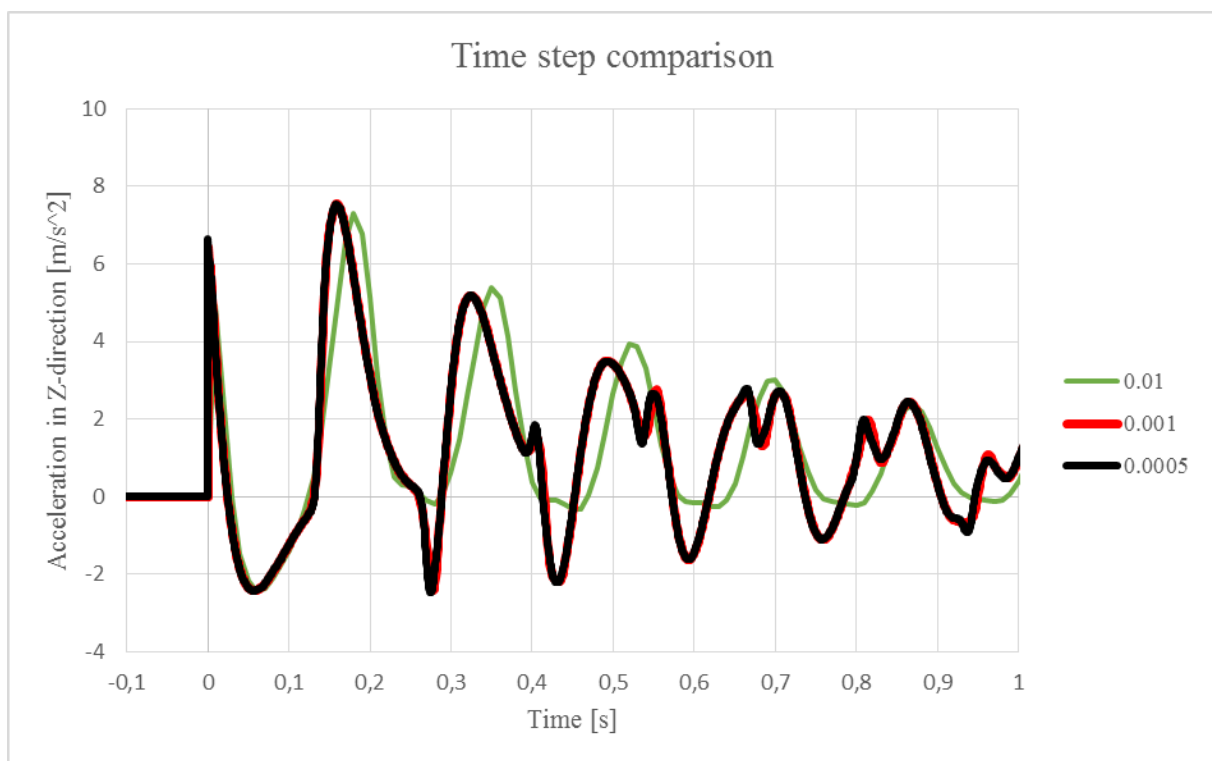


Figure 28: Impact of time step in Orcaflex. Figure shows EDP acceleration from EQD with waves and current and serves only illustrative sensitivity purposes.

Figure 28 shows deviations between the different time steps. Larger time steps are not considered as reasonable. A time step of 0.001 second is considered to give sufficient accurate results with reasonable simulation time. The results converge against the time step of 0.0005 second. The figure shows little deviation between 0.001 and 0.0005 second time step.

8.4.2 Coefficients

The used coefficients are based on common practice in the industry. A sensitivity analysis is performed to evaluate the impact of the results from Orcaflex. Extreme drag coefficients are also included to show the impact of EDP trajectory and are not considered to be realistic.

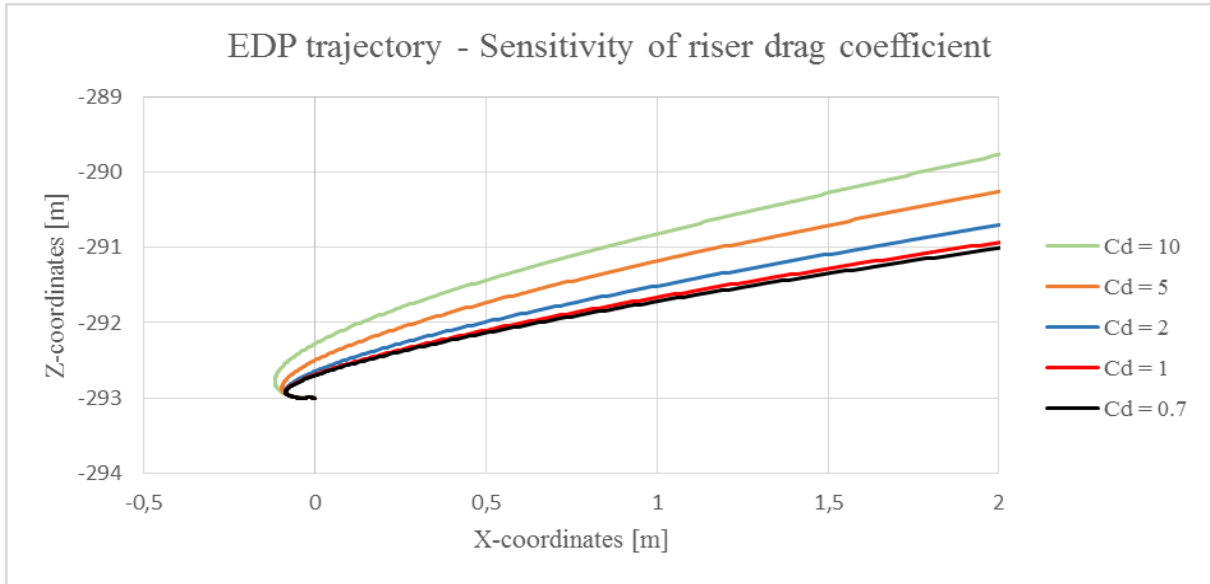


Figure 29: EDP trajectory - Sensitivity of riser drag coefficient

Figure 29 show that the difference between a drag coefficient of 0.7 and 1.0 influences the trajectory of the EDP minimal.

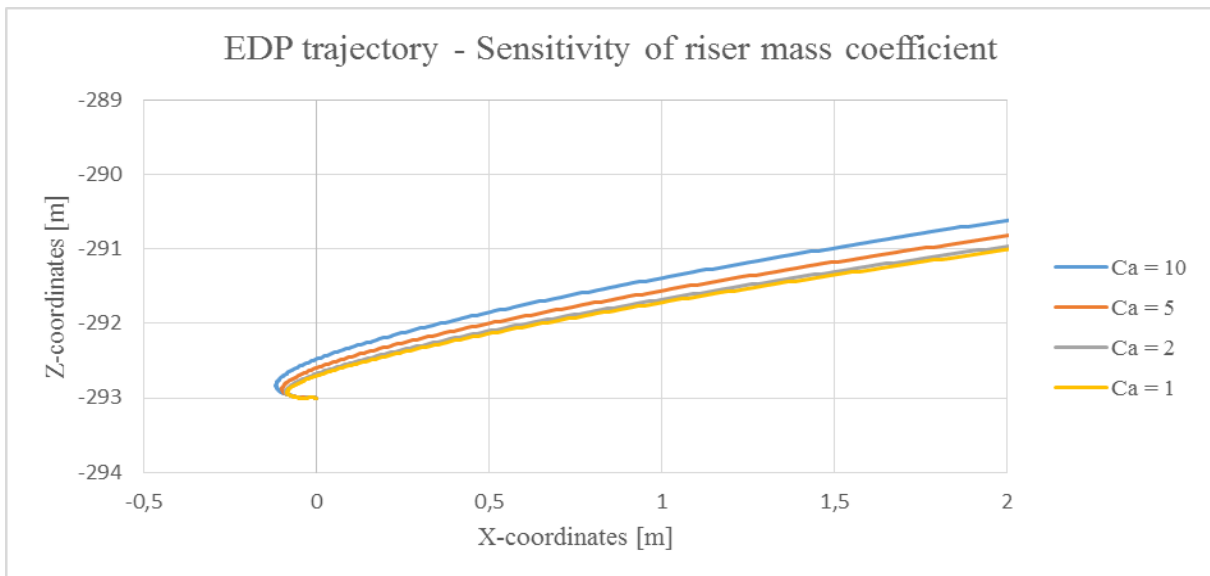


Figure 30: EDP trajectory - Sensitivity of riser added mass coefficient

Figure 30 shows similar trend as presented in Figure 29. The difference in EDP trajectory is even smaller for different added mass coefficients. This means that the choice of both drag and added mass coefficients are not critical to this part of the thesis.

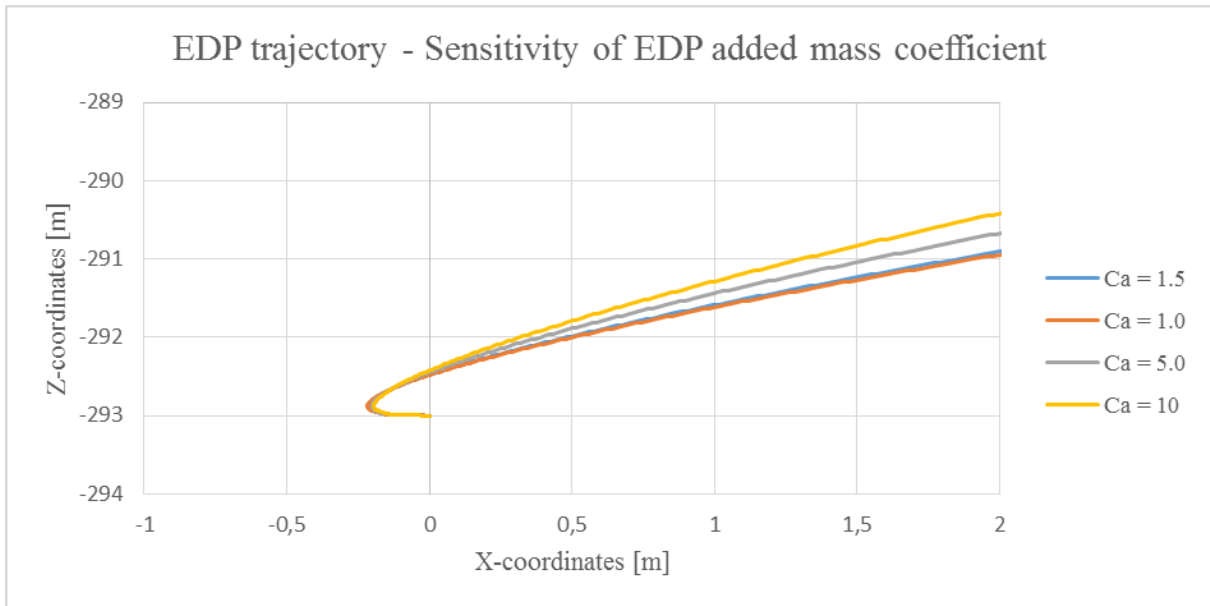


Figure 31: EDP trajectory - Sensitivity of EDP added mass coefficients

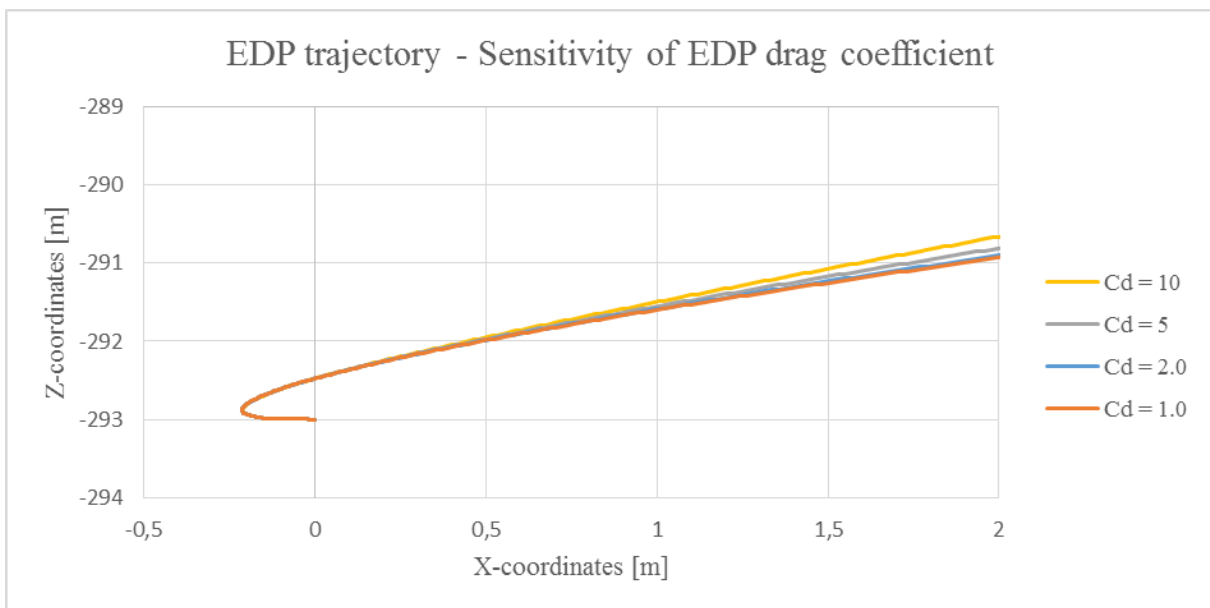


Figure 32: EDP trajectory - Sensitivity of EDP drag coefficient

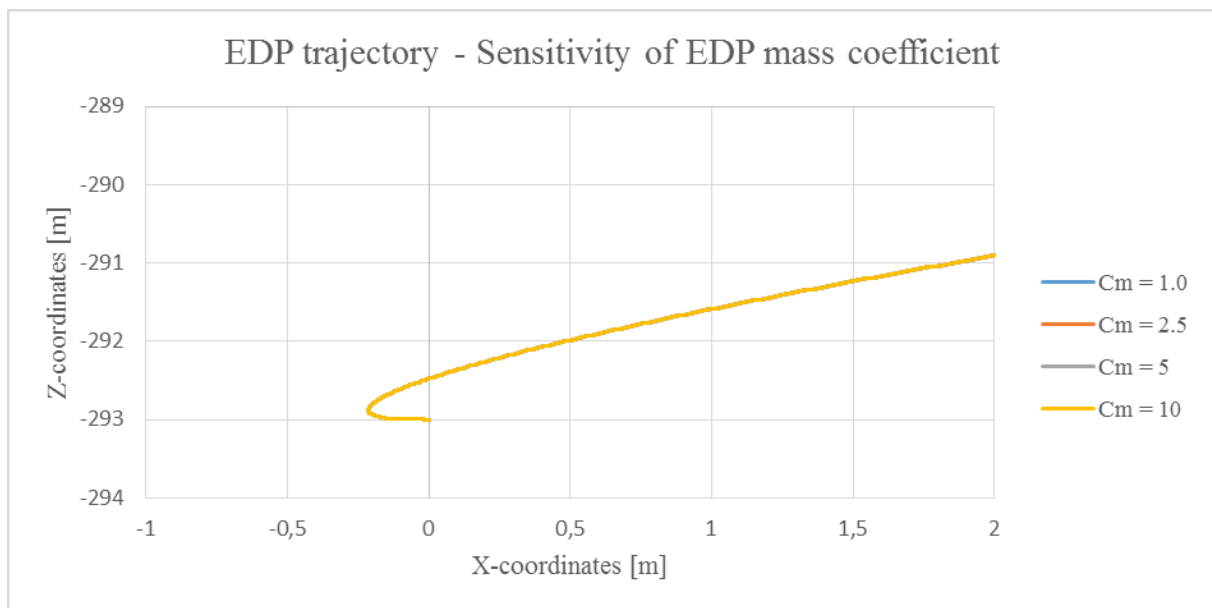


Figure 33: EDP trajectory - Sensitivity of EDP mass coefficient

Figure 31, Figure 32 and Figure 33 show minor difference of trajectory with use of realistic coefficients. The trajectory of the EDP observed in Figure 33 is similar for all coefficients. This is because Orcaflex considers the water particle acceleration relative to earth in this calculation. As the model in Orcaflex does not contain any waves or current, the trajectory of the EDP will not be affected.

9 Results from EQD

To clarify the motions due to riser properties and effect of water damping the EQD is first simulated with no environmental forces. Results for 300 meters WD are fully presented below. The results from 500 and 1000 meters are fully presented in the appendices. For 300 meters WD the semi-submersible is modelled with a static offset of 10° in Orcaflex. As for 500 and 1000 meters WD, the offset of the semi-submersible is modelled according to Figure 14: Remaining compensator stroke as a function of offset. Only the main conclusions from these scenarios will be discussed. As the recoil system is not fully developed in this thesis, the first 5 seconds after disconnect are the primary time interval of interest.

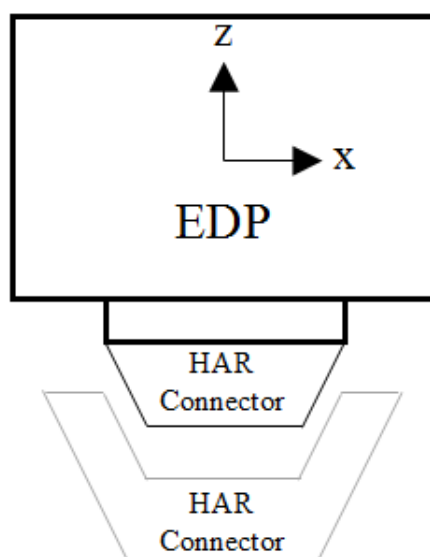


Figure 34: Configuration of EDP and HAR connector with coordinate system

Figure 34 gives an overview of the EDP and the HAR connector. The coordinate system is set to the center of the EDP, as shown in the figure. When addressing motions and positions of the EDP, all values are extracted from the center of the EDP unless otherwise specified.



Figure 35: GE Oil & Gas HAR connector (Not to scale) [20]

Figure 35 shows the HAR connector assembly provided by GE Oil and Gas and STL. The actual connector is positioned in the middle of the structure. The surrounding steel joints are the guiding structure. Analyzing the geometry of the HAR connector compared with the trajectory of the EDP during disconnect will give the opportunity to estimate the impact load to the guide base structure. Due to confidentiality the geometry of the connector will not be presented, but the results can easily be used to establish the points of potential impact.

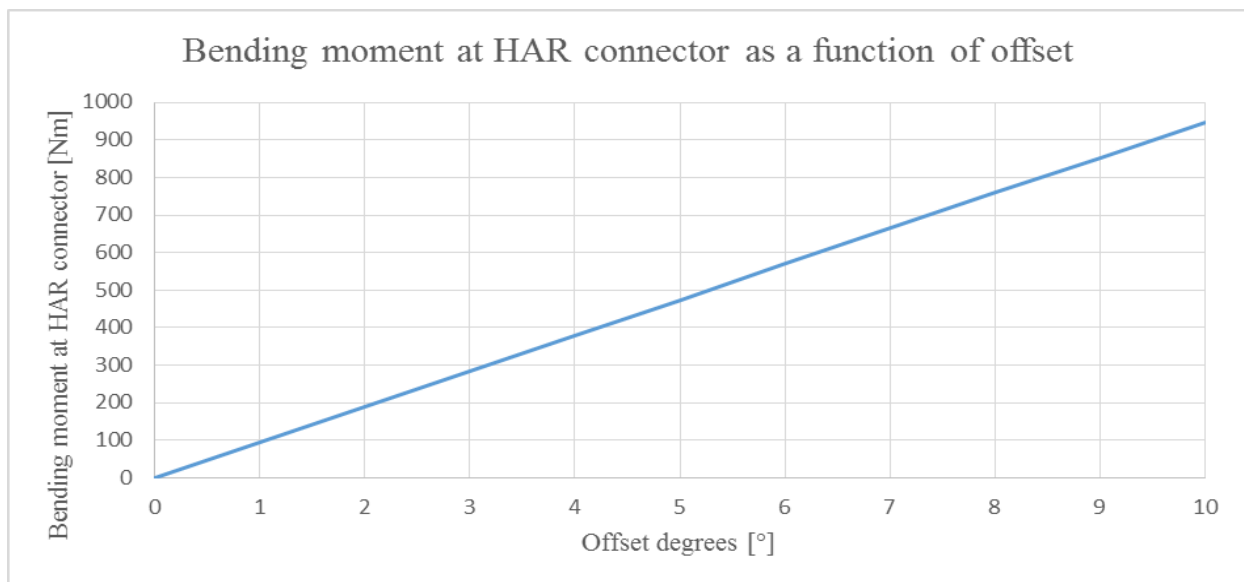


Figure 36: Bending moment at 300 meters WD as a function of offset

The bending moment shown in Figure 36 is statically determined by simulations in Orcaflex. Maximum bending moment subjected to the HAR connector is approximately 950 kNm.

9.1 EQD with no environmental forces

This section of the analysis excludes both waves and current to clarify the motions. 300 meters WD is considered representative for the NCS and is therefore used as main example.

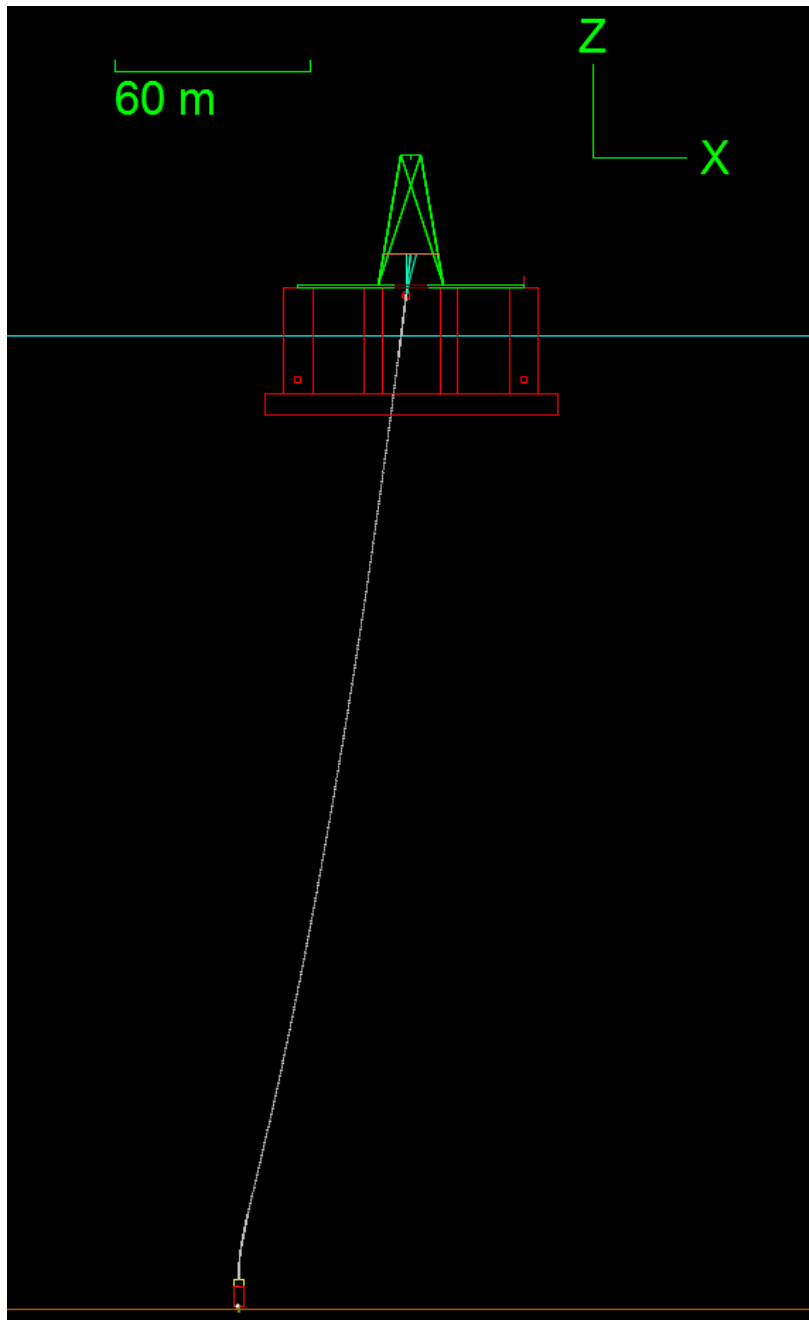


Figure 37: Global set-up in Orcaflex with 300 meters WD and 10° offset

Figure 37 shows the established model in Orcaflex at 300 meters WD with 10° offset and 15 Te overpull.

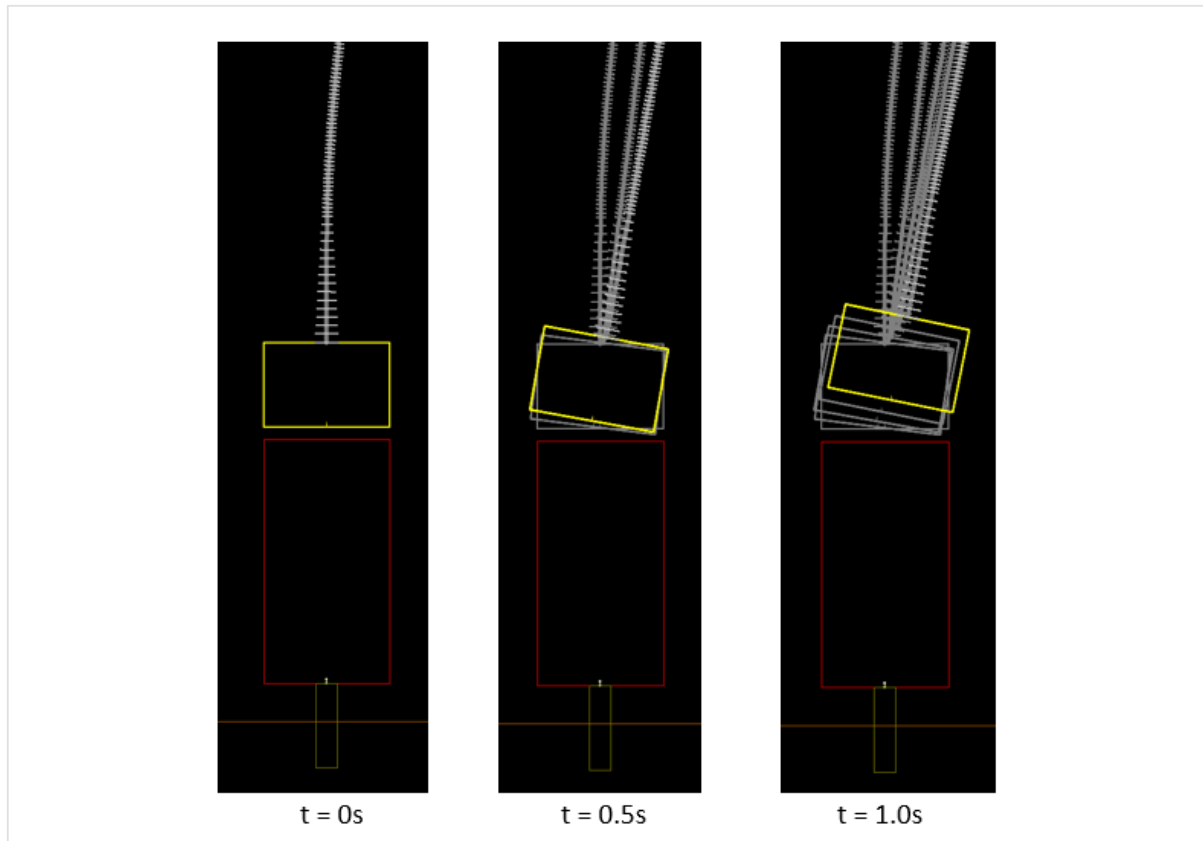


Figure 38: Initial motions of the EDP after EQD

The HAR connector is released at $t = 0$. Figure 38 shows an initial rotation of the EDP to straighten the curvature of the riser and hence reducing the bending moment in the riser.

The accelerations and velocities are separated by X and Z-direction to clarify the forces subjected to the EDP. The results presented are limited to the first 5 seconds post EQD. Main observations are indicated below each figure. The results are discussed in section 11.

EDP acceleration and velocity in Z-direction:

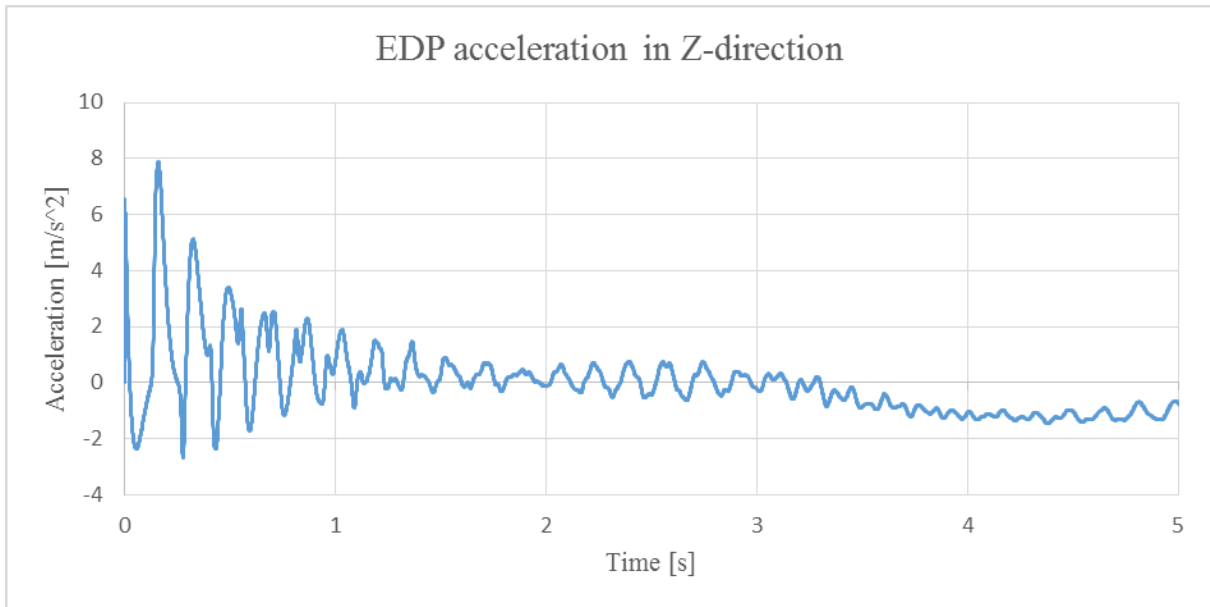


Figure 39: EDP acceleration in Z-direction in 300 meters WD

The period in Figure 39 is 0.18 second and maximum acceleration in Z-direction is 7.9 m/s^2 .

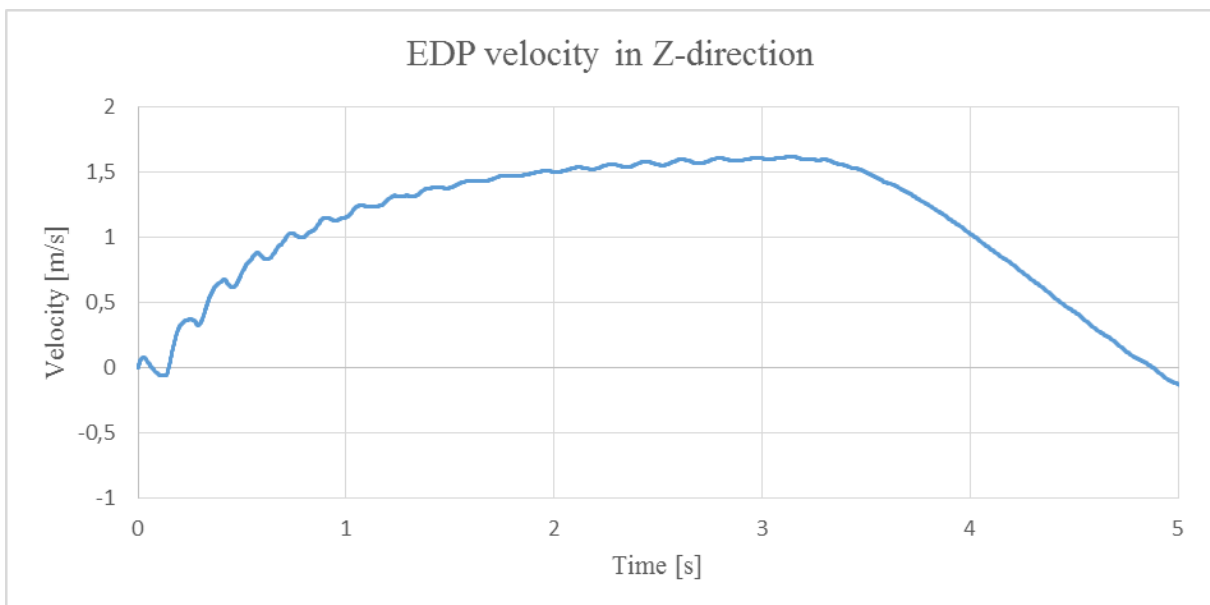


Figure 40: EDP velocity in X-direction in 300 meters WD

The maximum observed velocity in X-direction is 1.6 m/s.

EDP acceleration and velocity in X-direction:

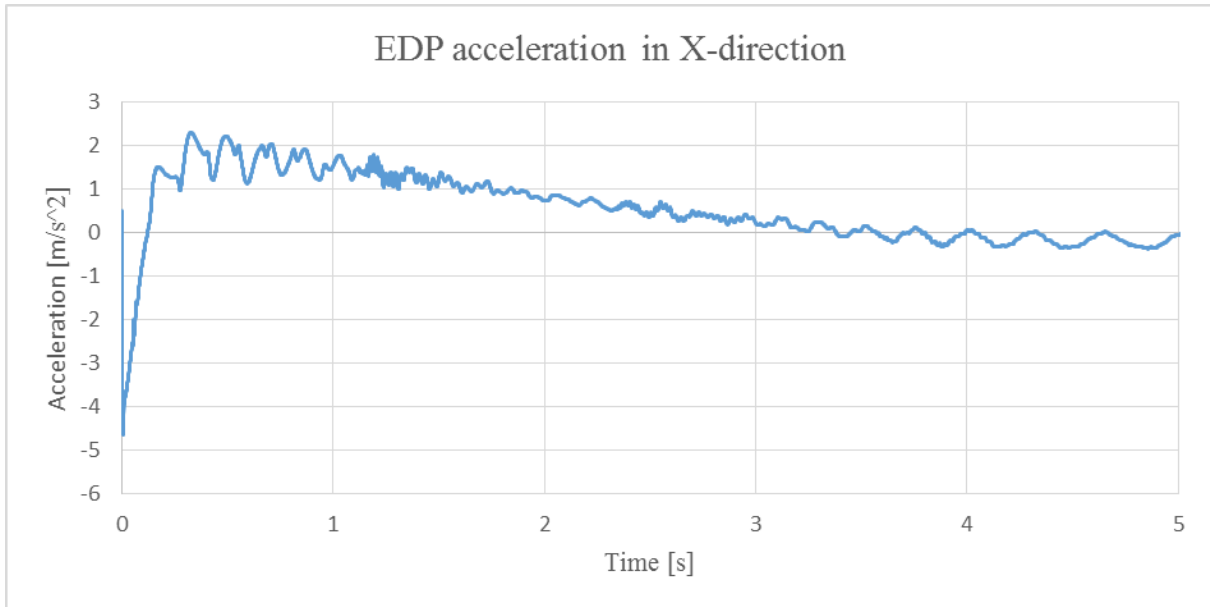


Figure 41: EDP acceleration in X-direction in 300 meters WD

Figure 41 shows that the maximum absolute acceleration in X-direction is 4.7 m/s^2 .

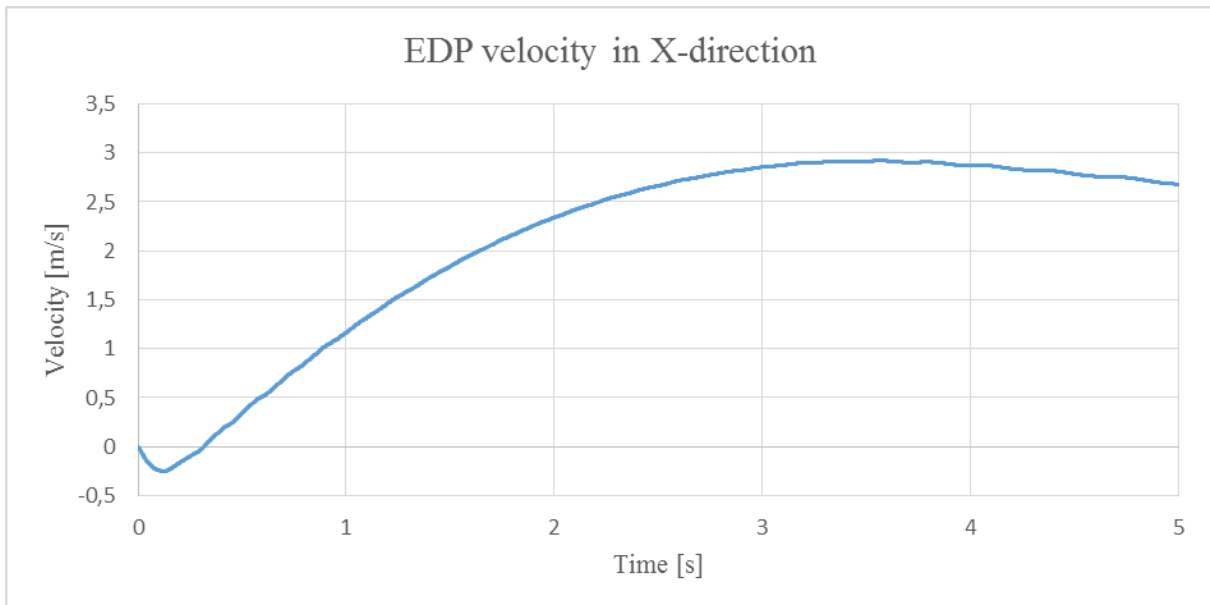


Figure 42: EDP velocity in X-direction in 300 meters WD

Figure 42 shows that the minimum velocity in X-direction is -0.25 m/s .

EDP position in X and Z-direction as a function of time:

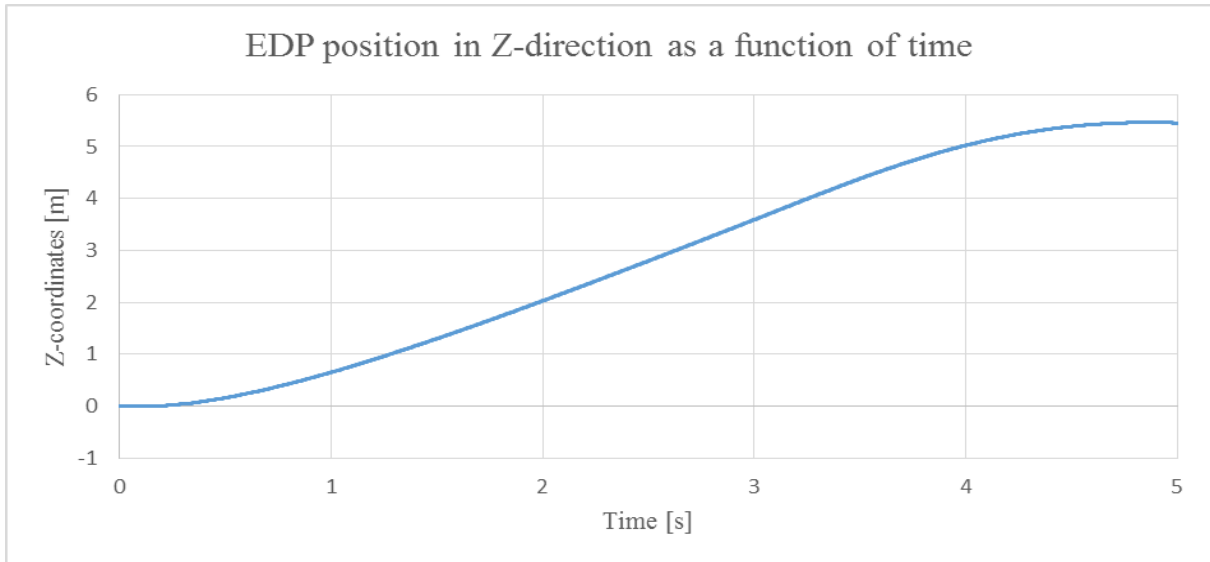


Figure 43: EDP position in Z-direction for 300 meters WD

Figure 43 shows that the EDP gains clearance from the stack-up after approximately 0.3 second.

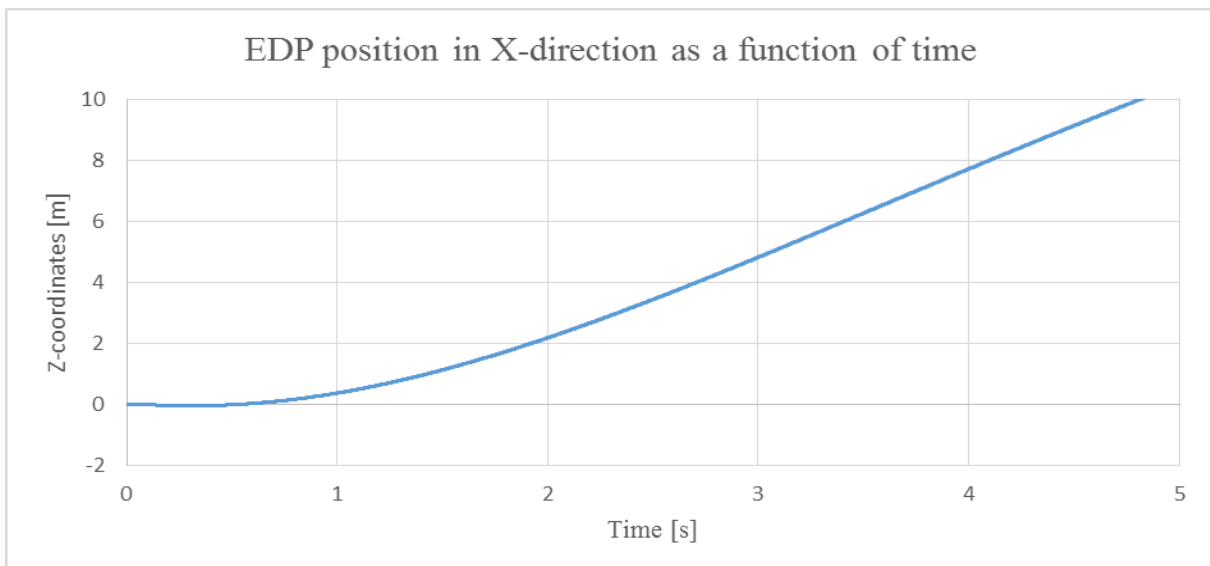


Figure 44: EDP position in X-direction for 300 meters WD

Figure 44 shows the EDP gains displacement in positive X-direction after approximately 0.8 second.

Trajectory of the EDP measured at origo:

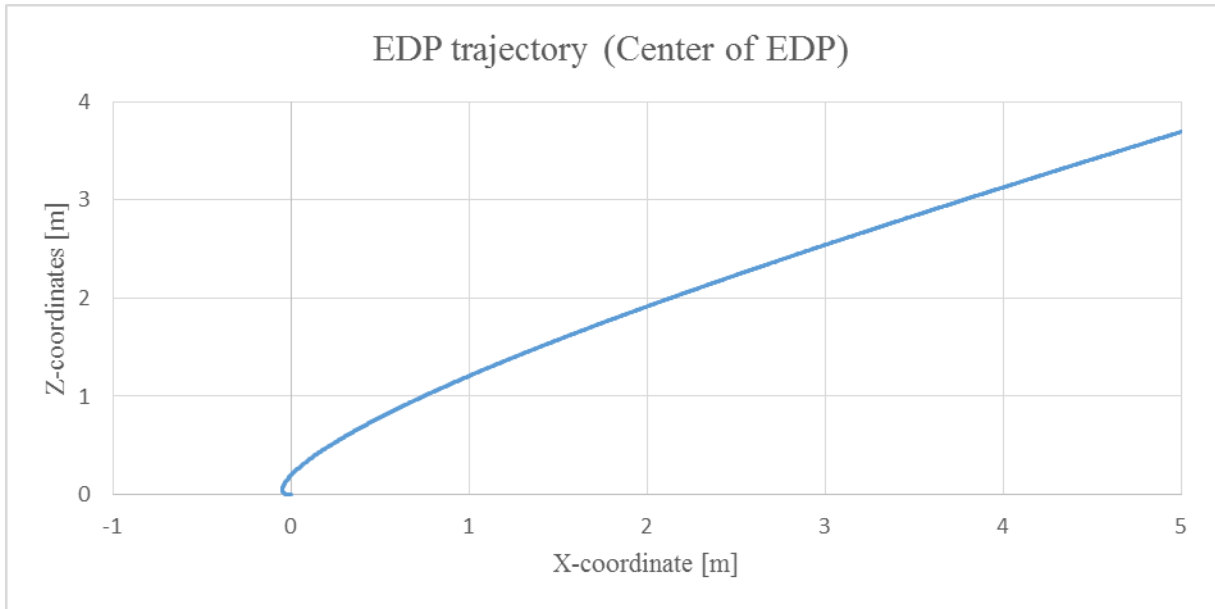


Figure 45: EDP trajectory

Figure 45 shows that the EDP is removed from the stack-up with approximately 45° .

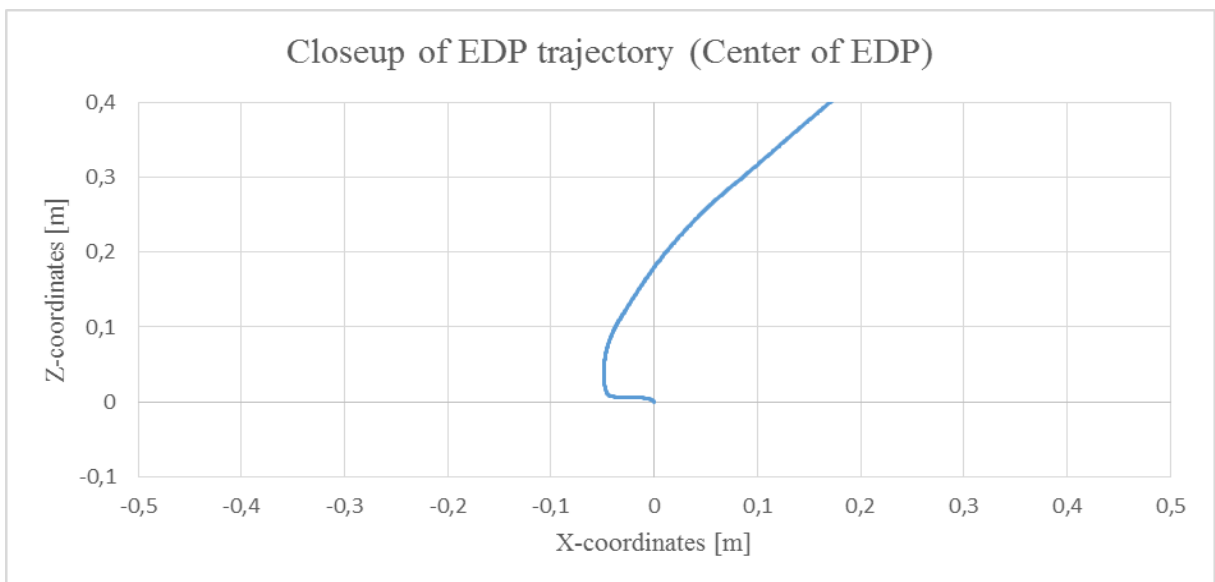


Figure 46: Initial EDP trajectory

Figure 46 shows that the initial motion of the EDP is 0.05 meter in negative X-direction.

Rotary motion of the EDP:

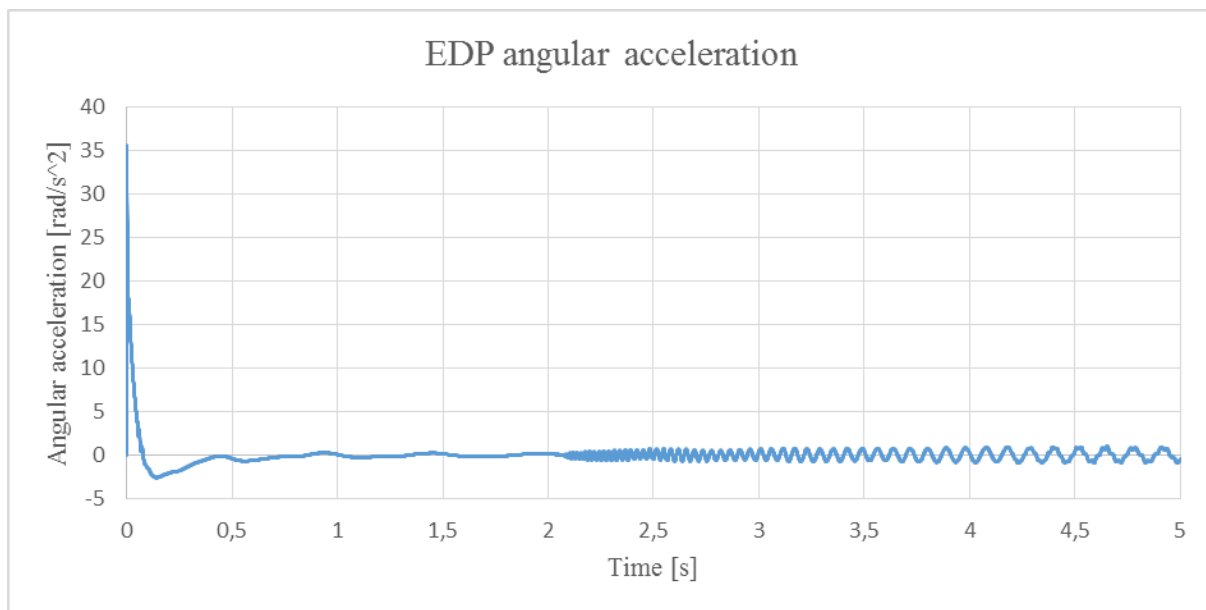


Figure 47: EDP angular acceleration

Figure 47 shows that the maximum initial angular acceleration is approximately 35 rad/s^2 .

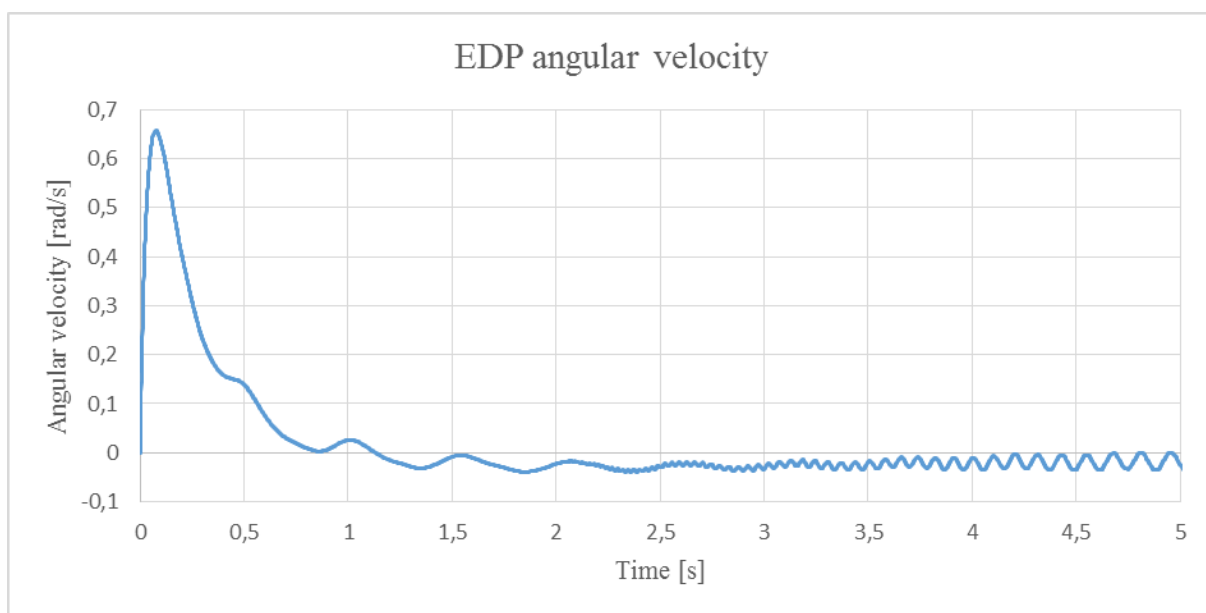


Figure 48: EDP angular velocity

Figure 48 shows that the maximum angular velocity is 0.65 rad/s .

| Peak values during EQD without environmental forces | | | | | | |
|---|--------------|---------------|--------------|--------------|---------------|------|
| | a_z | a_x | v_z | v_x | α | |
| | time | time | time | time | time | time |
| 300 meters WD | 7.90 0.16 | -4.66 0.01 | 1.61 3.14 | 2.92 3.57 | 36.90 0.00 | |
| 500 meters WD | 8.01 0.25 | -4.36 0.01 | 1.75 3.63 | 2.73 3.75 | 35.60 0.00 | |
| 1000 meters WD | 6.41 0.46 | -3.87 0.00 | 1.55 5.08 | 2.63 4.49 | 34.81 0.00 | |

Table 20: Key output obtained from Orcaflex

Peak acceleration and velocity in X- and Z-direction and angular acceleration from the simulation in Orcaflex are presented in Table 20. The table also shows when the values occur in the simulation. It is observed that both maximum acceleration in X-direction and maximum angular acceleration occurs simultaneously.

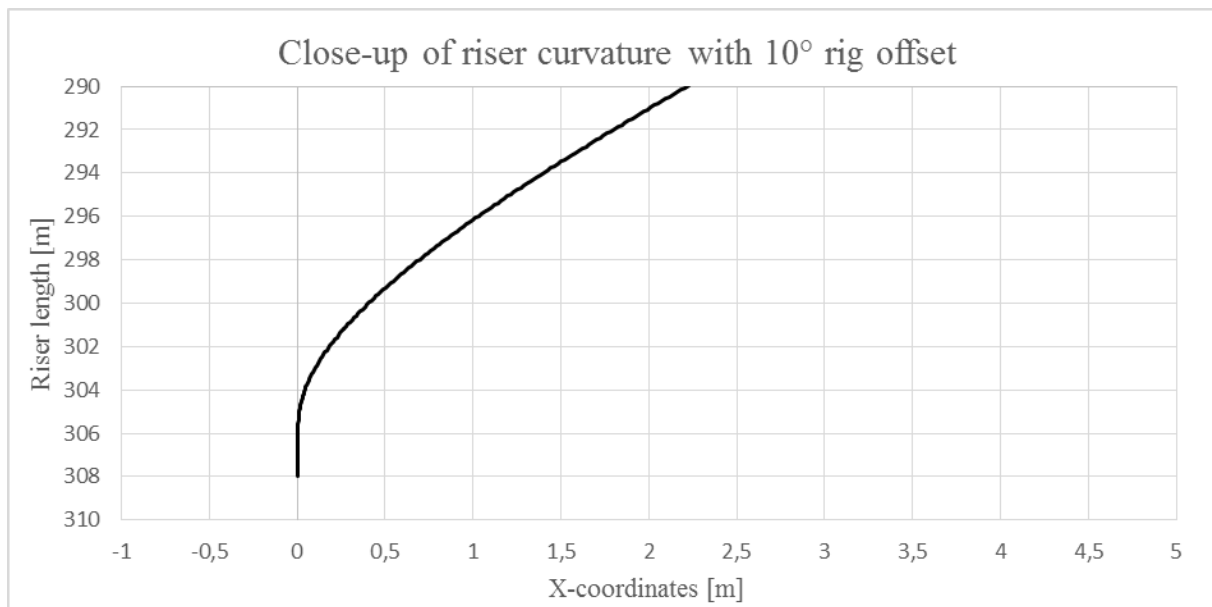


Figure 49: Close-up of riser curvature with 10° rig offset

Figure 49 shows the curvature of the lower part of the riser. The curvature causes the bending moment located at the HAR connector.

9.2 EQD with environmental forces

For developing realistic results, environmental forces have to be included. Maximum significant wave height is set to 4 meters with a period of 10 seconds. Stokes 5th spectra is used in the simulation to represent the wave condition in the Norwegian continental shelf (NCS). The current profile is taken from a known field in the NCS and extrapolated for the two other scenarios. Two different scenarios are considered to give the extreme values. The main objective is to remove the EDP as quickly as possible away from the stack-up and the best scenario of disconnect is when the semi-submersible has the largest positive velocity in Z-direction. The worst scenario of disconnect will then be when the semi-submersible has the largest negative velocity in Z-direction. The first point of interest is $t = 20.4$ shown in Figure 50 and Figure 51. This point gives the largest positive velocity of the semi-submersible. The second point is $t = 25.4$. This point gives the largest negative velocity of the semi-submersible. The semi-submersible's heave motions will not correspond to the actual sea state, but this thesis will not explain more details about this as it is only the motion of the semi-submersible that are of primary interest. Figure 50 and Figure 51 are extracted from Orcaflex and shows the motion and velocity in Z-direction of the semi-submersible.

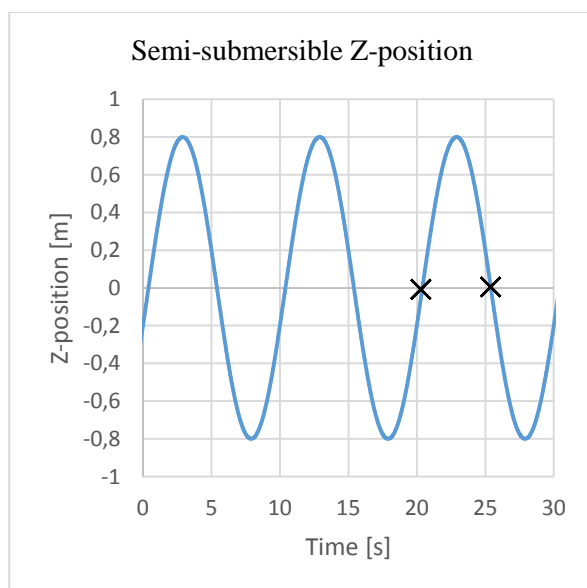


Figure 51: Z-position

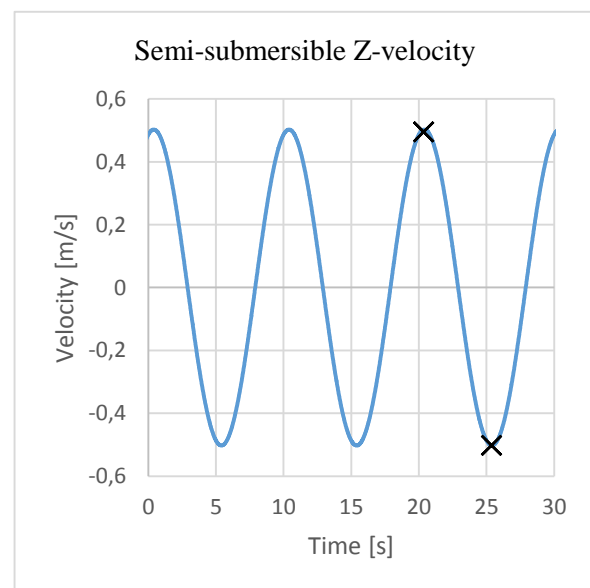


Figure 50: Z-velocity of semi-submersible

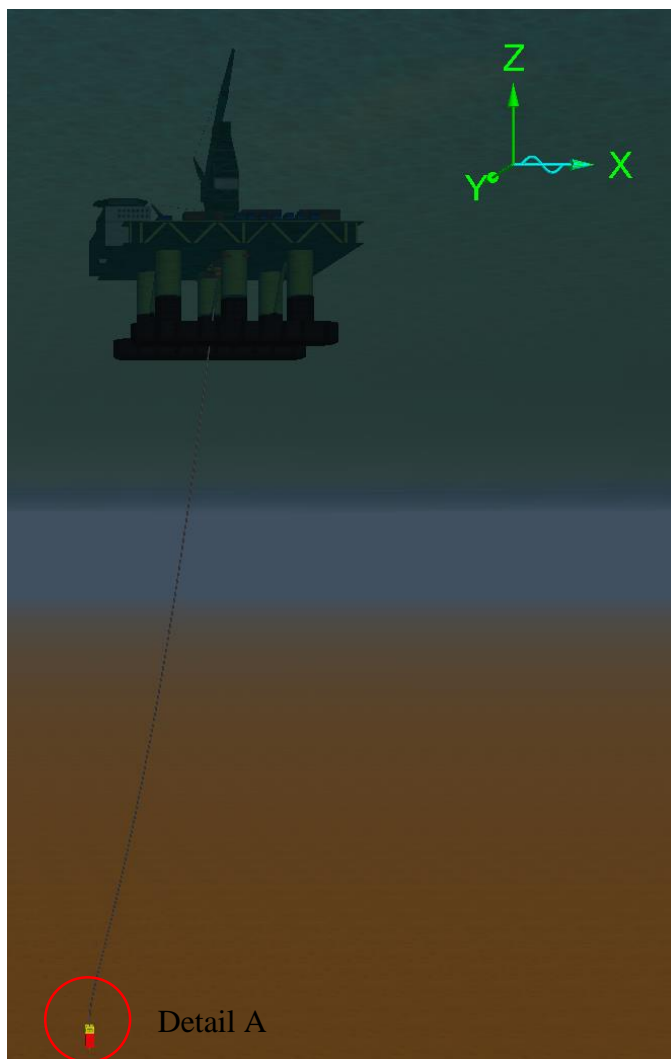


Figure 53: System set-up in Orcaflex

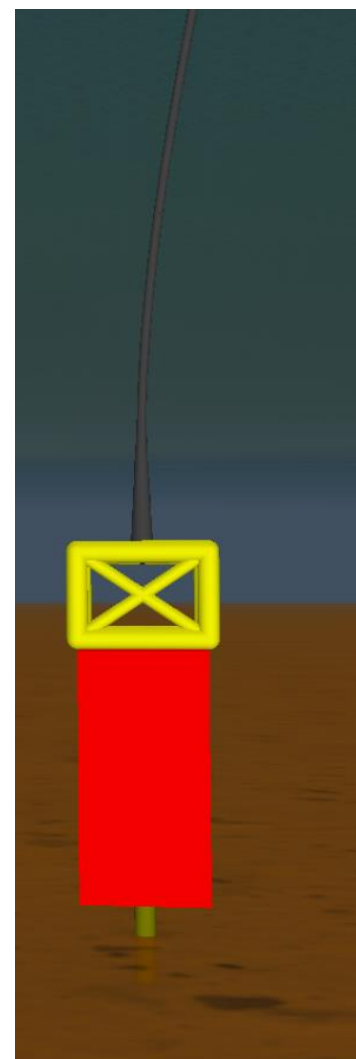


Figure 53: Detail A

The rig is modelled with an offset of 10° in positive X-direction. The wave and current directions are also in positive X-direction as shown in Figure 53. By checking the values of tension prior and post EQD, the new model can be verified similarly to the simplified example.

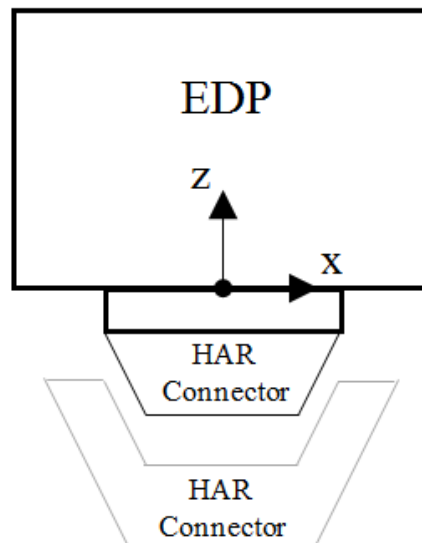


Figure 54: Configuration of EDP and HAR connector with coordinate system

The main difference occurring while including the environmental forces is the acceleration in Z-direction. A brief comparison is presented in section 10 of this thesis. This is the main reason for changing the position of the coordinate system. The largest accelerations and velocities will occur at the edges of the EDP because of the initial rotational motion. To extract these values from Orcaflex, the coordinate system is set according to Figure 54.

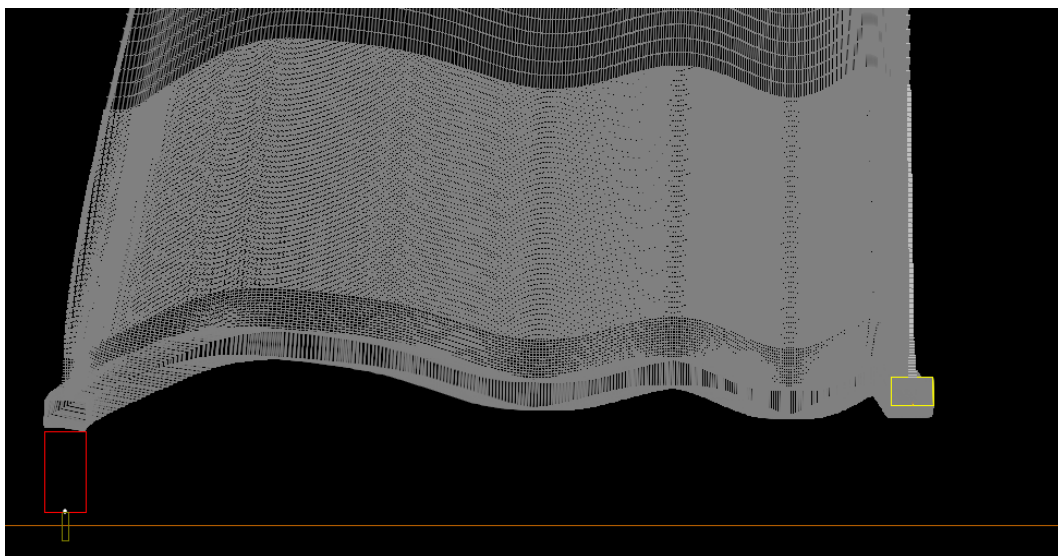


Figure 55: Orcaflex simulation - Trajectory of EDP for 300 meters WD and 10° offset

Figure 55 shows the trajectory for the EDP and riser with the specified conditions. The observed period correspond to the wave period of 10 seconds.

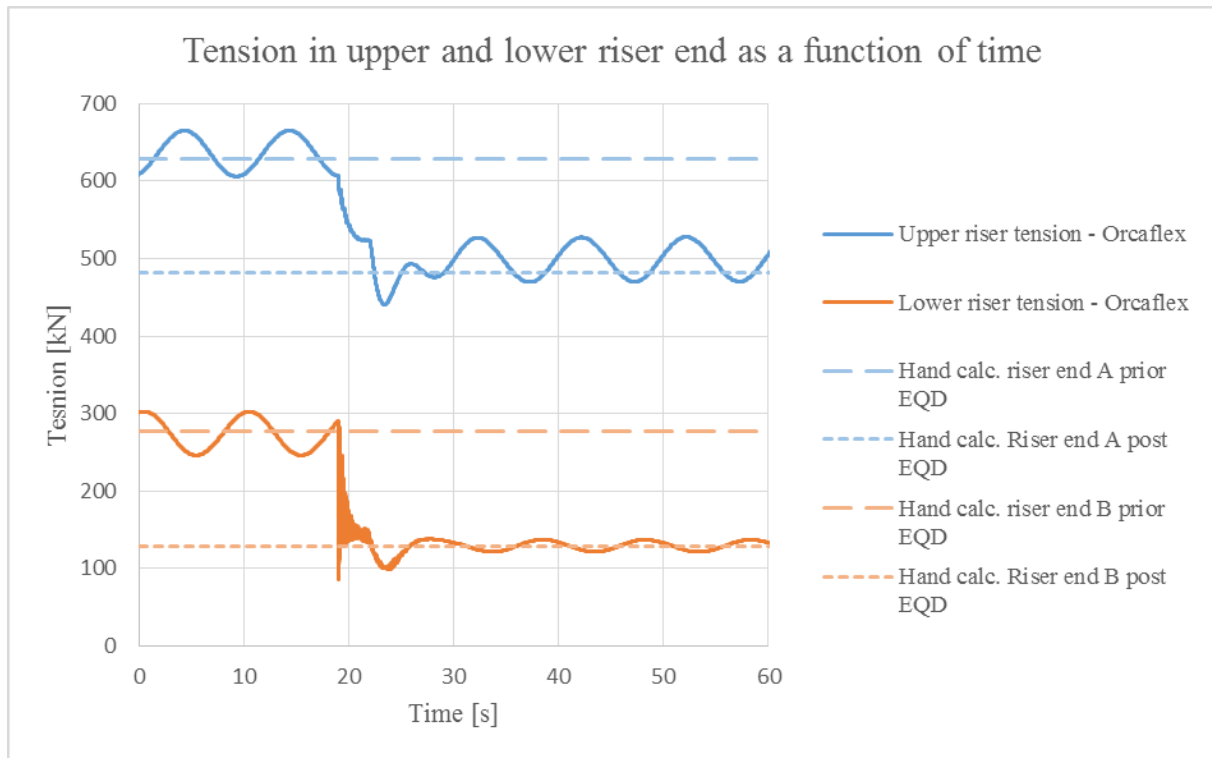


Figure 56: Tension verification of global model settings

Figure 56 shows both manually calculated tension values and Orcaflex output for the four different tension cases. In this particular scenario, EQD is initiated at $t = 19$ seconds, which can be observed in the figure. The oscillations in tension prior to the EQD are caused by the heave motions of the semi-submersible and the damping effect in the spring/dampers that represents the HCS system. Post EQD oscillations are caused by the waves only, as the riser is connected to the semi-submersible.

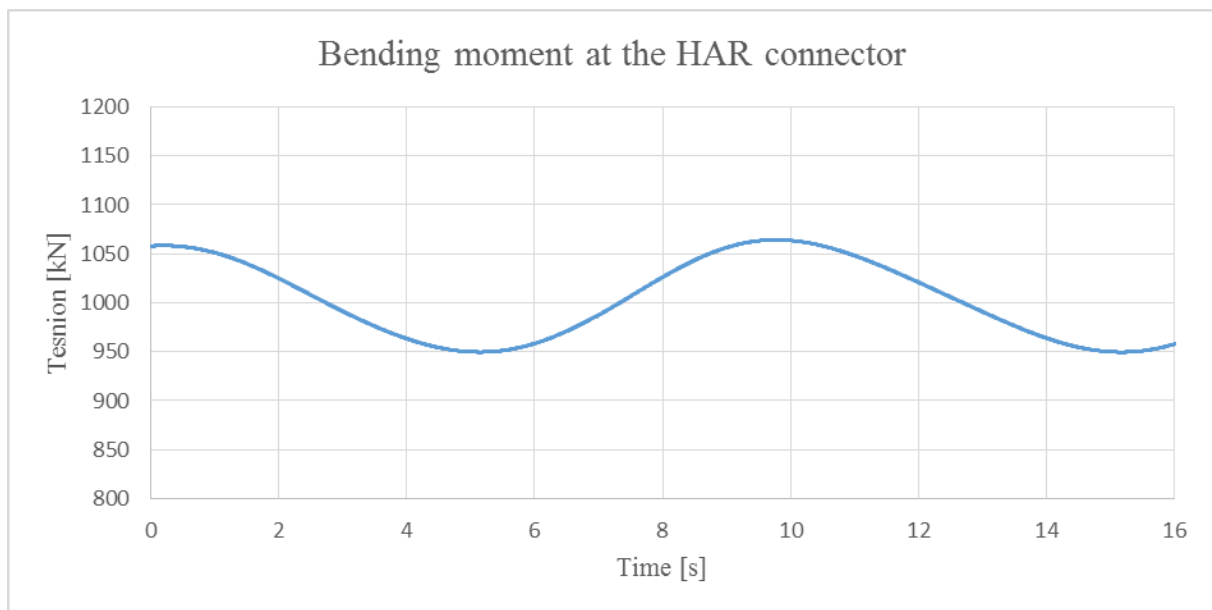


Figure 57: Bending moment at HAR connector

The rig offset combined with waves and current resulted in bending moments shown in Figure 57. The maximum bending moment occurring with waves and current is 1064 Nm. The wave period of 10 seconds can be observed in the figure. The oscillation in bending moment is caused by the heave motion of the ship combined with damping of the modelled HCS.

As discussed in this section there are two points of interest of emergency disconnect. The following graphs will emphasize the differences in acceleration, velocity and trajectory of the EDP.

EDP acceleration and velocity in Z-direction:

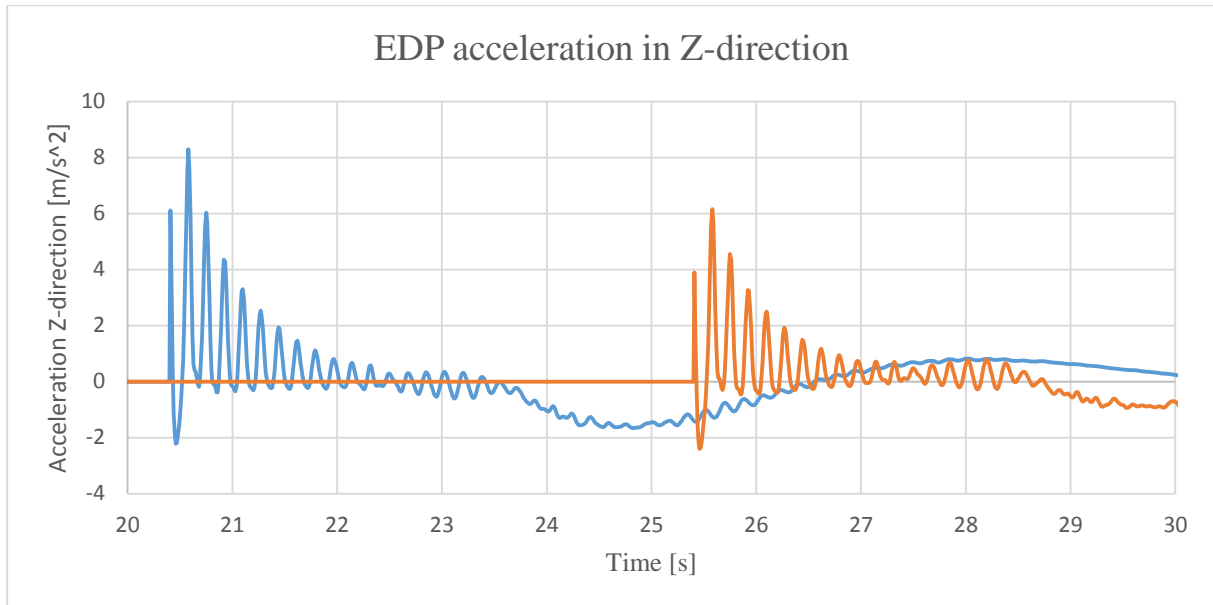


Figure 58: EDP acceleration in Z-direction

Figure 58 show both cases in EQD. The blue line represents initiated EQD at 20.4 seconds, and the orange line represents initiated EQD at 25.4 seconds. The maximum acceleration difference is 2 m/s^2 for the two scenarios. The period of the oscillating acceleration is approximately 0.18 second.

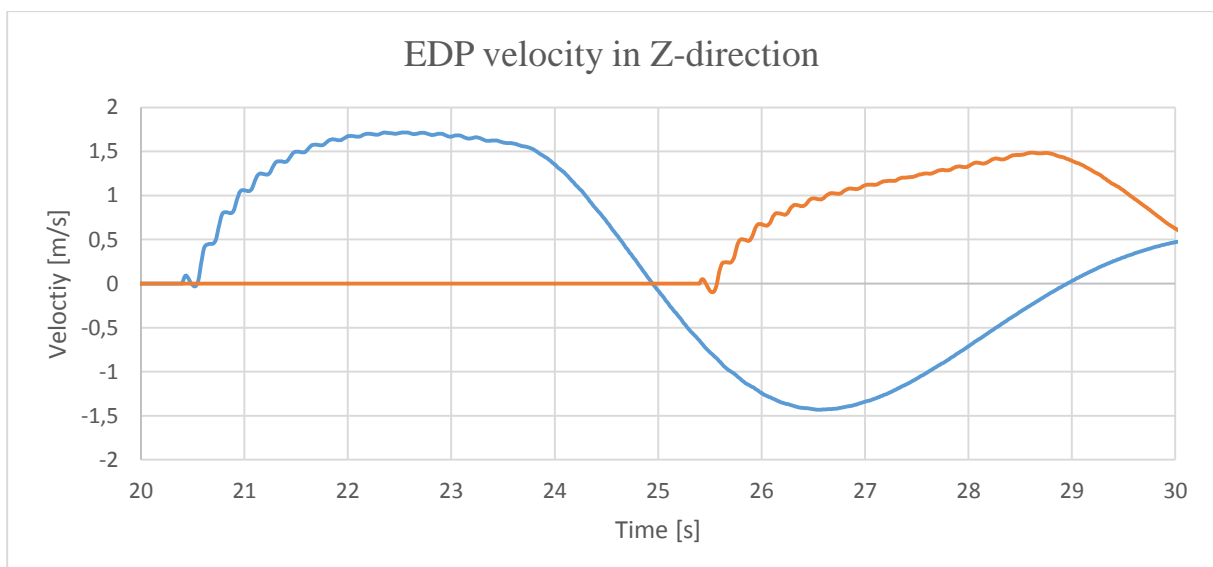


Figure 59: EDP velocity in Z-direction

EDP acceleration and velocity in X-direction:

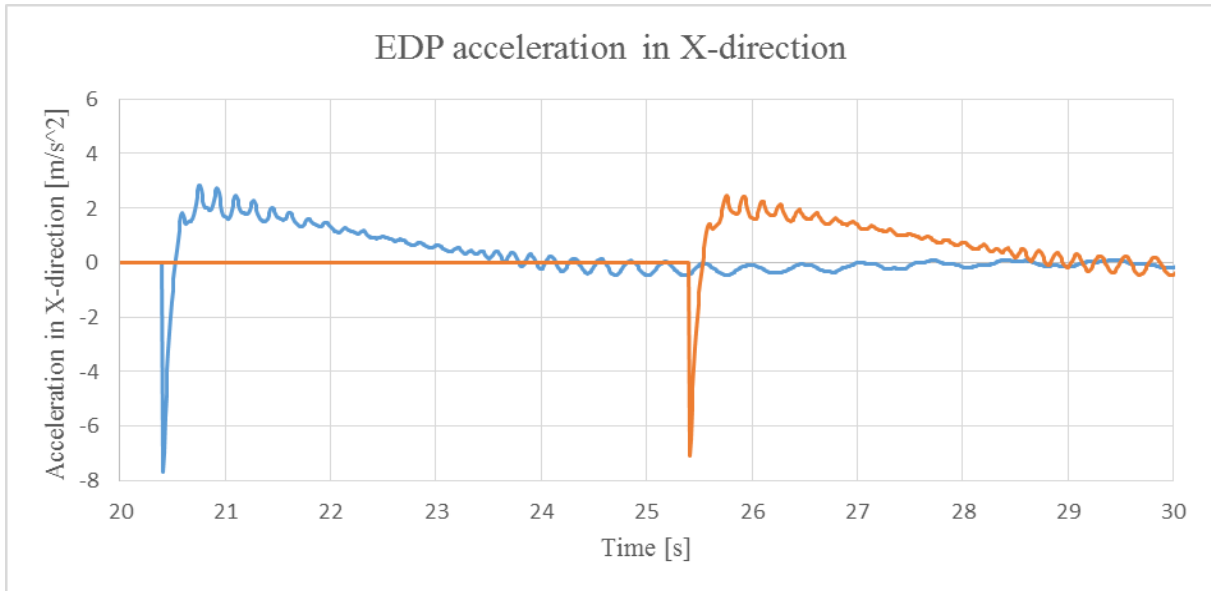


Figure 60: EDP acceleration in X-direction

Figure 60 shows small difference in acceleration in X-direction. The acceleration shown is only for comparison reasons.

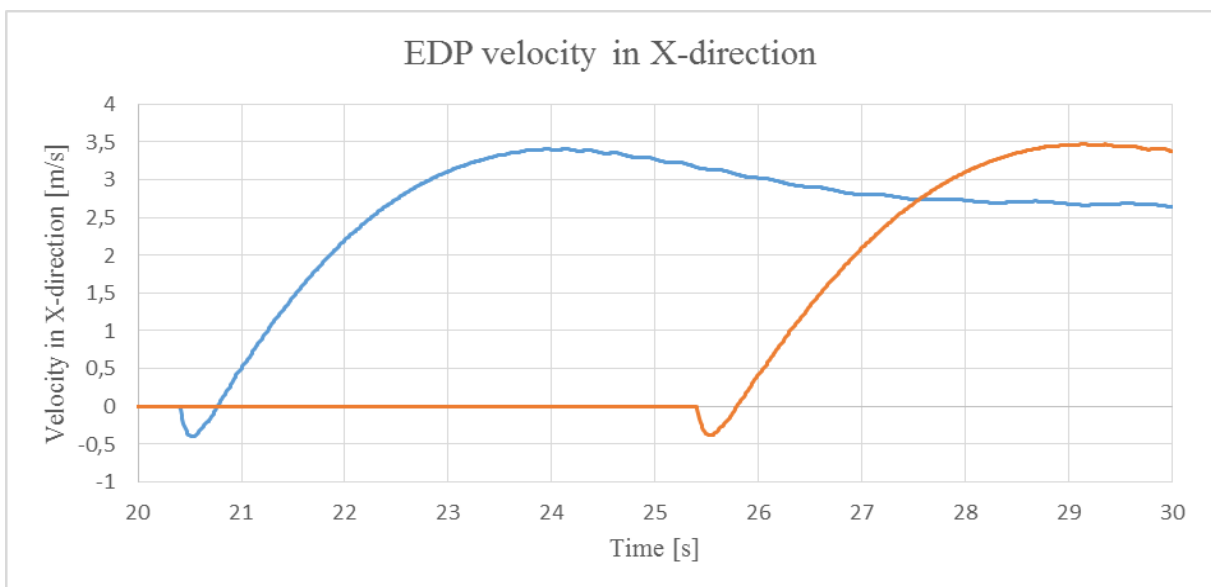


Figure 61: EDP velocity in X-direction

Figure 61 show that the initial velocity in negative X-direction is approximately 0.4 m/s for both cases.

EDP position in X and Z-direction as a function of time:

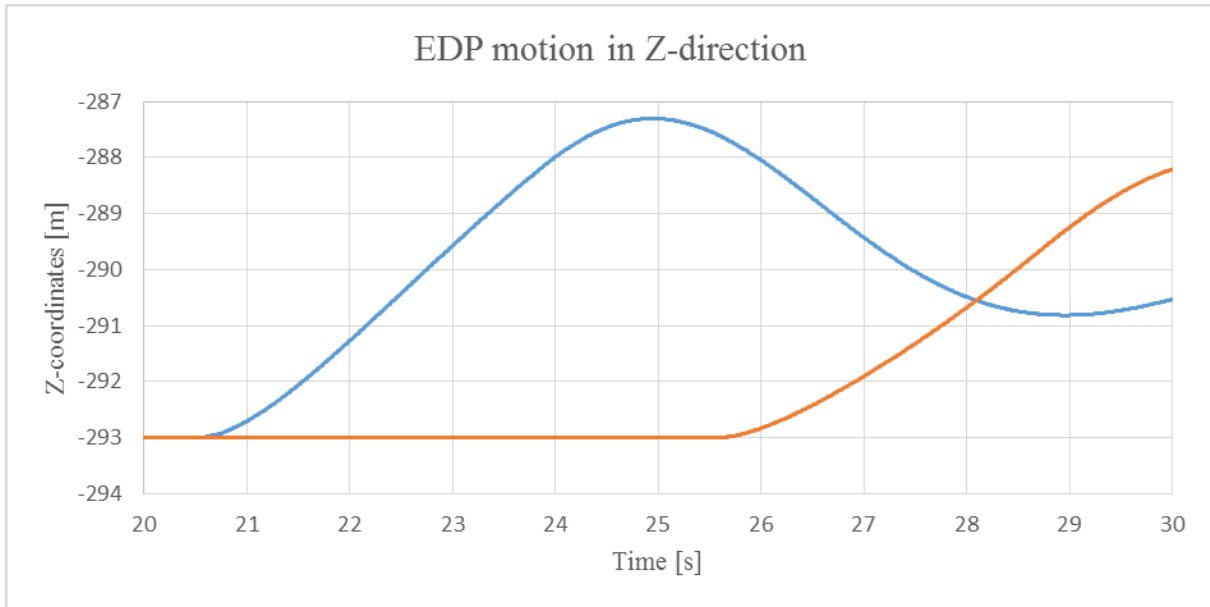


Figure 62: EDP motion in Z-direction

Figure 62 shows a higher gradient of motion in Z-direction for the EQD initiated at 20.4 seconds.

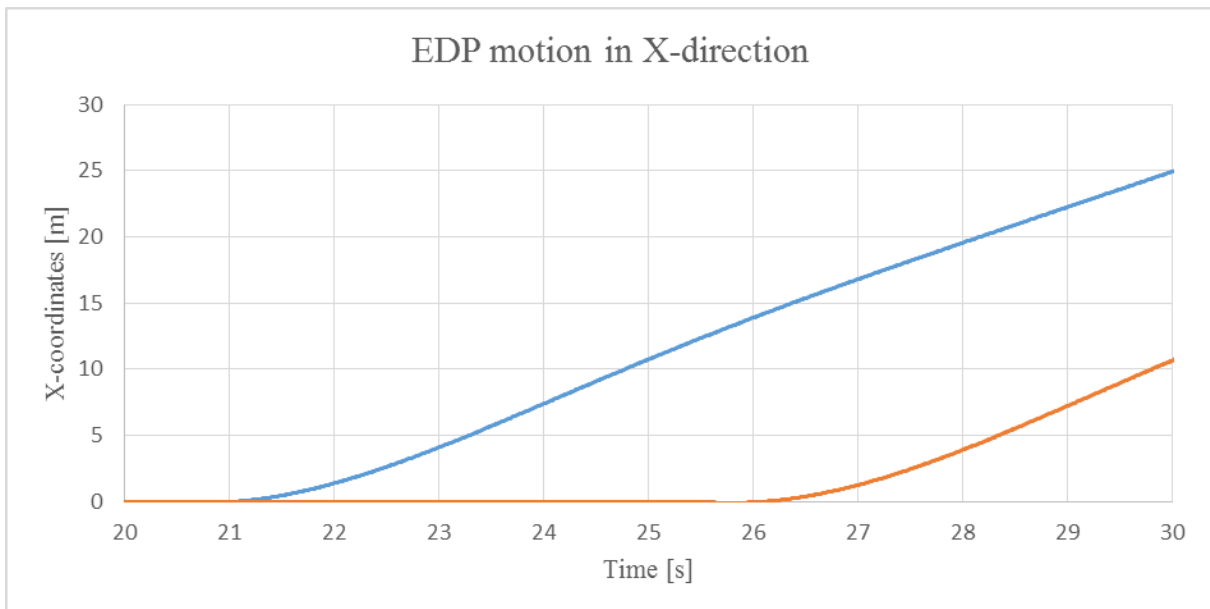


Figure 63: EDP motion in X-direction

Figure 63 shows a similar gradient for motion in X-direction for the two scenarios
 Trajectory of the EDP measured at origo:

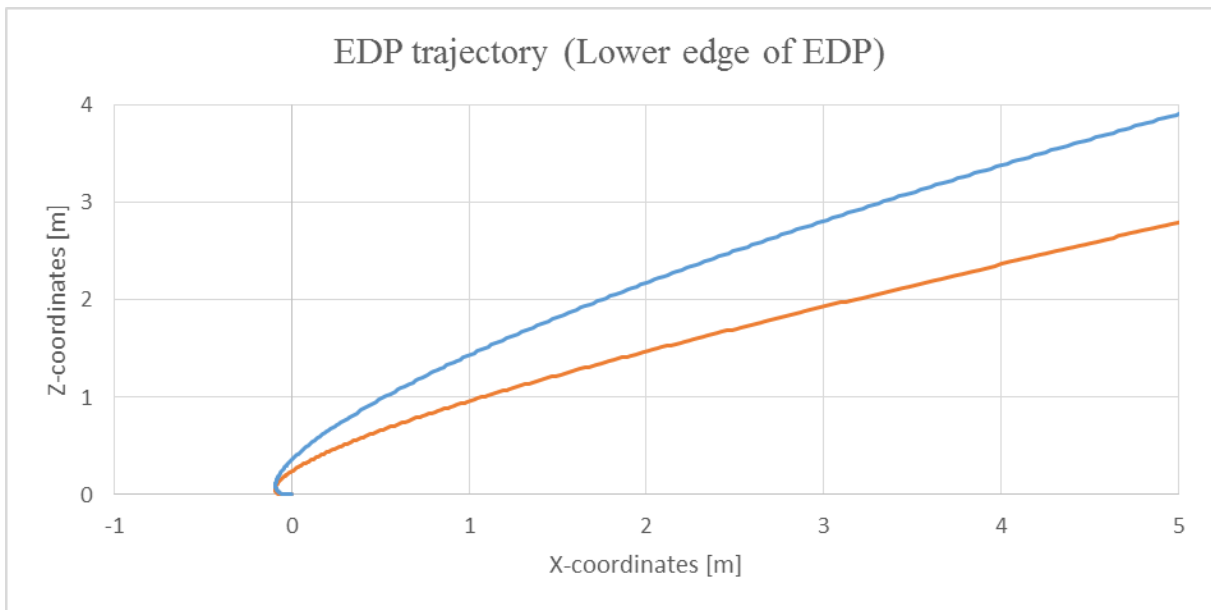


Figure 64: EDP trajectory (Lower edge of EDP)

Figure 64 shows that the EDP gains less displacement in Z-direction for the case of initiating EQD when the semi-submersible has a maximum negative velocity.

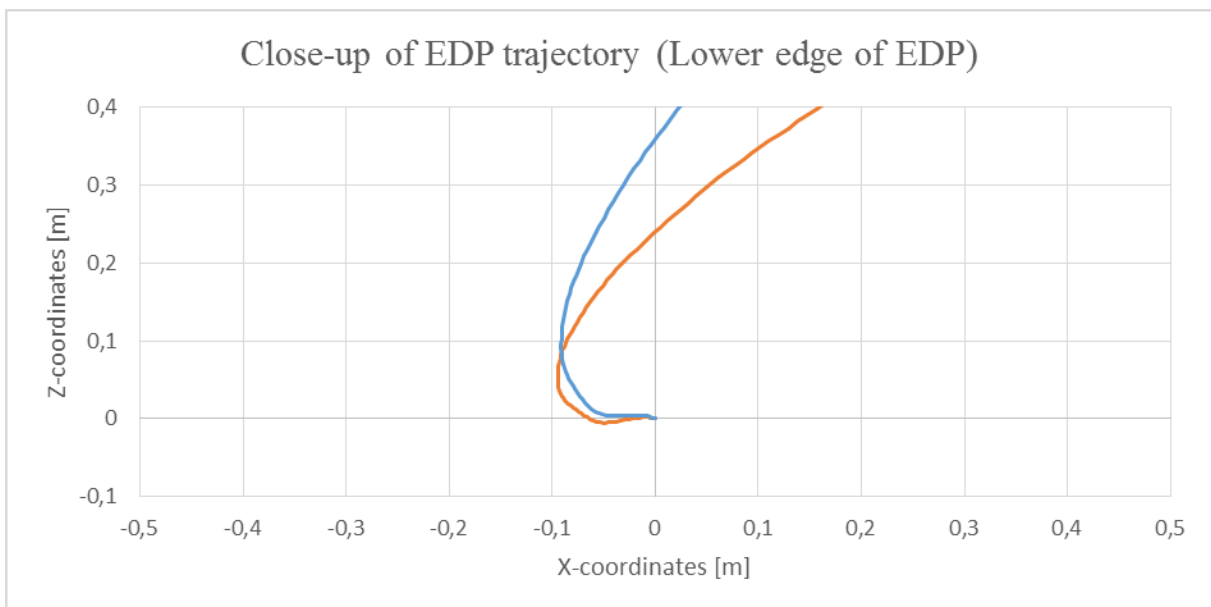


Figure 65: Close-up of EDP trajectory (Lower edge of EDP)

Figure 65 shows initial local trajectory of the lower edge of the EDP. A negative displacement of approximately 0.1 meters is observed.

Rotary motion of the EDP:

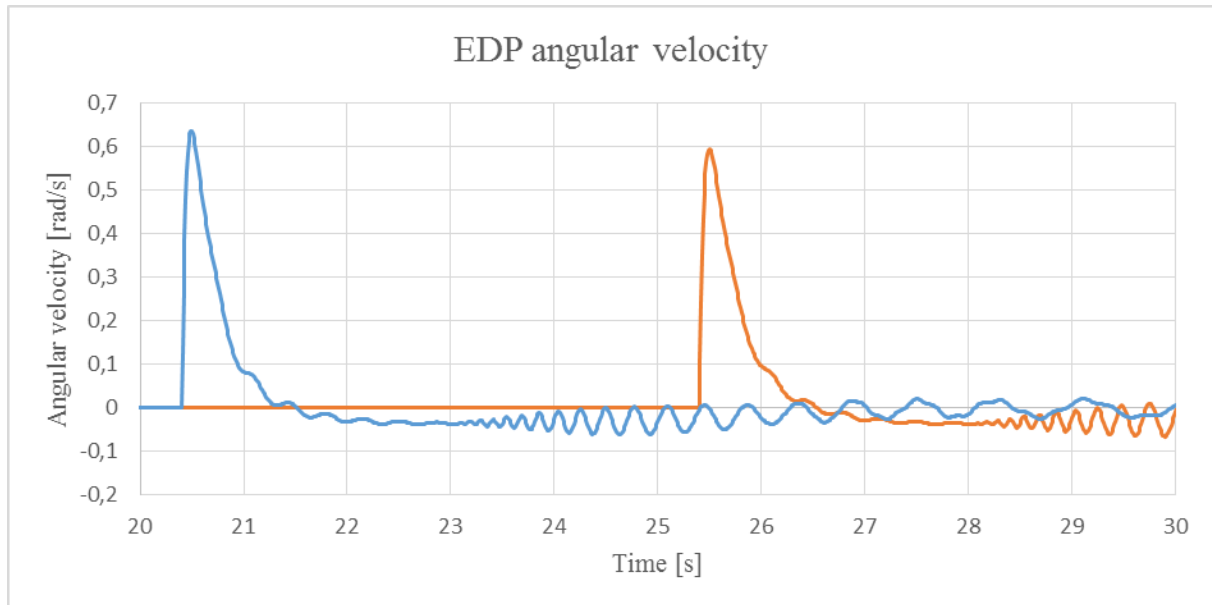


Figure 66: EDP angular velocity

Figure 66 shows that the angular velocity reaches a peak of 0.64 rad/s during initiated EQD at 20.4 seconds. This corresponds approximately to 37 deg/s, and is considered a large angular velocity. However, the velocity decreases rapidly with time which limits the impact of motion. The oscillations that evolve after some seconds after EQD are caused by the response of the riser connection and together with hydrodynamic forces.

Figure 65 show that the EDP will have an initial negative motion in X-direction prior to the dominating motion in positive X-direction. The figure also highlights the relative big difference in initiating an EQD while the vessel is heading upwards or downwards in the wave.

10 Comparison of results

10.1 Different water depths

As the axial natural period is different for each system this affects the accelerations. The presented comparison is based on similar conditions as section 9.2, but including water depths of 500 and 1000 meters.

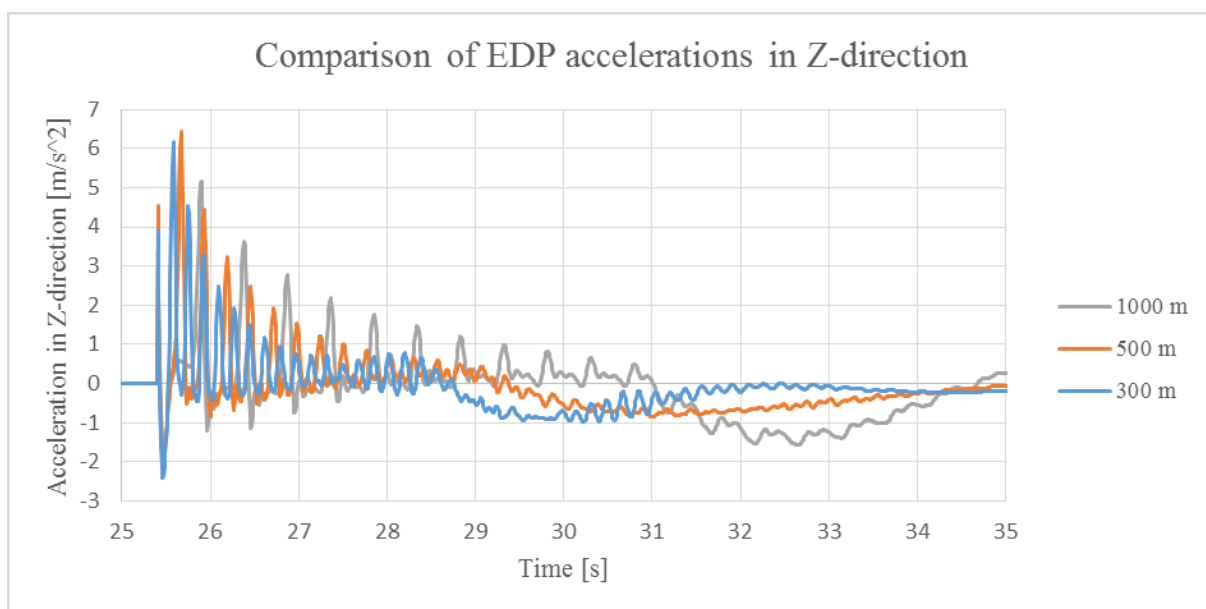


Figure 67: Comparison of Z-accelerations

Figure 67 shows a comparison of the acceleration in Z-direction for the three cases. The system set-up in 1000 meters WD reaches a less peak acceleration than the other two cases, but it is observed to have a lower damping. This means that the peak velocity is approximately similar.

| Description | Value | Annotation |
|--------------------------|-------|------------|
| Axial period 300 meters | 0.18 | s |
| Axial period 500 meters | 0.26 | s |
| Axial period 1000 meters | 0.49 | s |

Table 21: Comparison of axial periods

Table 21 shows the difference in axial periods for the three cases.

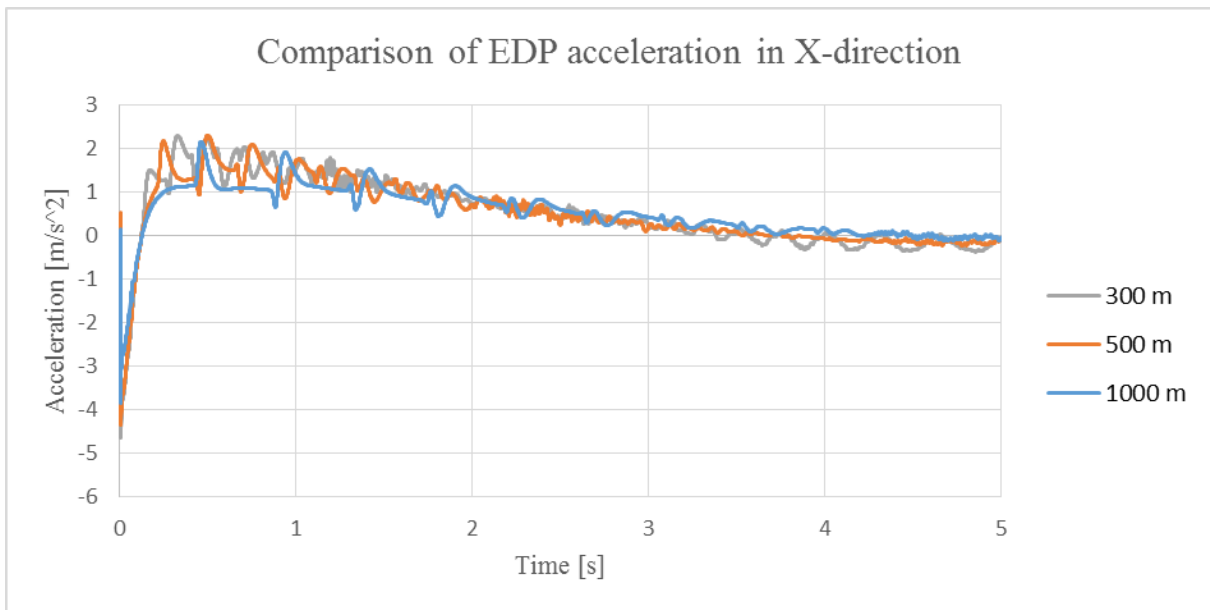


Figure 68: Comparison of EDP acceleration in X-direction without environmental loads

Figure 68 shows the difference of horizontal acceleration. The initial acceleration at $t = 0$ shows that the maximum acceleration occurs at 300 meters WD.

Center of EDP trajectory:

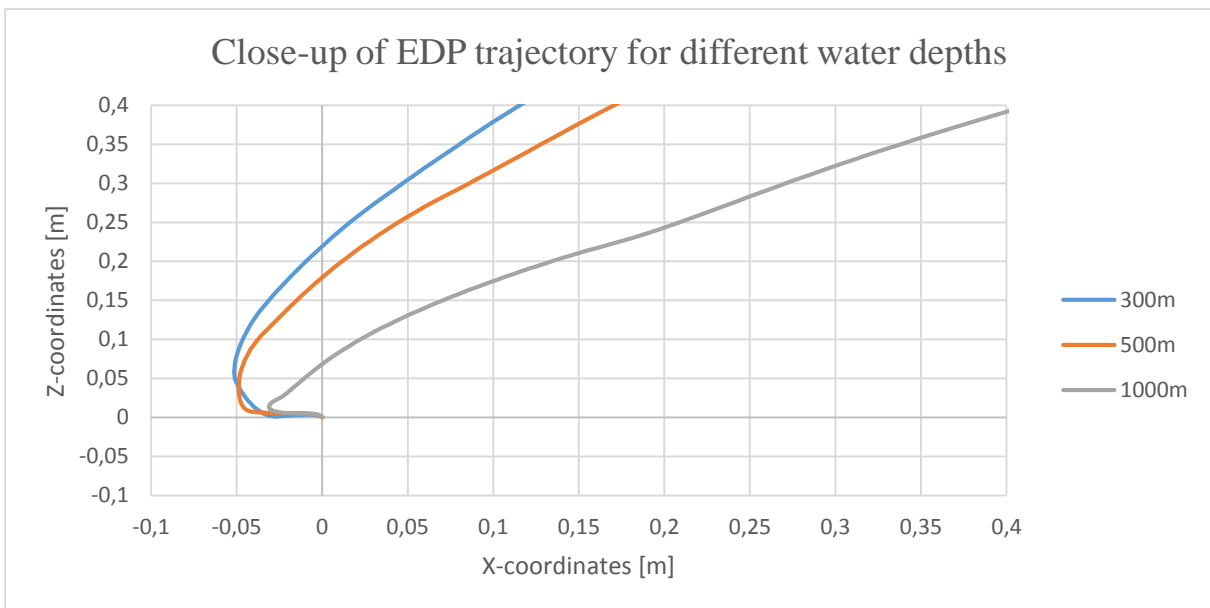


Figure 69: Comparison of EDP trajectories

The EDP trajectory for 1000 meters WD has a considerable smaller angle of removal.

Local trajectory of EDP:

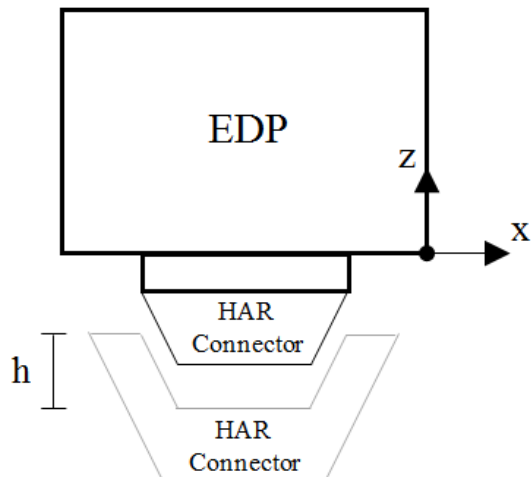


Figure 70: Configuration of lower edge coordinate system

One of the critical points of the EDP is the lower corner towards the offset direction as shown in Figure 70.

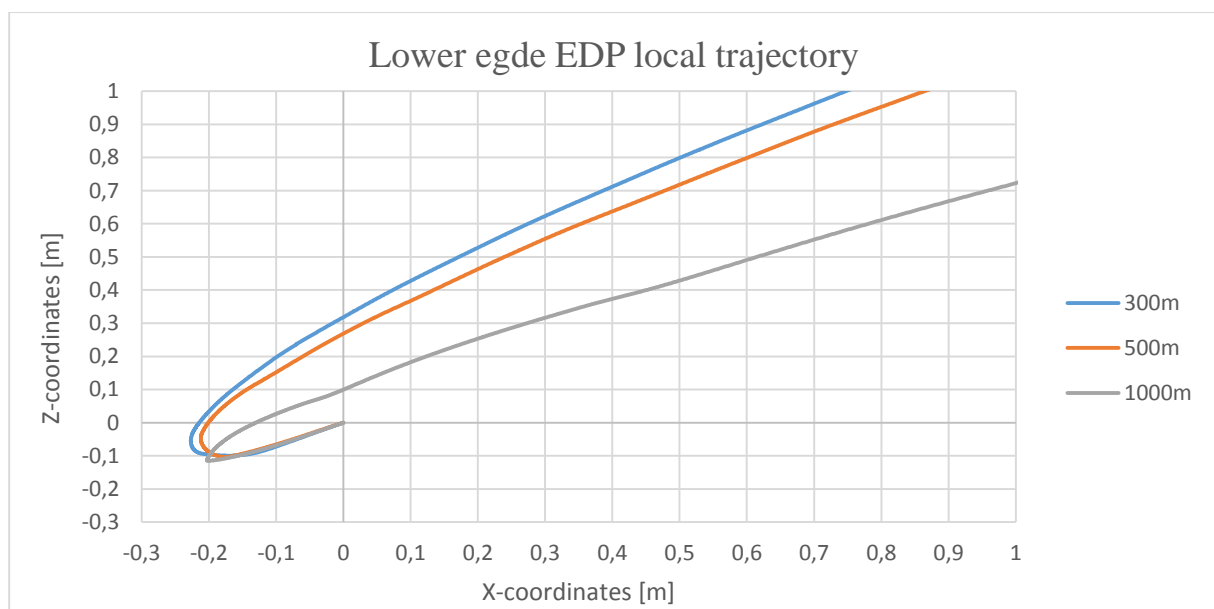


Figure 71: Lower edge of EDP local trajectory

Figure 71 shows the local trajectory of the lower edge of the EDP. This part of the EDP has an initial negative motion in both X- and Z-direction.

10.2 Environmental conditions

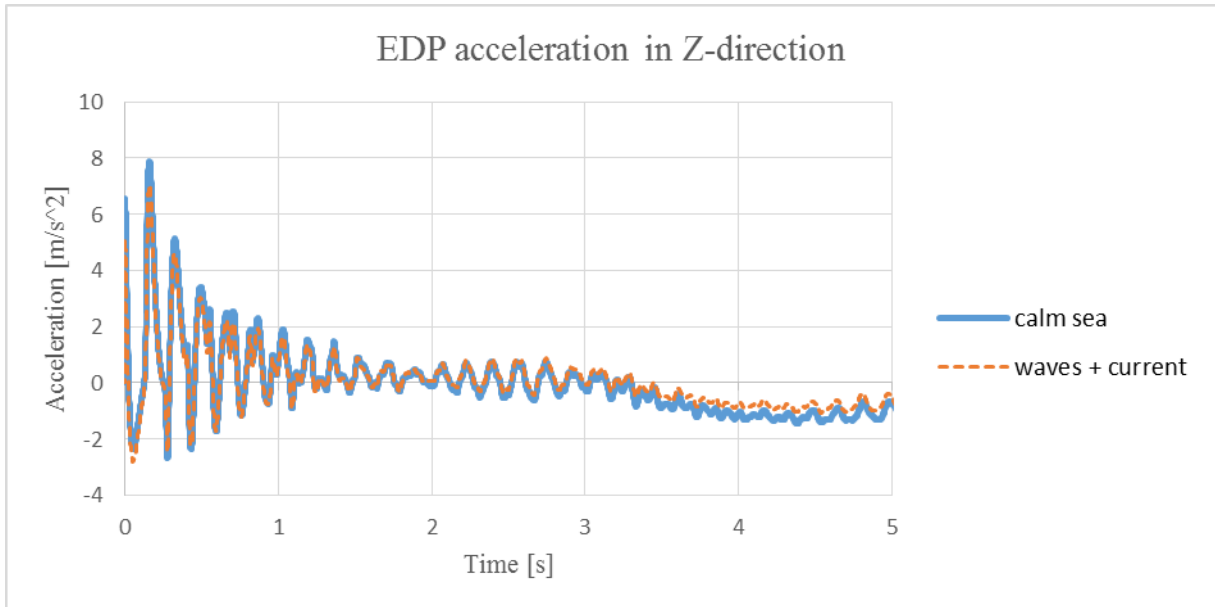


Figure 72: Comparison of EDP acceleration in Z-direction with and without environmental loads

Figure 72 shows that the acceleration in Z-direction is slightly decreased for the case including environmental forces.

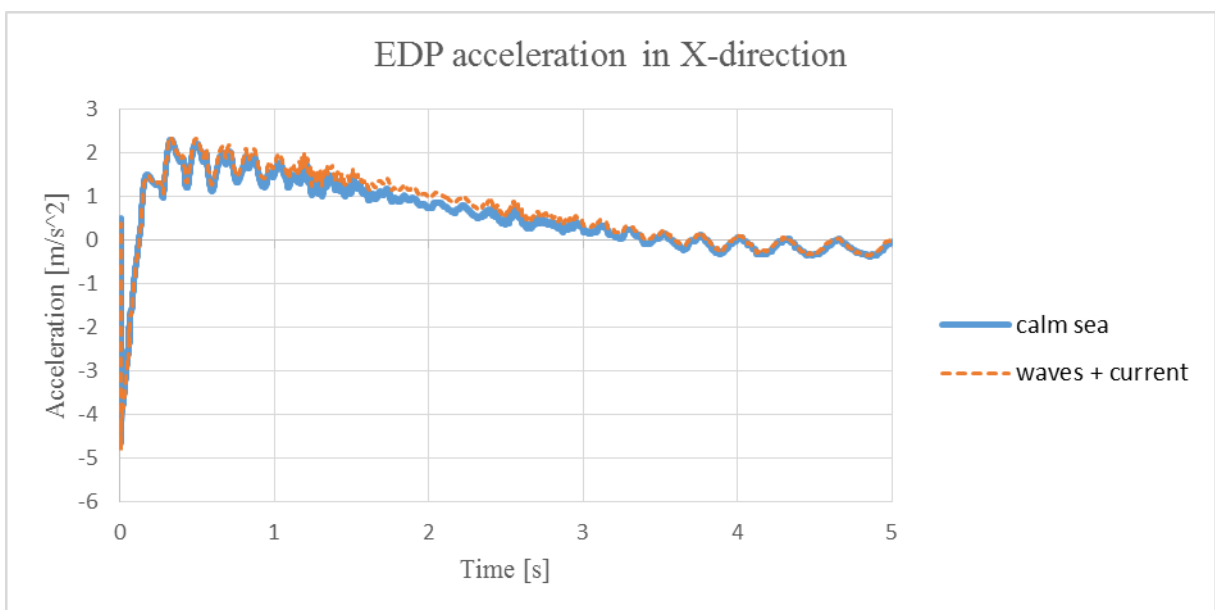


Figure 73: Comparison of EDP acceleration in X-direction with and without environmental loads

Figure 73 shows negligible difference in EDP acceleration in X-direction.

11 Discussion

When the bending moment at the HAR connector is released, the riser searches an equilibrium position. The instant acceleration in X-direction of the EDP is a result of the counter force from the added mass and drag force from the water to the riser. While the sensitivity analysis was performed, it was observed that an increase of the coefficients of the riser caused a considerable higher acceleration of the EDP in X-direction. Results from Orcaflex shows that a large initial angular acceleration dominates immediately after release. This was expected to occur, as the EDP consists of a large mass compared to the riser. Maximum acceleration in horizontal direction occurs simultaneously with the angular acceleration.

The output from Orcaflex has been verified by hand calculations and data from GE Oil and Gas. The combination between WORS configuration and geometric offset resulted in a bending moment of approximately 1000 kNm. This matches well the bending moments for other global riser analysis performed with different software products. The bending moment capacity of the HAR connector prior to failure is 3430 kNm [21]. Subsea Technology Ltd states that their connector can handle unlimited disconnect angle as long as the bending moment does not exceed the maximum capacity. This means that the rig may have a larger offset if the HCS allows this.

As the main target of an emergency disconnect is to quickly remove the riser and EDP away from any structure at the seabed, the worst case scenario is considered as low acceleration in Z-direction combined with a large acceleration in X-direction. The damping effect associated with the HCS causes the tension to vary along with the heave motion of the semi-submersible and generates interest of initiating EQD in different sea states. Several analyzes were performed to find the critical scenario where the acceleration in Z-direction is small, and acceleration in X-direction is large. This is considered to have the largest potential impact load on surrounding structures.

Hand calculations are considered to coincide well with the output given from Orcaflex. The acceleration in Z-direction in 300 meters WD deviated with approximately 10%, which is considered acceptable. The acceleration in Z-direction obtained from the WORS at 1000 meters WD was noticeable smaller due to the increased inertia of the system. It should be noted that the rig offset for 500 and 1000 meters is not equal to 10° as it is limited by the physical HCS stroke limits. The overpull at the HAR connector was similar for each case, but the associated bending moments was reduced. This also resulted in reduced horizontal accelerations for the cases of 500 and 1000 meters WD.

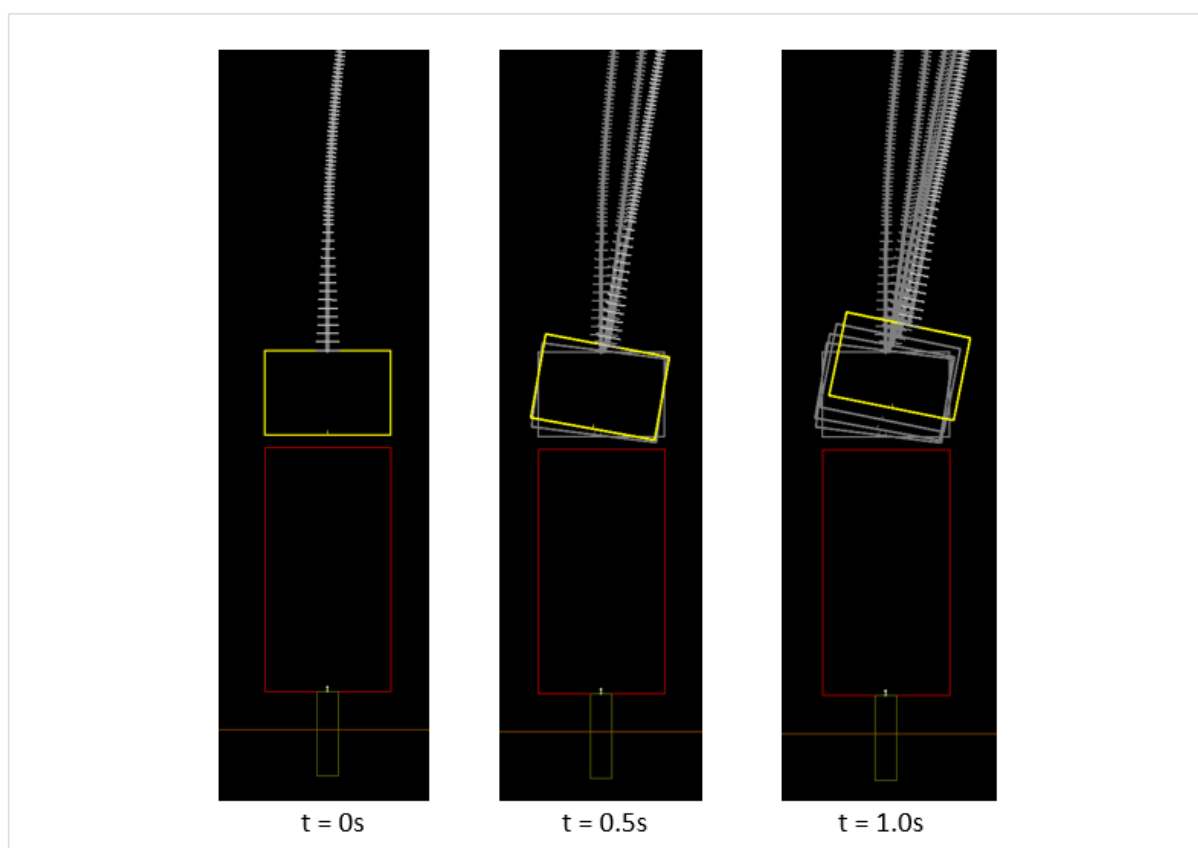


Figure 38: Initial motions of the EDP after EQD

There are two kinds of impact load to consider; impact load due to angular velocity and impact load due to motion in X-direction. Figure 38 shows the initial motions of the EDP after EQD with no environmental loads. The EDP has an initial rotation of 12.6° within the first second. The rotational motion of the EDP and HAR connector is not considered to damage the HAR connector, as the design of the connector allows for initial rotational

motion. However, the guiding structure may be revised. Figure 73 shows a slightly higher acceleration in X-direction for the case including environmental loading. This is seen reasonable as the current affects the acceleration in that direction. The EDP velocity in negative X-direction peaks at 0.25 m/s with a displacement of 210 mm. Due to limited access of the geometry of the HAR connector, an impact analysis is not possible to perform. However, the results may be used to locate the potential point of impact and further investigation. Another impact scenario is during movement of the EDP in positive X-direction. The upper part of the HAR connector may collide with the guiding structure surround the connector, depending on the height, "h", shown in Figure 70. With a comparison of the height of the connector and the trajectory, a potential impact situation may be established.

It is suggested that the alignment guiding structure is revised. The present alignment guides do not allow for negative displacement, i.e. the rotational motion will cause the guiding pin to collide with the guiding receiver. It is recommended to eliminate the physical obstructions at the lower alignment structure, making it possible for the connector to rotate with minimum 13° without risk of damage.

12 Conclusions

Emergency disconnect with excessive rig offset during workover operations has been analyzed and discussed during this work. The main objective of this thesis was to establish the forces and trajectory of the EDP after initiated EQD. The main effort has been on modelling different EQD scenarios in Orcaflex.

The dynamic analysis showed that the critical initial dominating forces on the EDP were angular acceleration combined with horizontal acceleration. The acceleration in vertical direction occurs approximately 0.1 second after initiated EQD. The main difference of initiating EQD in different water depths was the trajectory due to different acceleration in vertical direction. Large water depths add inertia to the system with respect to the length of the riser. This resulted in a lower acceleration in vertical direction causing the angle of trajectory to decrease. The horizontal acceleration is found to oscillate with a period of 0.18 second and reaches a peak acceleration of 7.9 m/s^2 . The oscillation is caused by the natural frequency of the system. The maximum acceleration in horizontal direction was found to be 4.7 m/s^2 . This caused a maximum displacement of 210 mm of the EDP in horizontal direction. However, the velocity related to the displacement in horizontal direction is limited to maximum 0.25 m/s and is considered to pose a minor risk of damage. Based on the assumption of operational HCS damping effect, the critical point of disconnect in wave conditions was also established. The worst case scenario was as expected found to occur when the vessel had the maximum velocity downwards because of the heave motion. The largest difference in acceleration in vertical direction depending on timing of EQD was found to be 2 m/s^2 and affected the trajectory angle as shown in Figure 64 at page 75.

The initial rotation of the EDP and the HAR connector is 12.6° within the first seconds after release. This may damage the guiding structure surrounding the connector depending on the rig offset direction. It is recommended to revise the alignment guides in the guiding structure of the HAR connector to prevent collision during large offset EQD.

13 Uncertainties

Orcaflex is a well-known software and widely used by the offshore industry. However, Orcaflex is dependent of reliable input data. The boundary conditions of the riser have a contribution to the result. In this analysis the upper end of the riser is assumed to behave as a free hinge. In reality the riser will be connected to the semi-submersible and cause a bending moment to the equipment on the vessel. The HAR connector is treated as a steel joint with limited bending capabilities. It is not used actual material properties and geometry of the connector. The intention was to give a reasonable approximation. The hydrodynamic coefficients will always be uncertain unless they are verified by testing. The model in Orcaflex was built on typical coefficients values from the industry and gives a reasonable approximation to the problem.

14 Further work

Due to large simulation time in Orcaflex, the presented results that include waves are only consisting of Stokes 5th order waves. To establish further extreme values of EQD, JONSWAP wave spectra should also be assessed. A conservative method would be to locate the largest wave and run several simulations surrounding this wave. A quantitative analysis with EQD in different combinations of wave period and wave height would gain even more confidence in EDP trajectory. The analysis should also be field specific to gather more environmental data. The behavior of the semi-submersible should also be closer investigated with correct and realistic RAO settings.

This thesis lacks further analysis of impact loading. A structural and geometric analysis of a specific HAR connector would give more precise answers to what damage the EQD can cause. The associated overpull at the HAR connector should also be analyzed to locate the best suitable tension to the WORS.

15 References

- [1] "Islandoffshore.com," [Online]. Available: <http://www.islandoffshore.com/?c=9452>. [Accessed 9 January 2015].
- [2] D. Lawson, "OE Digital Edition," 01 July 2013. [Online]. Available: <http://www.oedigital.com/engineering/item/3469-drilling-emergency-release-connectors-designed-for-high-bending-moment>. [Accessed 09 June 2015].
- [3] Rigzone.com, "How Does Coiled Tubing Work?," [Online]. Available: https://www.rigzone.com/training/insight.asp?insight_id=324&c_id=22. [Accessed 2 February 2015].
- [4] O. T. Gudmestad, Marine Technology and Operations, Theory and Practice, University of Stavanger, 2014.
- [5] T. E. Solli and DNV, "OTC 22586 - Workover/Well Intervention and Regulatory Challenges," in *Offshore Technology Conference*, Rio de Janeiro, 2011.
- [6] ISO, "ISO 13628-7 - Petroleum and natural gas industries - Design and operation of subsea production systems - Part7: Completion/workover riser systems," 2005.
- [7] GE Oil & Gas, "ge-intervention.com," [Online]. Available: http://ge-intervention.com/media/110521/low-res-ge_subsea_intervention_a4-082113-2.pdf. [Accessed 02 June 2015].
- [8] Subsea1, "Workover Riser System," 5 September 2010. [Online]. Available: http://subsea1.com/index/page?page_id=11083. [Accessed 2 February 2015].
- [9] Y. Bai and Q. Bai, *Subsea Pipelines and Risers*, Oxford: Elsevier Ltd, 2005.
- [10] Email from Robert Olsen, *Riser joint figure*, Stavanger, 2015.
- [11] Subsea1, "Subsea1.com," alf, NCE Subsea, Statoil, DETNORSKE, BP, FMC, Aker Solutions, ibruk, 5 September 2010. [Online]. Available: <http://subsea1.com/index/search?content=edp>. [Accessed 28 January 2015].
- [12] Subsea Technologies Ltd, "Xtreme Release (XR) Connector™," 2014. [Online]. Available: <http://www.subseatek.com/XR-Connector>. [Accessed 10 June 2015].

- [13] Subsea Technologies Ltd, "Xtreme Release Connector™," [Online]. Available: <http://www.subseatek.com/images/upload/downloads/DN-1096-GD-2%20Rev%20%20B%20-%20XR%20Email.pdf>. [Accessed 10 June 2015].
- [14] Offshore Energy Today, "GE's Subsea Systems executes first major contract," 09 April 2014. [Online]. Available: <http://www.offshoreenergytoday.com/ges-subsea-systems-executes-first-major-contract/>. [Accessed 10 June 2015].
- [15] D. Kurunakaran, Lecture notes: Riser Design, University of Stavanger, 2014.
- [16] Ø. Vollen, Statikk og fasthetslære, Kristiansand: NKI Forlaget, 2008.
- [17] DNV RP-H103, *Modelling and analysis of marine operations*, 2011.
- [18] Orcina, "OrcaFlex Examples - B Drilling Risers," 08 06 2015. [Online]. Available: <http://www.orcina.com/SoftwareProducts/OrcaFlex/Examples/B%20Drilling%20Risers/index.php>.
- [19] Orcina Ltd, *Orcaflex Manual, version 9.8a*, Cumbria: Orcina.
- [20] GE Oil & Gas, *Doc no: A110600-25*.
- [21] "Xtreme Release Connector," Subsea Technologies Ltd, [Online]. Available: <http://www.subseatek.com/images/upload/downloads/DN-1096-GD-2%20Rev%20%20B%20-%20XR%20Email.pdf>. [Accessed 11 June 2015].
- [22] H. O. Hovland, Analysis of global forces in the wellhead/wellhead connector as a function of wellhead lateral support and stiffness, Stavanger: Universitetet i Stavanger, 2014.
- [23] S. Matre, "Developing concept for subsea heavy well intervention," Universitet i Stavanger, Stavanger, 2008.
- [24] Island Offshore, "Light Well Intervention," [Online]. Available: <http://www.islandoffshore.com/?c=9452>. [Accessed 2 February 2015].
- [25] O. T. Gudmestad, *Linear wave theory - Lecture compendium*, Stavanger, 2014.
- [26] Standards Norway, *NORSOK N-003 - Actions and action effects*, 2007.
- [27] D. W. Allen, "OTC 8703 - Vortex-Induced Vibration of Deepwater Risers," in *Offshore Technology Conference*, Houston, Texas, 1996.

Appendix A

Results obtained from Orcaflex in 500 meters WD with waves and current. Measurements correspond to the coordinates system described in section 9.2.

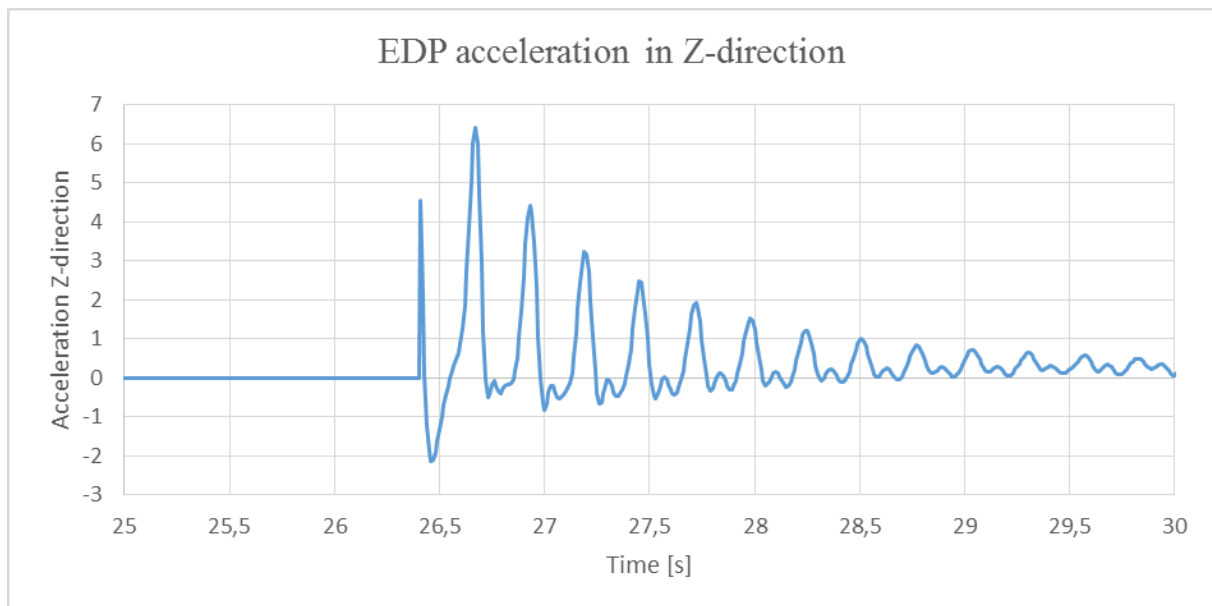


Figure A1: EDP acceleration in Z-direction

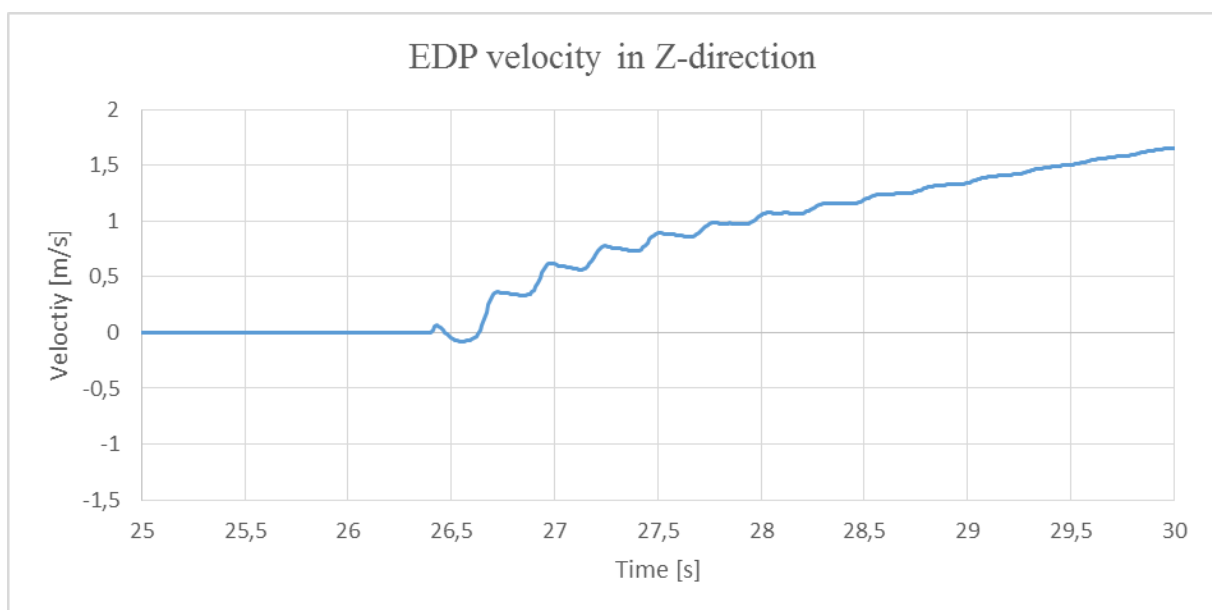


Figure A2: EDP velocity in Z-direction

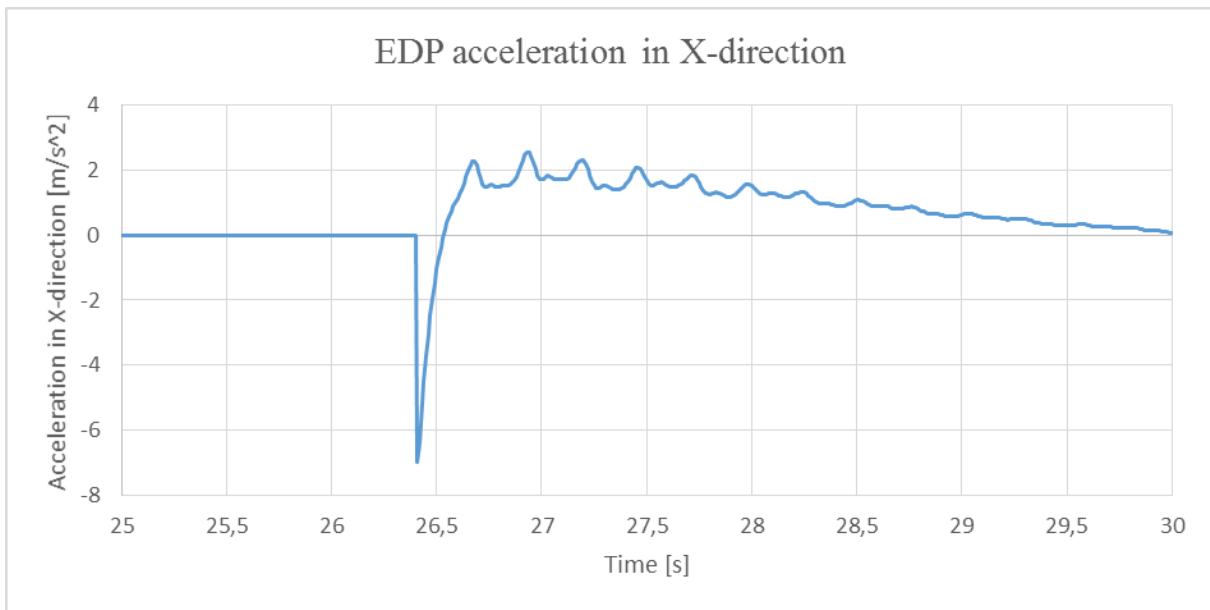


Figure A3: EDP acceleration in X-direction

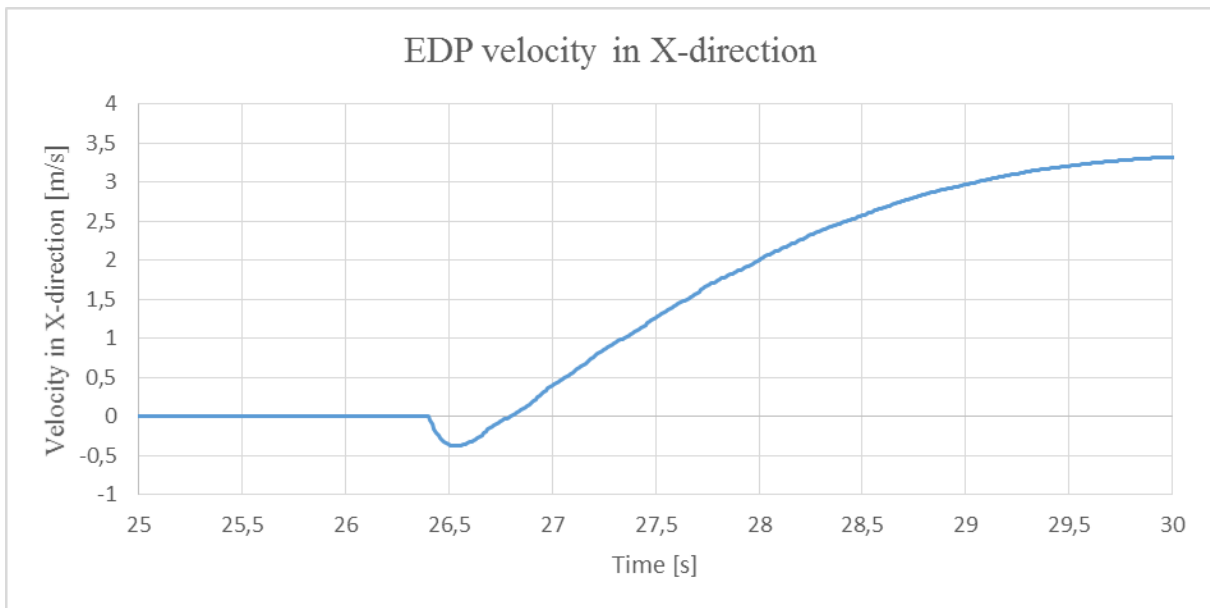


Figure A4: EDP velocity in X-direction

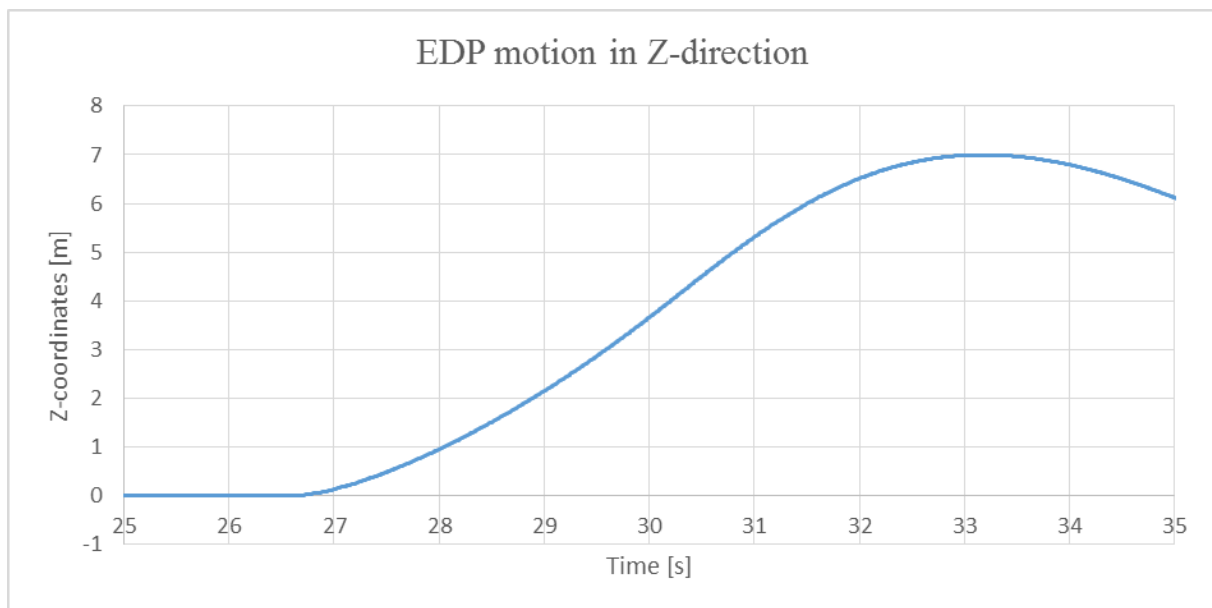


Figure A5: EDP motion in Z-direction

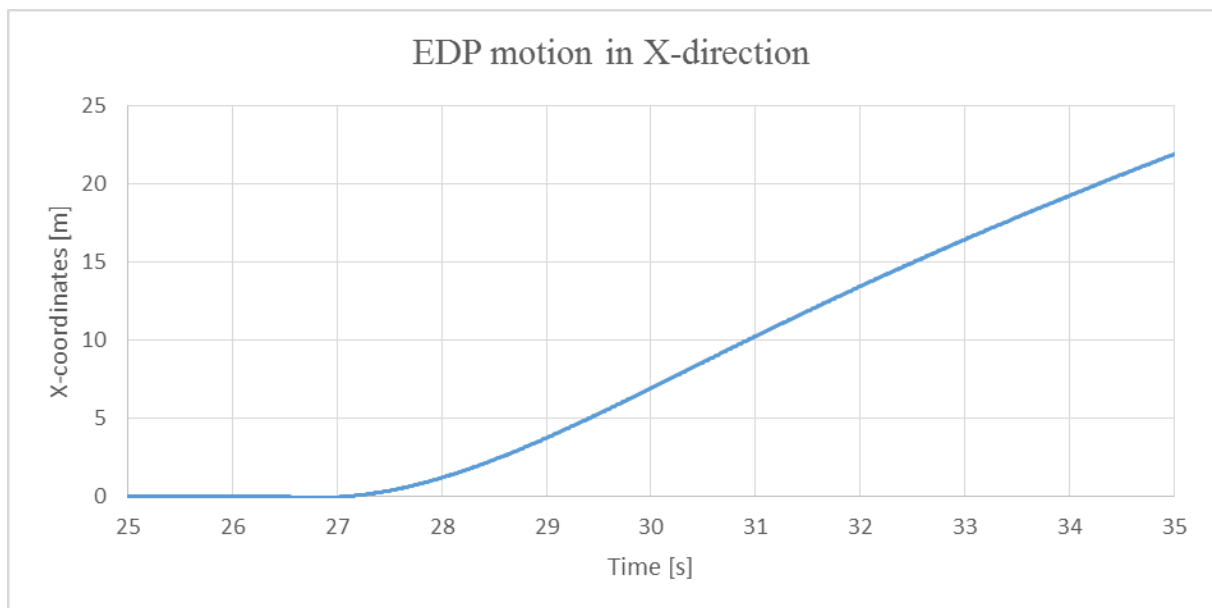


Figure A6: EDP motion in X-direction

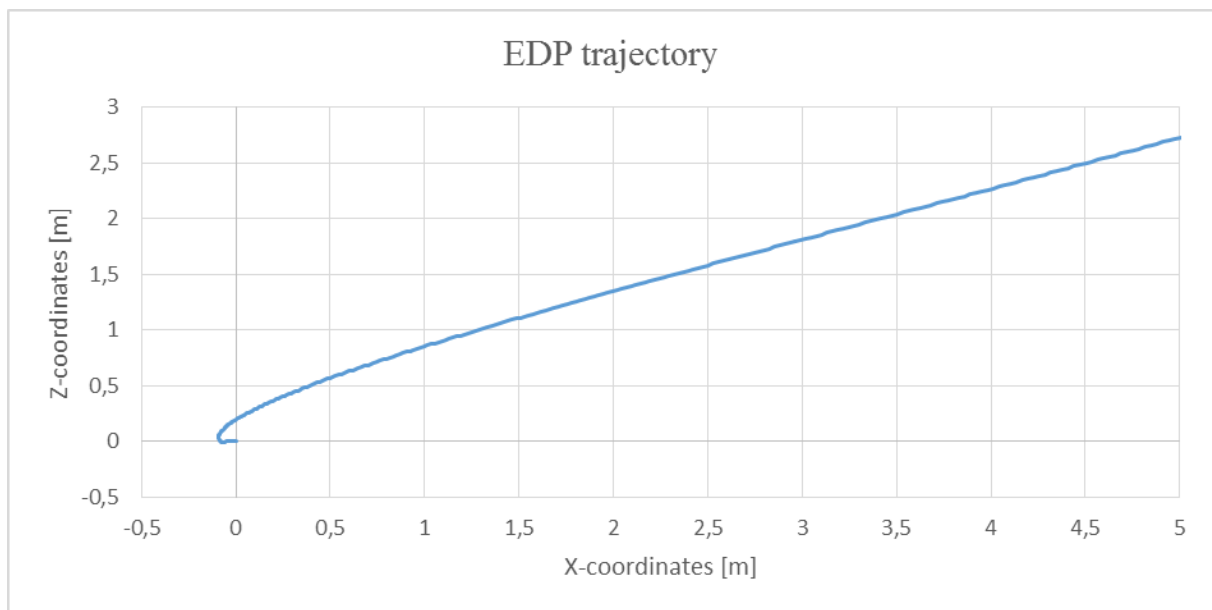


Figure A7: EDP trajectory

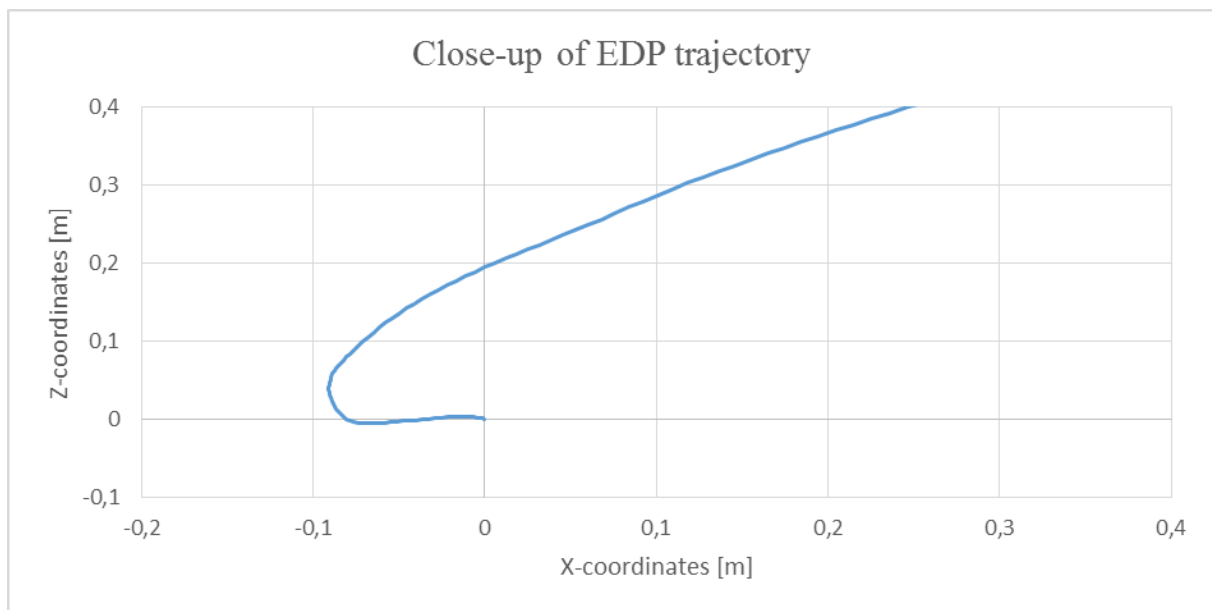


Figure A8: Close-up of EDP trajectory

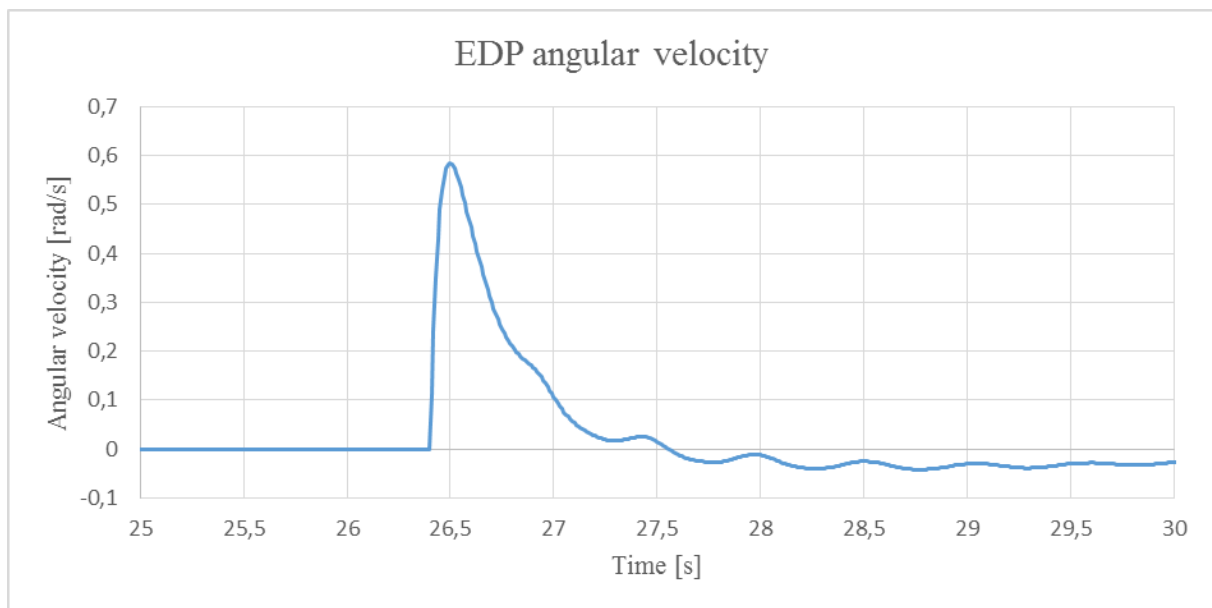


Figure A9: EDP angular velocity

Appendix B

Results obtained from Orcaflex in 1000 meters WD with waves and current. Measurements correspond to the coordinate system described in section 9.2.

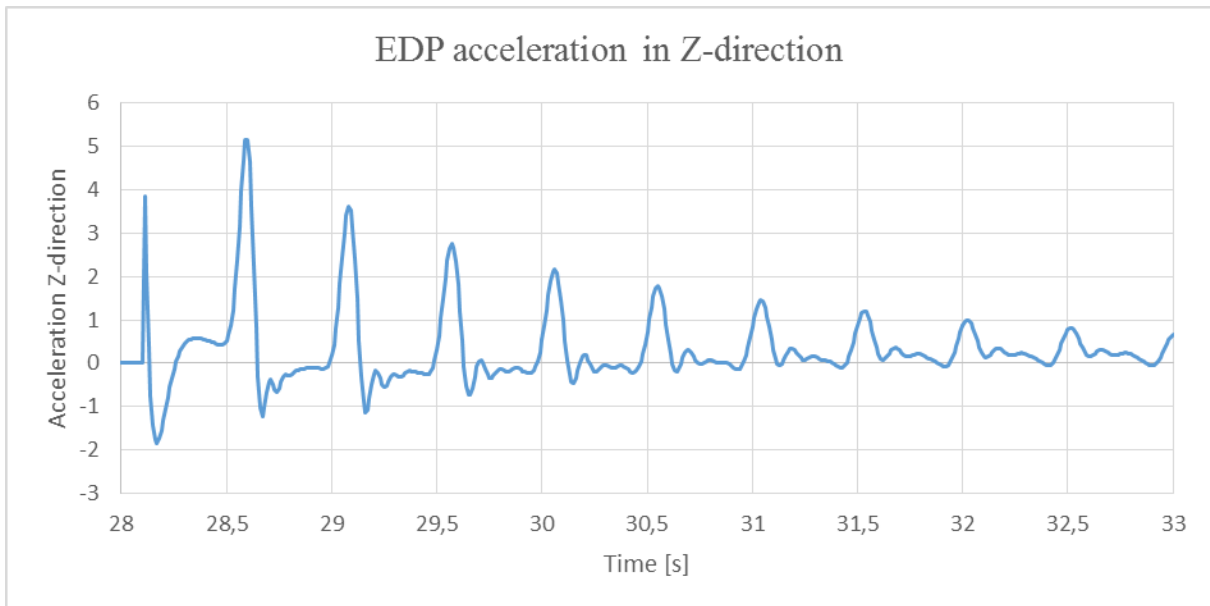


Figure B1: EDP acceleration in Z-direction

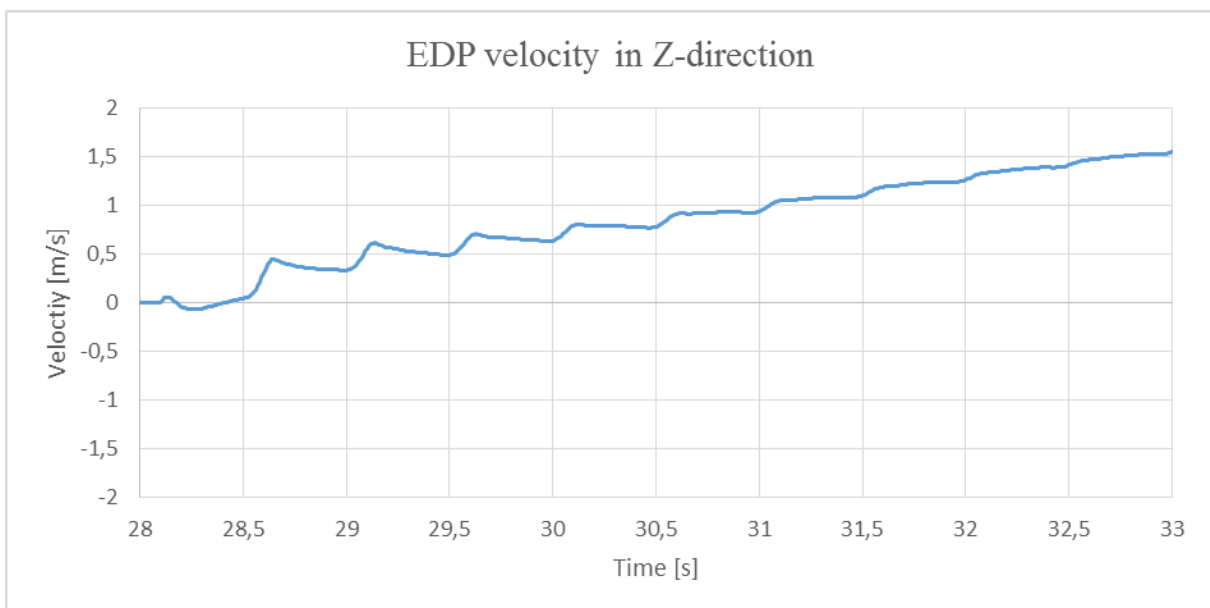


Figure B2: EDP velocity in Z-direction

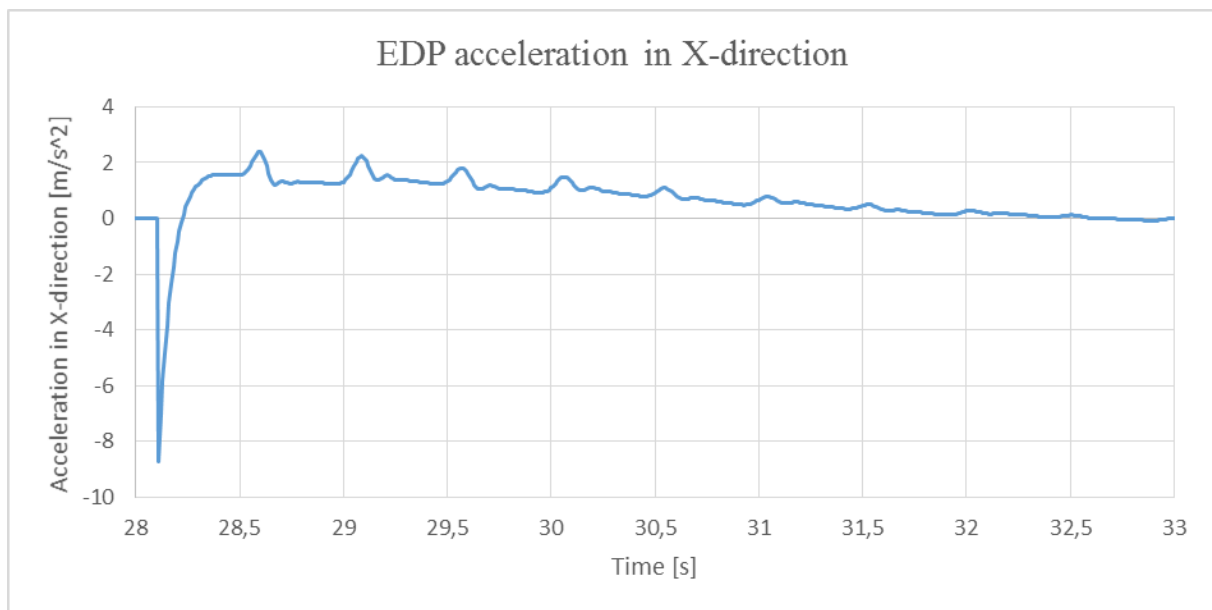


Figure B3: EDP acceleration in X-direction

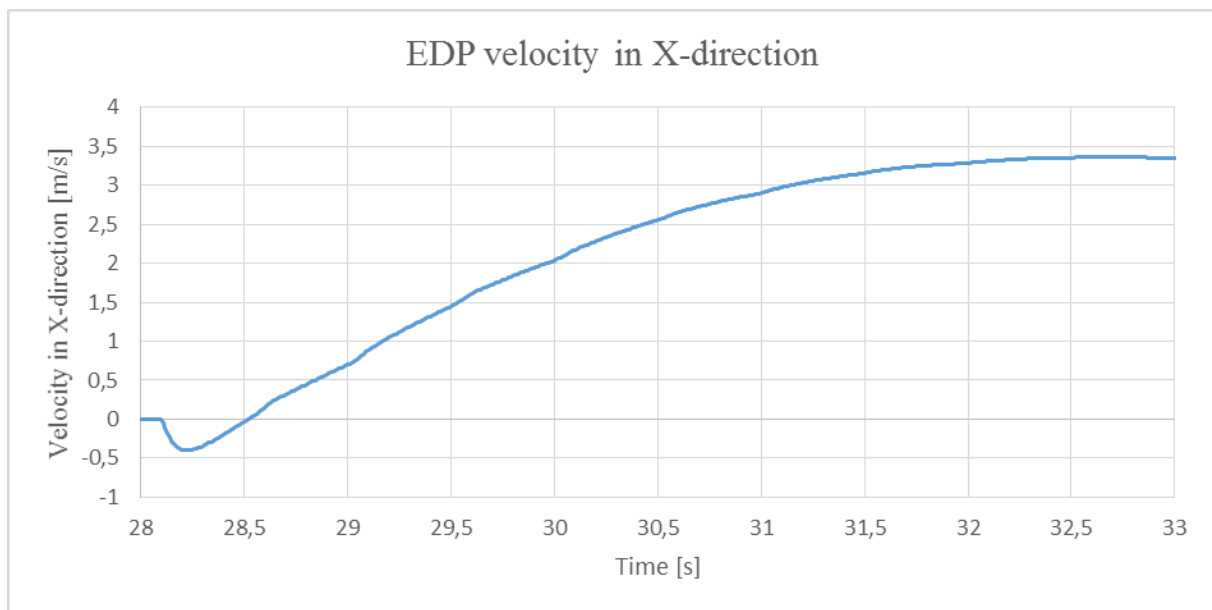


Figure B4: EDP velocity in X-direction

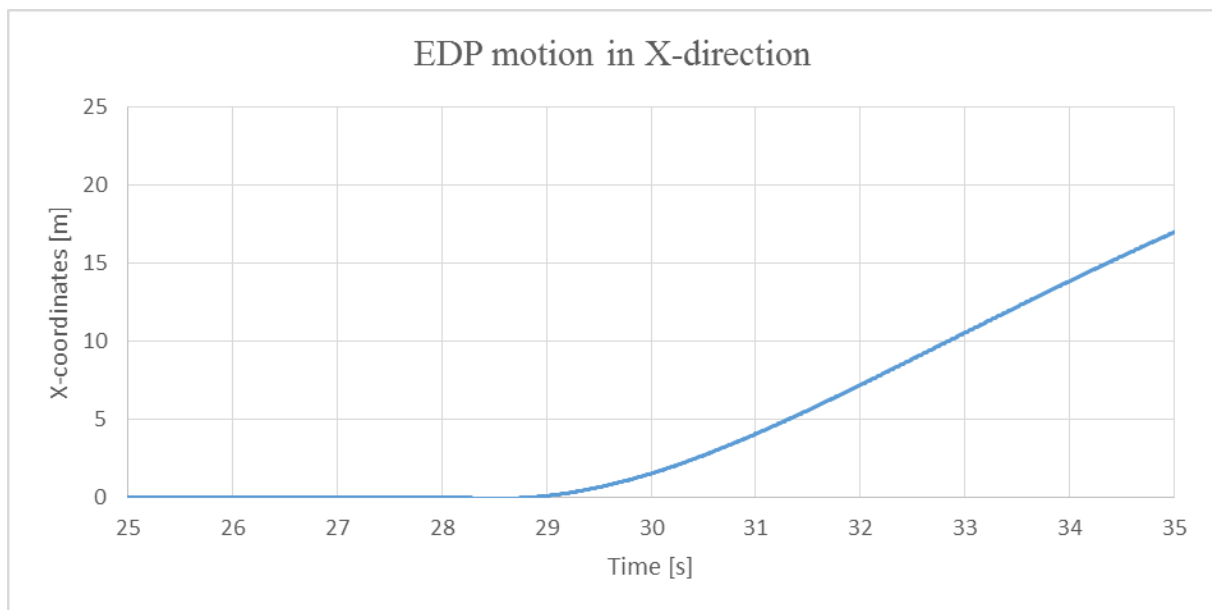


Figure B5: EDP motion in X-direction

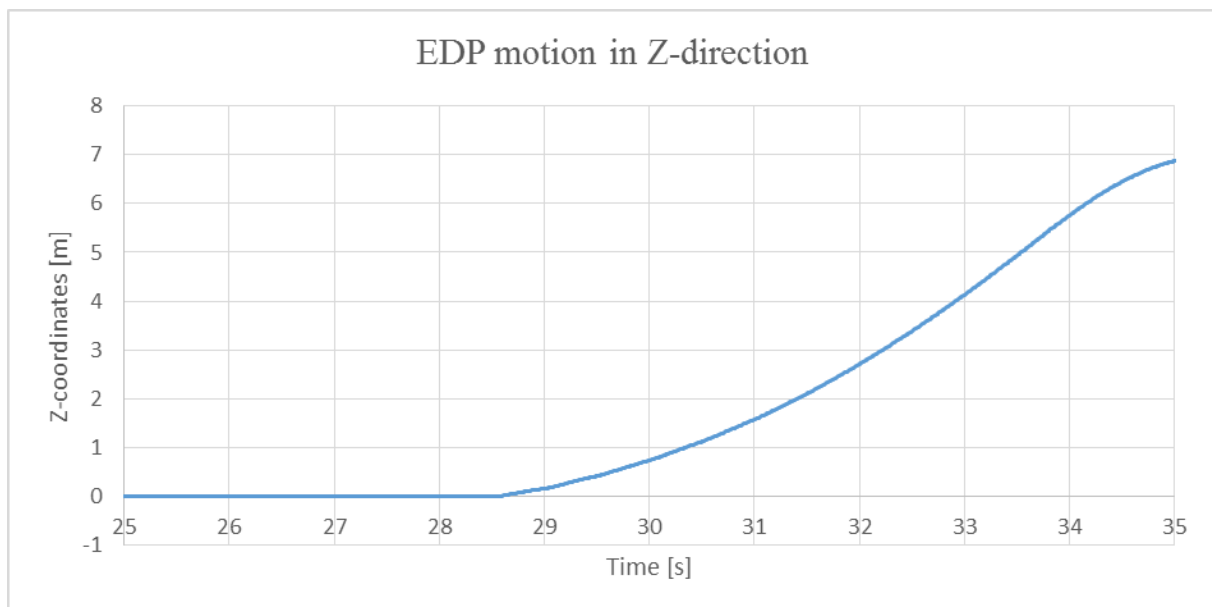


Figure B6: EDP motion in Z-direction

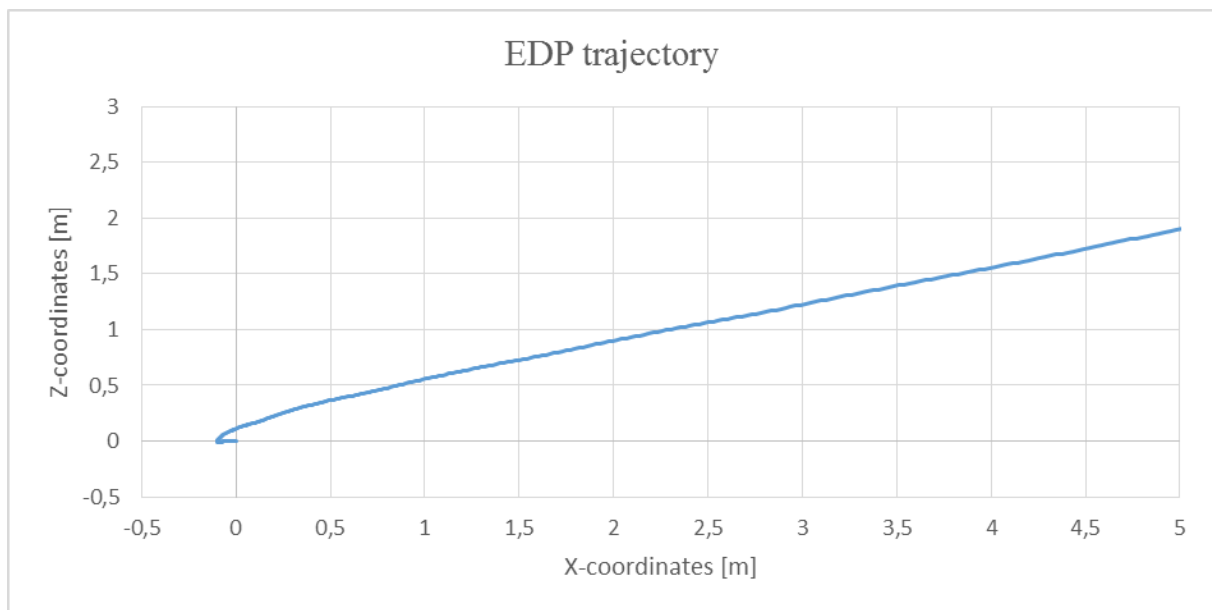


Figure B7: EDP trajectory

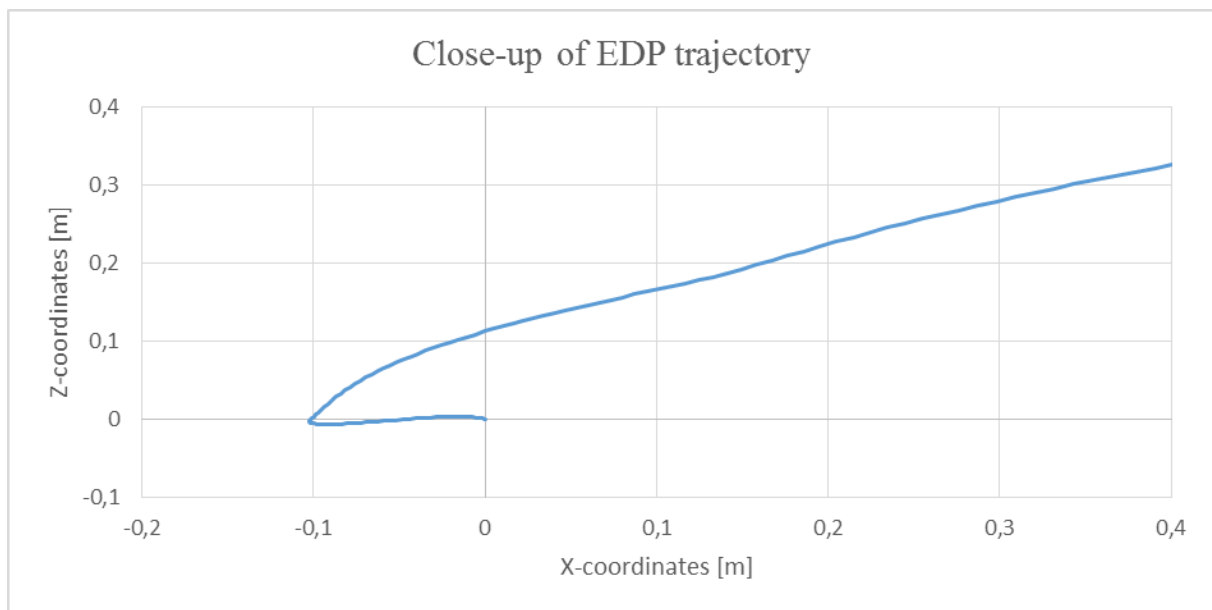


Figure B8: Close-up of EDP trajectory

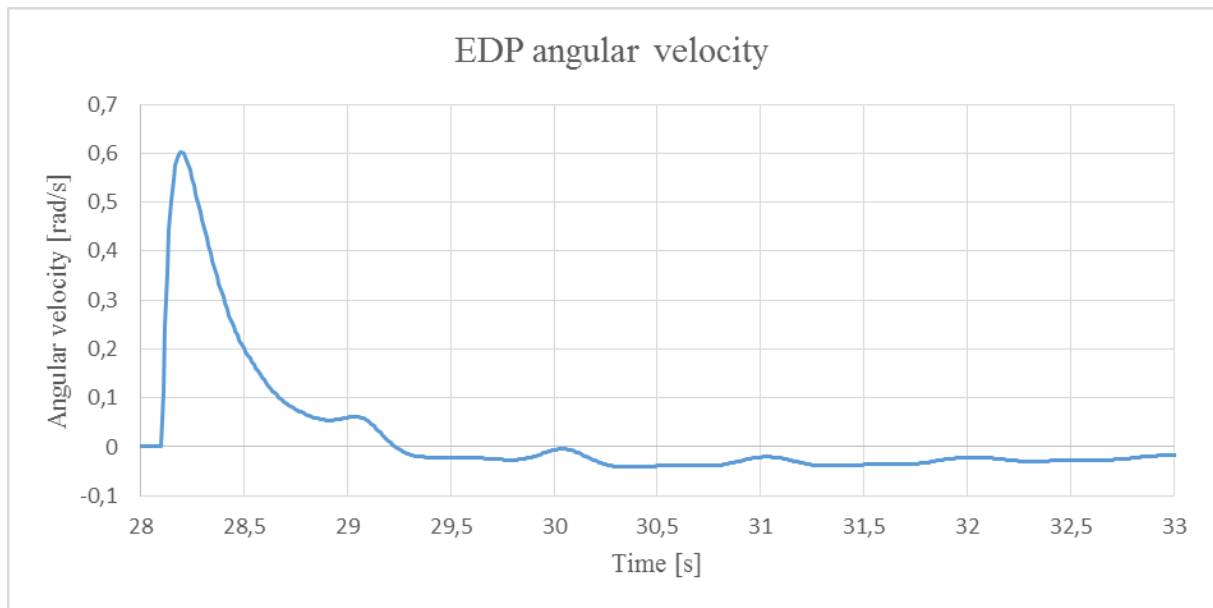


Figure B9: EDP angular velocity